

# Excellence in Chemistry Research

## Announcing our new flagship journal

- Gold Open Access
- Publishing charges waived
- Preprints welcome
- Edited by active scientists



## Meet the Editors of *ChemistryEurope*



**Luisa De Cola**

Università degli Studi  
di Milano Statale, Italy



**Ive Hermans**

University of  
Wisconsin-Madison, USA



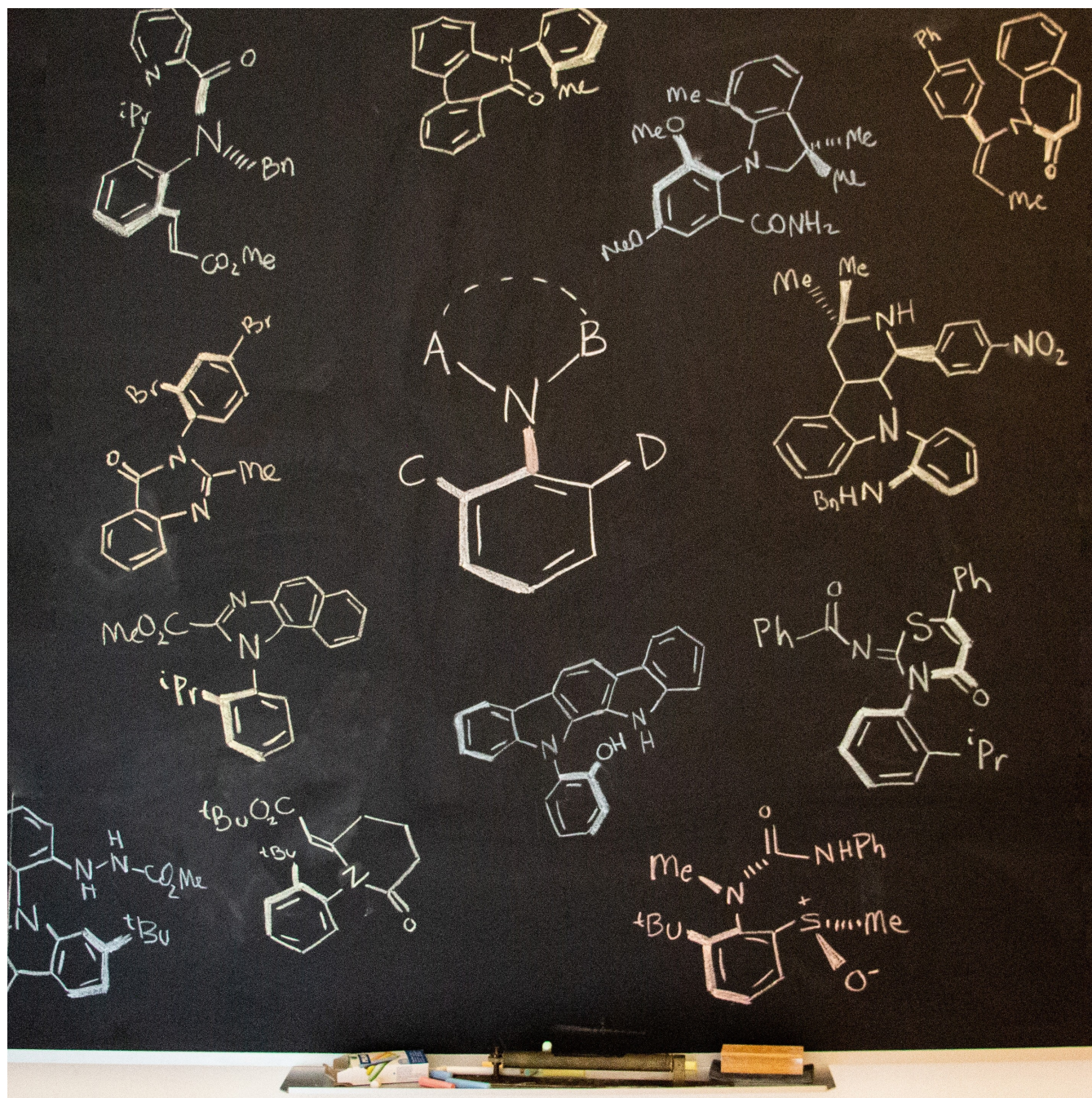
**Ken Tanaka**

Tokyo Institute of  
Technology, Japan

# Asymmetric Synthesis of Axially Chiral C–N Atropisomers

Patricia Rodríguez-Salamanca,<sup>[a]</sup> Rosario Fernández,<sup>\*[b]</sup> Valentín Hornillos,<sup>\*[a, b]</sup> and José M. Lassaletta<sup>\*[a]</sup>

*Dedicated to Professor Joan Bosch on the occasion of his 75th birthday*



**Abstract:** Molecules with restricted rotation around a single bond or atropisomers are found in a wide number of natural products and bioactive molecules as well as in chiral ligands for asymmetric catalysis and smart materials. Although most of these compounds are biaryls and heterobiaryls displaying a C–C stereogenic axis, there is a growing interest in less common and more challenging axially chiral C–N atropisomers. This review offers an overview of the various methodologies available for their asymmetric synthesis. A brief introduction is initially given to contextualize these axially

chiral skeletons, including a historical background and examples of natural products containing axially chiral C–N axes. The preparation of different families of C–N based atropisomers is then presented from anilides to chiral five- and six-membered ring heterocycles. Special emphasis has been given to modern catalytic asymmetric strategies over the past decade for the synthesis of these chiral scaffolds. Applications of these methods to the preparation of natural products and biologically active molecules will be highlighted along the text.

## 1. Introduction

Atropisomers, the most recognized class of compounds featuring axial chirality, comprise conformers with restricted rotation around a single bond that allow their isolation in a stable form. The configurational stability of these compounds depends on the rotational energy barrier and is generally determined by the number and size of substituents at the *ortho*, *ortho* positions relative to the stereogenic axis. The presence of larger substituents led to higher energy barriers and thus more configurationally stable products. In order to isolate atropisomers by analytical methods, a half-life for their interconversion of at least 1000 s is required, which is equivalent to a barrier of rotation of 90–100 kJ mol<sup>-1</sup>.<sup>[1]</sup>

Atropisomerism was first reported in 1922 by Christie and Kenner after their isolation of 6,6'-dinitro-[1,1'-biphenyl]-2,2'-dicarboxylic acid atropisomers by using brucine as a resolution agent.<sup>[2]</sup> Nonetheless, the importance of axial chirality in organic synthesis began to be widely recognized after 1980, when BINAP was implemented as a highly efficient ligand in asymmetric hydrogenation reactions.<sup>[3]</sup> During the subsequent decades, enantiomerically pure atropisomers have become desirable synthetic targets and tools in the field of asymmetric catalysis with long-winded application as organocatalysts and ligands for enantioselective transition-metal-catalyzed transformations.<sup>[4]</sup> Furthermore, axially chiral biaryl scaffolds are present in numerous natural products and biologically active

molecules in which the configuration of each enantiomer plays an important role in determining the final biological activity.<sup>[5]</sup>

A family of nonbiaryl atropisomers that have attracted considerable attention in recent years comprises those with restricted rotation around a C(sp<sup>2</sup>)-N(sp<sup>2</sup>) axis.<sup>[6]</sup> These chiral scaffolds are also present as key motifs in biologically active compounds (Figure 1A). In 1931, Adams described the first example of a compound with C–N axial chirality, a pyrrole derivative that could be obtained in enantiomerically pure form by resolution with brucine (compound **I**).<sup>[7]</sup> More recently, the groups of Curran and Clayden set the bases for the study, synthesis, and applications of C–N atropisomers<sup>[8]</sup> and, in recent years, a growing number of members of this family have been described. Many of them are natural products or present varied biological activities.<sup>[9]</sup> For example, quinazolinone derivative methaqualone **II** has sedative and hypnotic properties and has also been illegally used as a recreational drug,<sup>[10]</sup> while aniline derivative metolachlor **III** is one of the most important grass herbicides for use in maize.<sup>[11]</sup> Other relevant representatives include ancisheynine **IV**, a naphthylisoquinoline alkaloid isolated from *Ancistrocladus heyneanus*,<sup>[12]</sup> or murrastifoline A, B and F alkaloids, extracted from the root of *Murraya koenigii* plants, which constitute a family of axially chiral carbazole-derived C–N compounds,<sup>[13]</sup> whose configurational properties were studied by Bringmann in 2001 (compound **V**).<sup>[14]</sup> More recently, axially chiral metabolites (–)-marinopyrrole **Via** and (–)-marinopyrrole **Vib** were isolated by cultivation of an obligate marine *Streptomyces* strain and have shown excellent antibiotic activity against methicillin-resistant staphylococcus aureus.<sup>[15]</sup> Particularly relevant is the axially chiral quinazolinone derivative AMG 510 (Sotorasib) **VII**, a potent KRAS<sup>G12C</sup> inhibitor<sup>[16]</sup> that has been recently approved as an anti-cancer medication for the treatment of non-small-cell lung cancer (NSCLC). Remarkably, several types of axially chiral heterobiaryls show activity as kinase inhibitors. Selected representatives are quinazolinone **VIII**, a reversible inhibitor of Bruton's tyrosine kinase (BTK),<sup>[17]</sup> benzimidazole **IX**, a phosphoinositide 3-kinase PI3 K $\beta$  inhibitor,<sup>[18]</sup> and pyridone **X**, a potent p38 kinase inhibitor.<sup>[19]</sup> Interesting bioactivities have also been found in axially chiral *N*-aryl triazole derivatives. For example Lenisurad **X** is a hURAD1 inhibitor used for the treatment of goat,<sup>[20]</sup> while analogue **XII** is a glycine transporter GlyT1 inhibitor.<sup>[21]</sup> These types of compounds have also demonstrated their potential as

[a] P. Rodríguez-Salamanca, Dr. V. Hornillos, Prof. J. M. Lassaletta  
Instituto de Investigaciones Químicas (CSIC-US) and Centro de Innovación  
en Química Avanzada (ORFEO-CINQA)  
C/ Américo Vespucio, 49, 41092 Sevilla (Spain)  
E-mail: jmlassa@iiq.csic.es  
vhornillos@us.es

[b] Prof. R. Fernández, Dr. V. Hornillos  
Departamento de Química Orgánica (Universidad de Sevilla) and Centro de  
Innovación en Química Avanzada (ORFEO-CINQA)  
C/ Prof. García González, 1, 41012 Sevilla (Spain)  
E-mail: rfernand@us.es

© 2022 The Authors. Chemistry - A European Journal published by Wiley-VCH GmbH. This is an open access article under the terms of the Creative Commons Attribution Non-Commercial License, which permits use, distribution and reproduction in any medium, provided the original work is properly cited and is not used for commercial purposes.

chiral ligands for asymmetric catalysis, as exemplified by the selected examples VIII–XI shown in Figure 1(B).<sup>[22]</sup>

While the synthesis of axially chiral biaryls has been widely explored, the enantioselective construction of C–N heterobiaryls and other axially chiral compounds featuring a C–N stereogenic axis has been much less investigated and remains as a quite challenging task.<sup>[23]</sup> Their rotational stability generally relies on the steric factors of the substituents around the C–N axis as well as the structure of the nitrogen moiety. Thus, most of these axially chiral C–N atropisomers contain substituents in the *ortho* position of the aromatic unit attached to nitrogen. The structural properties of the C–N axis often led to a decrease in the configurational stability, which increases the difficulty of their enantioselective synthesis.

The aim of the present review is to provide an updated outline of the different strategies and methodologies developed for the asymmetric synthesis of compounds with restricted rotation around a C–N bond, with special emphasis on catalytic asymmetric methodologies. The manuscript includes methods for the synthesis of axially chiral anilides XII, indole and carbazole derivatives XIII, pyrroles and triazoles XIV, benzimidazoles XV, imides XVI, six-membered lactam derivatives XVII, quinazolinones XVIII, and thiazinones XIX, among others (Figure 2).

Early contributions based on diastereoselective approaches using auxiliaries from the chiral pool, classical resolutions, co-crystallizations or chromatographic separations are presented for each group of compounds, but then the review emphasizes the different strategies developed for their catalytic asymmetric synthesis. These can be roughly classified according to the retrosynthetic pathways shown in Figure 3. Thus, target products featuring a C–N stereogenic axis can be accessed by *N*-functionalization of aniline derivatives, either intramolecularly (Figure 3A) or by cyclization (Figure 3B). There are also methodologies involving atroposelective de novo construction of heterocyclic (Figure 3C) or aromatic (Figure 3D) moieties of the final product. Modern C–H activation/functionalization strategies (Figure 3E) are also suitable tools for the atroposelective synthesis of these compounds. Alternatively, there are also approaches that focus on the direct generation of the C–N stereogenic axis (Figure 3F). Finally, examples of desymmetrization strategies based on transformations in either the aromatic (Figure 3G) or the heterocyclic (Figure 3H) part of heterobiaryls are also presented and discussed.

Patricia Rodríguez-Salamanca received in 2017 her Master in Organic Chemistry from the Autonomous University of Madrid, where she worked on iron-catalyzed hydroborylative cyclization of enynes. She commenced her PhD studies in the group of Asymmetric Catalysis at the Instituto de Investigaciones Químicas (CSIC-US) in 2018, exploring novel methodologies for the atroposelective synthesis of axially chiral biaryls involving dynamization processes.



Rosario Fernández received her Ph.D. (1985) at the University of Sevilla. She was a NATO postdoctoral fellow at the University of Paris-Sud (Orsay, France) from 1986 to 1987. In 1987, she returned to the University of Sevilla, where she was promoted to Associate Professor. In 2008 she became a Full Professor at the same University. She has been recognized with the 'Excelencia Investigadora' Award from the Royal Society of Chemistry (2019). Her current research interests include asymmetric synthesis and enantioselective catalysis, in both aspects, asymmetric metal catalysis and organocatalysis.



Valentín Hornillos (Toledo, 1978) obtained his Ph.D. from the University Complutense de Madrid in 2009, working on the synthesis of fluorescent lipid drugs. In 2007, he also spent four months in the Novartis laboratories in Vienna. From 2010 until 2015, he was a postdoctoral fellow in the group of Professor Ben Feringa at the University of Groningen and in 2015 he moved to the IIQ, CSIC in Seville as a Talent Hub Fellow. Since 2019, he has been a Ramón y Cajal researcher at the University of Seville. His research interests include the development of new transition metal-catalyzed enantioselective processes.



José María Lassaletta received his Ph. D. in 1990 at the University of Sevilla. He then performed postdoctoral stages at the 'Instituto de la Grasa y sus Derivados' (CSIC) and the University of Konstanz, (Germany), with Prof. R. R. Schmidt. In 1995 he moved to the 'Instituto de Investigaciones Químicas' (CSIC, Seville), where he was promoted to Tenured Scientist (1996), Research Scientist (2005), and Research Professor (2009). He has been recognized with the 'Felix Serratosa' Lecture (2011) and the 'Ignacio Ribas' Medal from the Royal Society of Chemistry (2017). His current interests focus on asymmetric homogeneous catalysis and the development of synthetic methodologies.



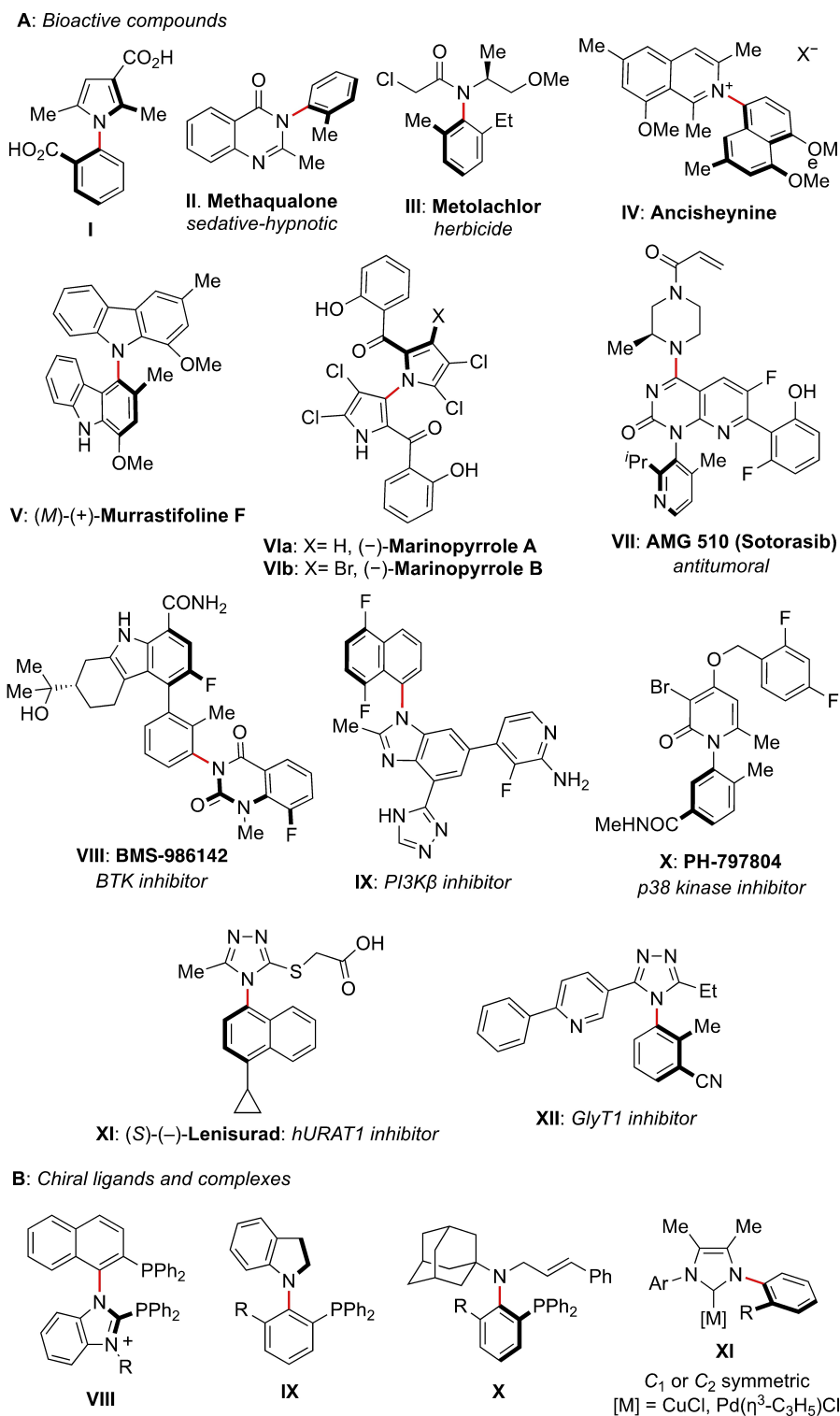


**Figure 1.** A) Naturally occurring and bioactive C–N-bonded axially chiral compounds. B) Selected ligands and complexes featuring C–N axially chirality.

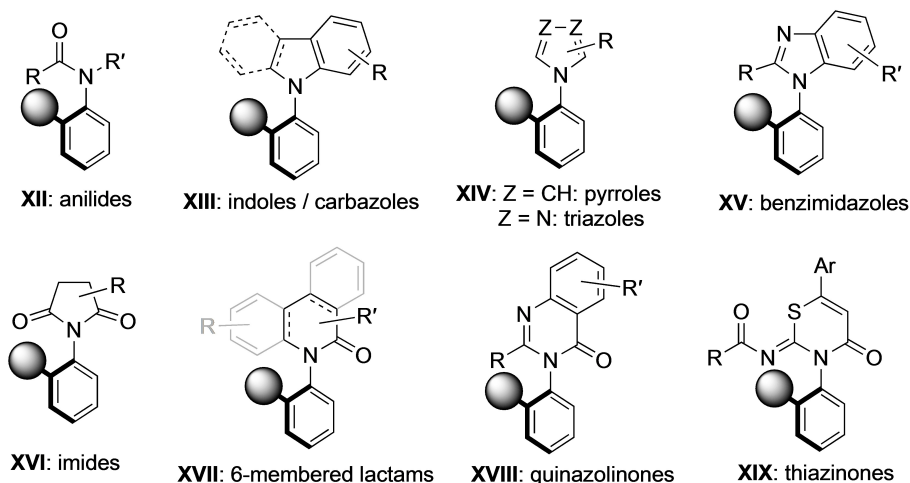


Figure 2. Representative families of atropisomers featuring a C–N chiral axis.

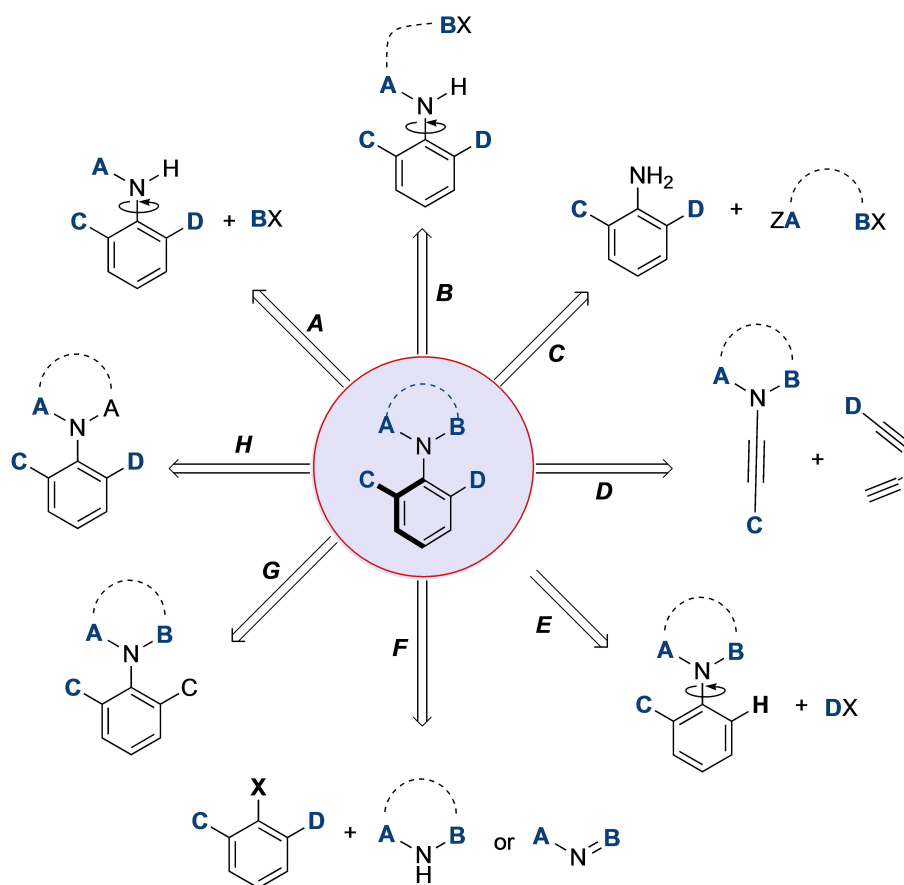


Figure 3. Strategies for the catalytic asymmetric synthesis of axially chiral C–N atropisomers.

## 2. Atropisomeric cyclic derivatives: anilides and related analogues.

### 2.1. Early examples and conventional resolution approaches

In the case of anilides, a bulky *ortho* substituent, such as the *tert*-butyl group, is frequently used to attain configurational stability. In 1994, Curran et al.<sup>[24]</sup> advanced the requirement of using large *ortho* substituents next to the C–N axis to increase their rotational barrier and thus prevent racemization at room temperature. Initially, they focused on the study of the configurational stability of racemic anilides **1** and their subsequent derivatization reactions, such as the 1,3 dipolar cycloaddition with benzonitrile oxide to afford a mixture of diastereomers **2a** and **2b** in a 97:3 ratio (Scheme 1).

These preliminary results fixed the bases for the development of a range of approaches for the synthesis of these compounds in enantiomerically pure form. Thus, Simpkins and co-workers<sup>[25]</sup> performed a kinetic resolution (KR) of racemate **3** to obtain enantioenriched  $\alpha$ -methylated product **4** together with unreacted 2-(*tert*-butyl)anilide (–)-**3** in 88% *ee*. The reaction proceeds through the generation of an enolate using substoichiometric amounts of a chiral lithium amide base, followed by quenching with MeI (Scheme 2). Although the kinetic resolution was not optimized, the strategy paved the way for the development of more efficient methods to obtain highly enantioenriched axially chiral anilides.

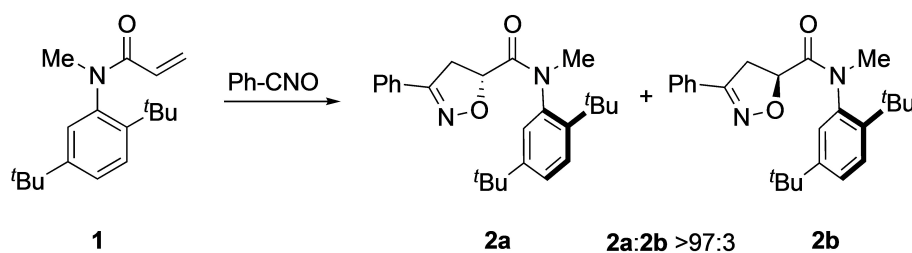
Taguchi<sup>[26]</sup> and co-workers employed a chiral pool approach to obtain enantiomerically pure anilide derivatives. Thus, the reaction of *N*-allyl-*o*-(*tert*-butyl)aniline **6** with 2 equivalents of lactic acid derivative **5** afforded a 3:1 separable mixture of diastereomeric carboxamides **7a** and **7b**. Subsequently, the

former was easily transformed into anilide **8**, obtained in 97% enantiomeric excess, as shown in scheme 3.

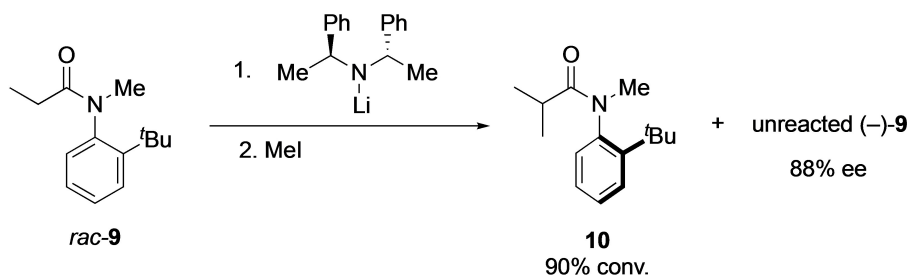
Following a related strategy, Simpkins and co-workers<sup>[27]</sup> also used a chiral pool approach based on lactic acid. Starting from  $\alpha$ -acetoxy anilide **9**, readily available after condensation of acetate **5** with *o*-(*tert*-butyl)aniline, alkylation with MEMCl afforded a mixture of stereoisomeric anilides **10a** and **10b** in 41% and 25% yield, respectively. Subsequently, these products were reduced using a  $\text{SmI}_2$ -LiCl system to afford enantioenriched products **11** with a slight loss of stereochemical integrity. This reaction was general for a wide variety of acetates and the method was also effective for the removal of  $\alpha$ -bromo and  $\alpha$ -benzyloxy functionalities (Scheme 4).

Furthermore, Taguchi co-workers<sup>[28]</sup> developed a chiral pool approach to access highly enantioenriched atropisomeric anilides based on the resolution of amide esters **13a** and **13b**, easily available from oxalyl chloride, (*R*)-pantolactone alkoxide **12** and *N*-allyl-(*ortho-tert*-butyl)aniline **6** (Scheme 5). Noteworthy, the chiral pantolactone **12** could be recovered and reused, and the efficient resolution of **13a** and **13b** by recrystallization makes large-scale preparation possible. The authors further performed the synthesis of enantiomerically pure  $\alpha$ -ketoamides **14** and  $\alpha,\beta$ -unsaturated anilides **15** from amide ester **13a**, without loss of stereochemical integrity.

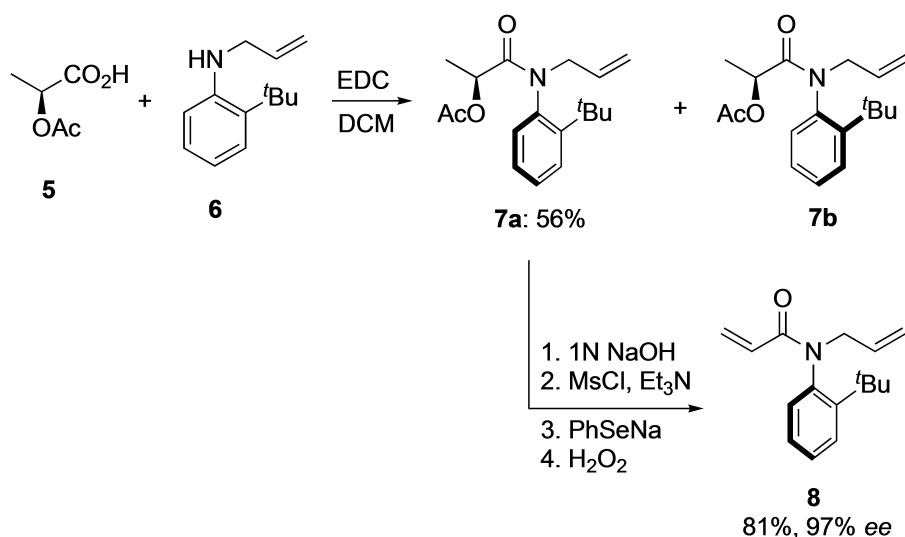
In 2000, Uemura and co-workers<sup>[29]</sup> reported the asymmetric synthesis of atropisomeric anilides through a kinetically controlled enantiotopic lithiation of prochiral chromium arene complex **16** (Scheme 6). Deprotonation with chiral lithium amide base **17**, followed by quenching with an electrophile (alkyl halides or carbonyl compounds) afforded axially chiral amides **18** with selectivities up to 97% *ee*. The high stereoselectivity could be associated with the conformational orientation of the prochiral chromium complex, where the amido carbonyl



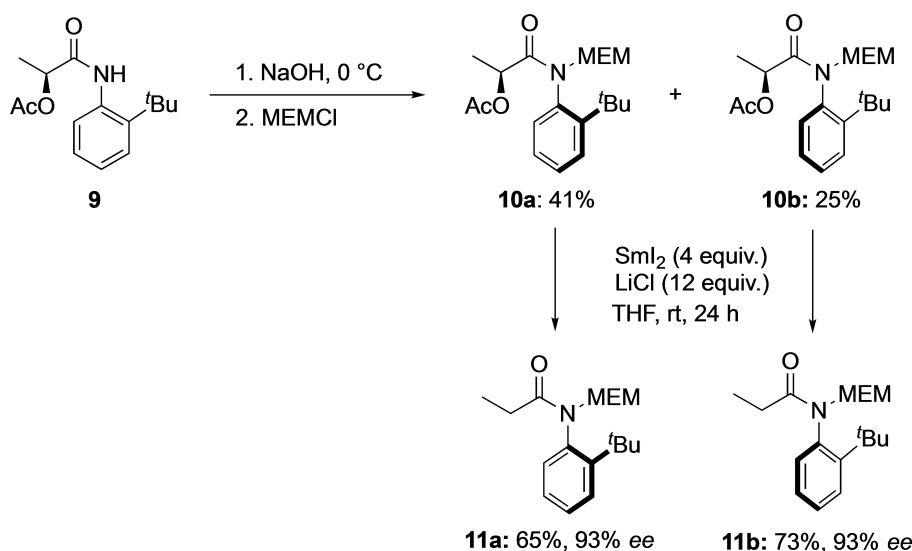
**Scheme 1.** Seminal studies toward the synthesis of axially chiral anilides. Enantiomers of **2a** and **2b** not shown.



**Scheme 2.** Kinetic resolution for the synthesis of 2-(*t*-butyl)anilides.



Scheme 3. Chiral pool approach to axially chiral anilide derivatives.



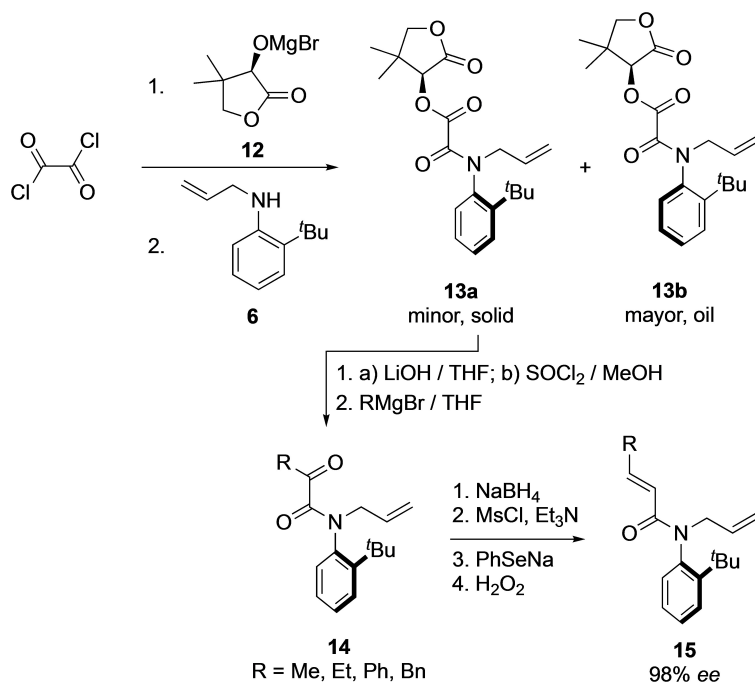
Scheme 4. Synthesis and reduction of axially chiral acetoxy anilides.

oxygen is oriented *trans* to the chromium atom in the complexed aryl group. Exposure of complex **18** to sunlight resulted in the removal of the ligand from the coordination sphere of chromium, providing pure anilides **19** without loss of optical purity.

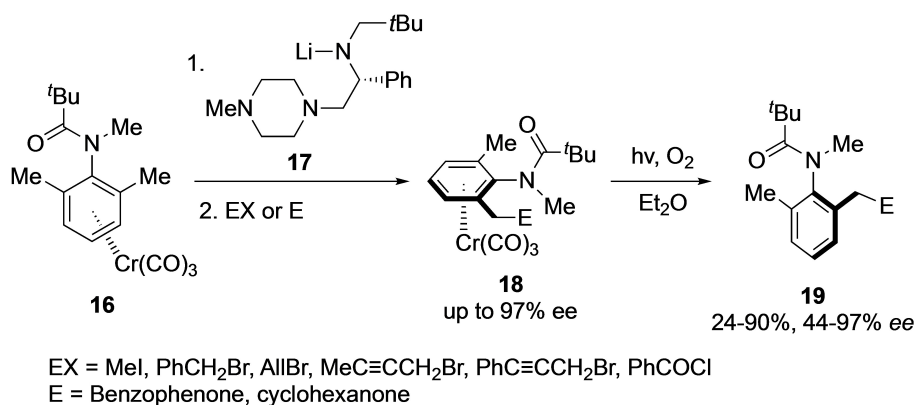
Building upon the above findings of Simpkins and Taguchi, the group of Curran<sup>[30]</sup> described an efficient method to obtain axially chiral enantiopure anilides based on a crystallization-induced asymmetric transformation (Scheme 7). Upon reaction with dimethyl-L-tartrate, racemic anilide **20** was converted into a 1:1.1 mixture of diastereomeric ketals **21**. Further selective recrystallization increased the diastereomeric ratio to 20:1. The enantiomeric excess of the final product **20** obtained after cleavage with  $\text{SmI}_2$  or hydrolysis under basic conditions was determined by the diastereomeric ratio of **21**, assuming that

these transformations proceed faster than the interconversion of the rotamers (racemization). On the other hand, the diastereomeric ratio drops when the crystallization occurs too rapidly. In these compounds, the nitrogen atom exhibits a pyramidal structure, with the *ortho-tert-butyl* group adopting a *syn* orientation relative to the vicinal N lone pair.

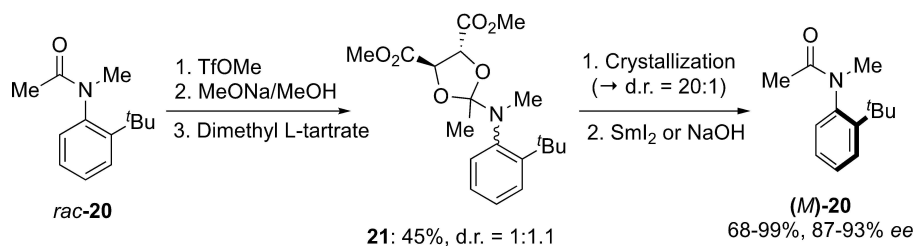
In 2009, Clayden et al. reported a kinetic resolution for the synthesis of atropisomeric ureas **23** based on the vanadium-catalyzed enantioselective oxidation of *ortho*-thiophenyl precursors **22** (Scheme 8).<sup>[31]</sup> Sulfoxidation proceeds with moderate enantioselectivities (up to 78% ee for ligand **L1** and  $\text{R}^1=\text{tBu}$ ,  $\text{R}^2=\text{Cy}$ ), and low selectivity factors except for one substrate ( $\text{R}^1=\text{tBu}$ ,  $\text{R}^2=\text{Me}$ ,  $S=300$ ). The half-life for racemization of the substrates was determined to be between 8 weeks [ $\text{R}^1=\text{CH}$ -



Scheme 5. Chiral pool approach for the synthesis of atropisomeric anilides.



Scheme 6. Asymmetric synthesis of atropisomeric anilides.

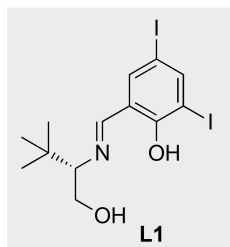
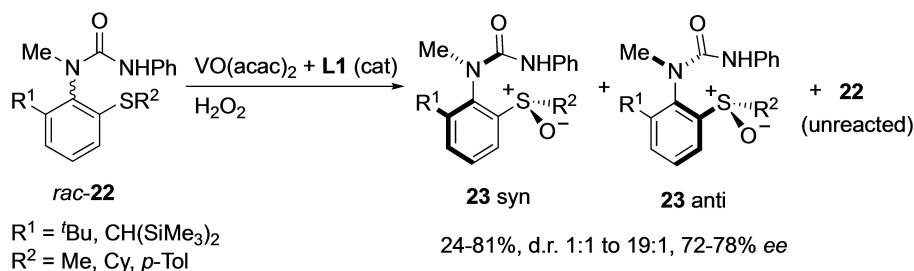


Scheme 7. Axially chiral enantiopure anilides by crystallization-induced asymmetric transformation.

$(\text{SiMe}_3)_2$ ,  $\text{R}^2=\text{Me}$ ] and 500 years ( $\text{R}^1=t\text{Bu}$ ,  $\text{R}^2=\text{Me}$ ), discarding any possibility of developing dynamic kinetic resolutions (DKR).

## 2.2. Atroposelective N-functionalization of aniline derivatives

The groups of Taguchi<sup>[32]</sup> and Curran<sup>[33]</sup> independently described the catalytic asymmetric synthesis of atropisomeric anilides **25**



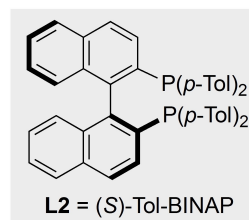
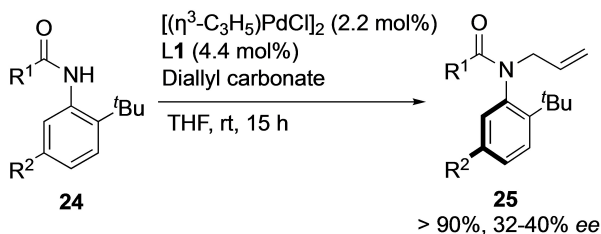
Scheme 8. Kinetic resolution of sulfanyl ureas.

and **27** by palladium-catalyzed allylation of achiral precursors **24** and **26**, using diphosphine ligands (*S*)-Tol-BINAP **L2** and (*S*)-BINAP **L3**, respectively (Scheme 9). Excellent yields were observed in both cases, but the enantioselectivities were rather low, a fact that was attributed to poor facial discrimination during the nucleophilic attack of the soft anilide anion on the

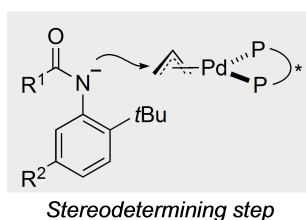
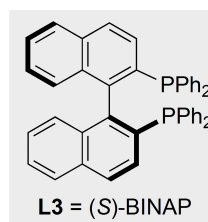
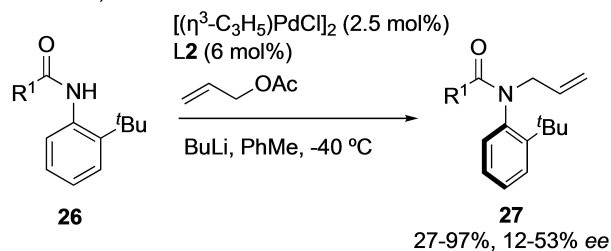
$\pi$ -allyl system, which occurs from the opposite side of the coordinated chiral ligand.

Aiming to overcome these difficulties, Taguchi et al.<sup>[34]</sup> described the synthesis of optically active atropisomeric anilide derivatives **29** through a catalytic asymmetric inter- and intramolecular *N*-arylation of achiral anilides **24**, using in this

## A: Taguchi, 2002:



## B: Curran, 2003:



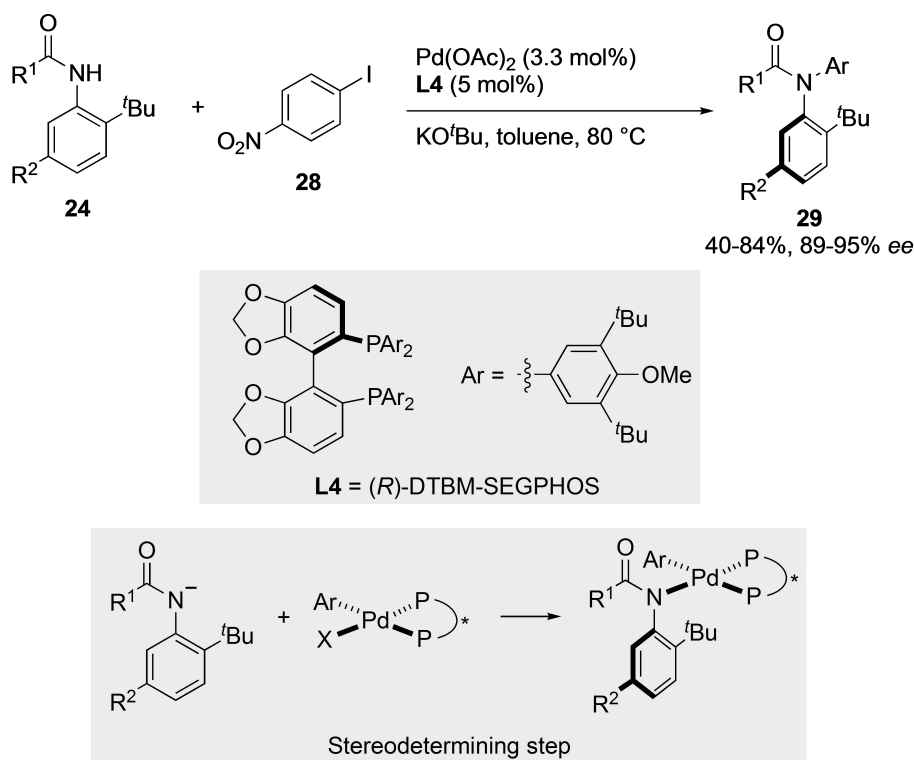
Scheme 9. Palladium-catalyzed asymmetric allylic alkylation for the synthesis of atropisomeric anilides.

case (*R*)-DTBM-SEGPHOS **L4** (Scheme 10). In this case, the anilide N atom attacks the Pd center instead of the allylic carbon in the stereodetermining step, so that the N-aryl bond lies in the proximity of the chiral ligand, making it therefore possible to reach high enantioselectivities. The absence of racemization under the reaction conditions was further confirmed by heating the product at 80 °C. On the other hand, a limited scope was shown for the method: the reaction was performed with 1-iodo-4-nitrobenzene as a unique electrophile.

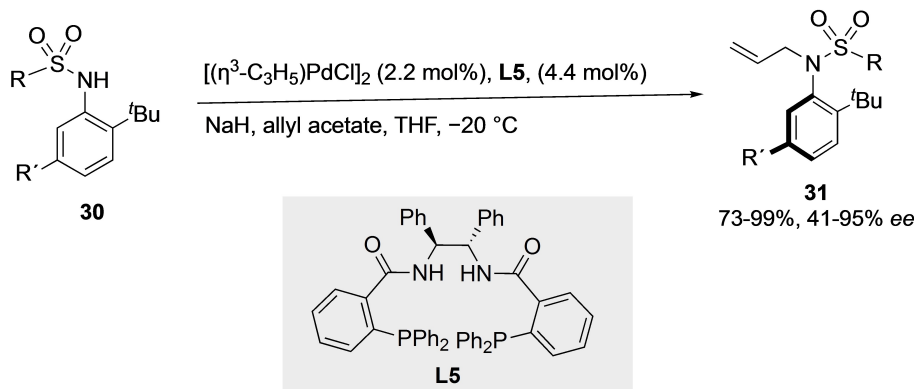
Kitagawa and co-workers<sup>[35]</sup> reported more recently the enantioselective synthesis of C–N axially chiral sulfonamides **31**, achieved through Pd-catalyzed *N*-allylation of precursors **30** with allyl acetate (Scheme 11). Using Trost's ligand **L5**, good

yields and high enantiomeric excesses were observed, especially for hindered substrates ( $R^1=^t\text{Bu}$ ).

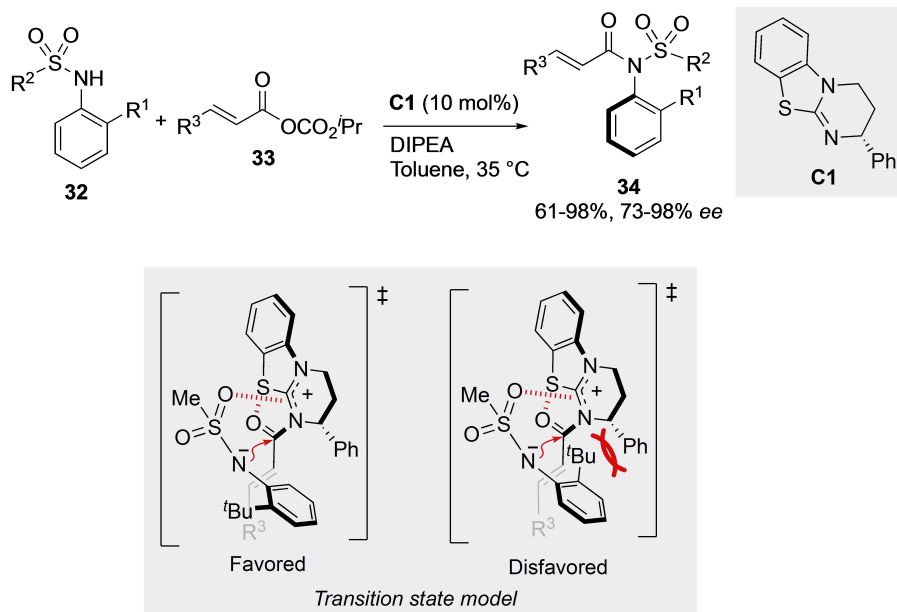
Very recently, Feng and co-workers reported a methodology for the asymmetric acylation of *N*-sulfonyl anilides **32** using  $\alpha,\beta$ -unsaturated carbonic anhydrides **33** as acyl transfer reagents and chiral isothiurea **C1** as the catalyst, yielding axially chiral *N*-acyl sulfonamides **34** (Scheme 12).<sup>[36]</sup> The reaction takes place under mild conditions using nonpolar solvents, and the use of a neutral base such as DIPEA was found to be key to obtain high enantioselectivities. Under the optimized conditions, a broad variety of carbonates were shown to be suitable substrates, although electron-poor derivatives gave better yields than electron-rich ones. Regarding the sulfonamide substrate, the



Scheme 10. *N*-arylation of achiral anilides.



Scheme 11. Atroposelective *N*-allylation of sulfonamides.



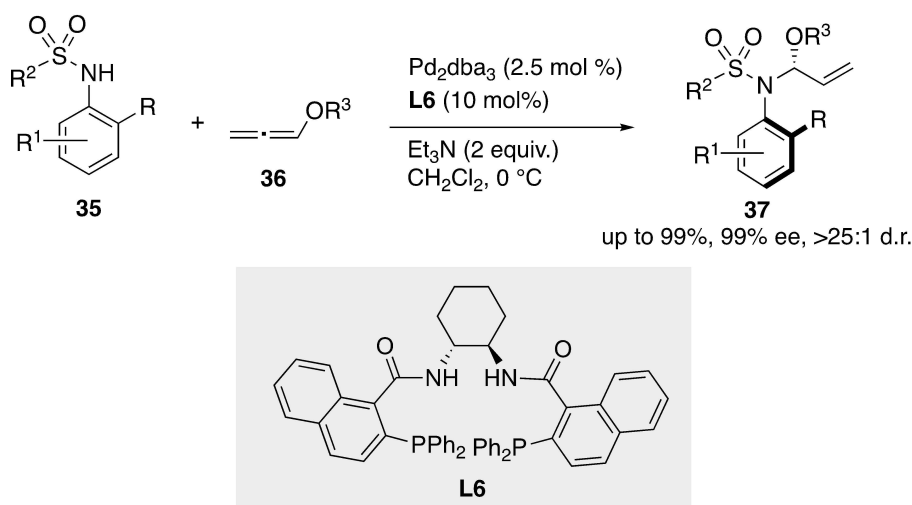
Scheme 12. Atroposelective acylation of sulfonamides

size of the *ortho* R' group directly correlates with the enantioselectivity. In the proposed enantiodetermining transition state model, the sulfonamide anion approaches from the opposite side of the phenyl group to avoid steric repulsion. Furthermore, the bulky *o*-*tert*-butyl group reduced the  $\pi$ - $\pi$  interactions between the substrate and catalyst, while the interaction between the oxygen of the sulfonyl moiety and the positive electronic charge on the imidazolium salt side was proposed to play an important role.

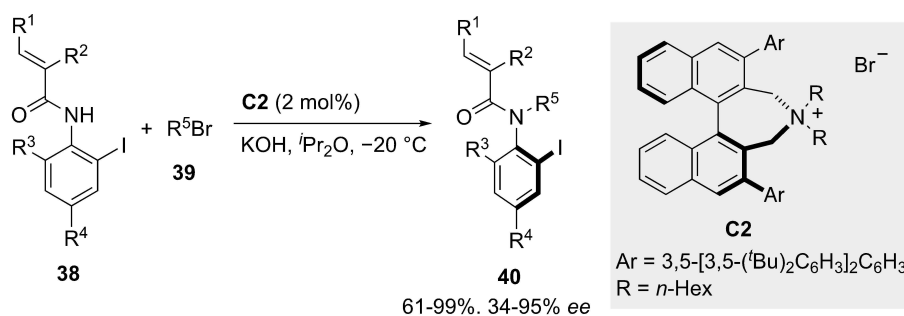
A late strategy developed to access axially chiral sulfonamides **37** makes use of a Pd-catalyzed atroposelective hydroamination of allenes **36** with substituted aryl sulfonamides **35** (Scheme 13).<sup>[37]</sup> Excellent enantio- and diastereoselectivities, as

well as a perfect branched-to-linear ratio were achieved by using Pd<sub>2</sub>(dba)<sub>3</sub> as the precatalyst and multidentate Trost type ligand **L6**. Moreover, the method benefits from wide functional group tolerance and, interestingly, substrates bearing uncommon *ortho* R groups such as ester, ketone, nitro, Cl, F, or OMe are well tolerated.

More recently, Maruoka et al.<sup>[38]</sup> described an efficient asymmetric synthesis of axially chiral *o*-iodoanilides **40** via phase-transfer catalyzed *N*-alkylation of precursors **38** with alkyl bromides **39** (Scheme 14). The key to obtaining high enantioselectivity relies on the ability of the chiral tetraalkylammonium bromide phase-transfer catalyst **C2** to discriminate between the *ortho* substituents in the anilide, a fact further supported by the



Scheme 13. Atroposelective hydroamination to axially chiral sulfonamides



**Scheme 14.** Phase-transfer-catalyzed *N*-alkylation of axially chiral *o*-iodoanilide.

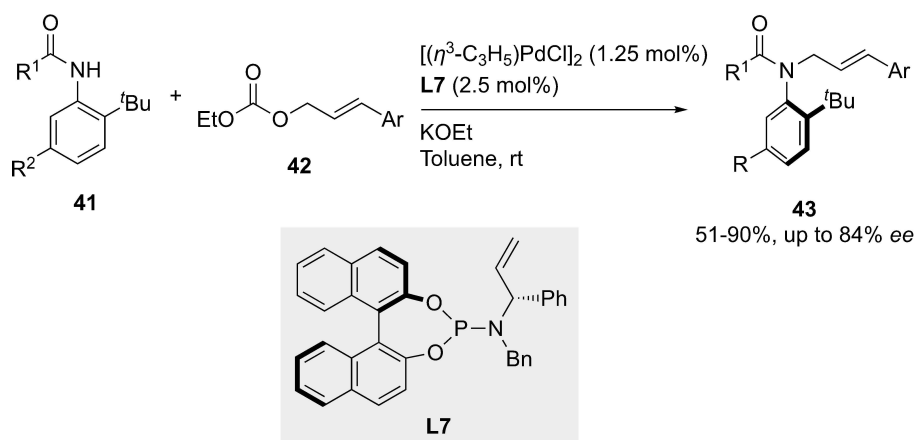
study of the crystal structure of the chiral ammonium/anilide anion complex.

In 2015, Feng and Du<sup>[39]</sup> studied the use of phosphoramidite-olefin **L7** as the ligand for the Pd-catalyzed asymmetric allylic alkylation of *ortho*-substituted anilides **41** with carbonate derivatives **42** to obtain axially chiral anilides **43** (Scheme 15). The choice of the base was found to have a strong impact on enantioselectivity, and KOEt was found to provide the best results. Importantly, the catalyst loading could be reduced to 1.25 mol% without affecting reactivity or enantioselectivity. A wide range of allyl carbonates were tolerated to give the corresponding axially chiral anilide product with moderate to good enantioselectivities and yields.

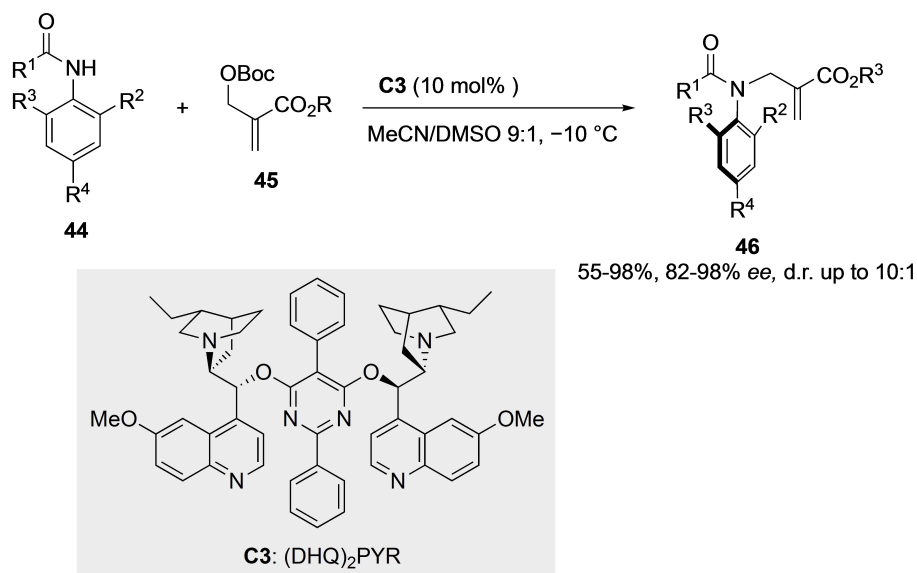
Few years later, Li and co-workers<sup>[40]</sup> reported an efficient Lewis base organocatalyzed allylic alkylation of similar anilides **44** to access axially chiral anilides **46**. Good yields and excellent enantioselectivities (up to 98% ee) were obtained using a biscinchona alkaloid catalyst **C3** in combination with Morita-Baylis-Hillman carbonates **45** (Scheme 16). A large influence of the solvents in reactivity and enantioselectivity was observed with MeCN giving the best results. The size of the substituents on the aromatic ring of the anilides also has a strong influence on selectivity. Thus, it was found that bulky groups, such as *t*Bu and I, in *ortho* position afforded the highest enantioselectivities. It should be mentioned that for aliphatic amides (R<sup>1</sup>=Et), the

chiral anilines were obtained with lower yield, probably due to the lower acidity of the NH group. It was also found that the configurational stability of products bearing electron-withdrawing groups in the aromatic benzoyl ring (R<sup>1</sup>) was higher than that with electron-donating groups. At all, most of the products showed high configurational stability at 25 °C in the solid state.

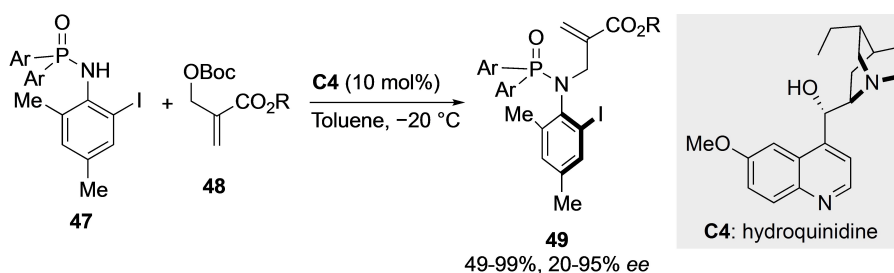
More recently, the same group described an efficient protocol for the construction of axially chiral phosphamides **49** via atroposelective allylic *N*-alkylation reaction of precursors **47** with Morita-Baylis-Hillman carbonates **48** using hydroquinidine **C4** as the catalyst.<sup>[41]</sup> *Ortho*-iodo-substituted anilide derivatives were selected as substrates considering the potential application of the resulting iodobenzene products as chiral hypervalent iodine catalysts (Scheme 17). It was found that the sterically hindered diphenyl phosphoryl group was beneficial for stability and stereoselectivity control. Phosphamides bearing different substitution patterns in combination with a wide range of carbonates resulted in a broad range of products, obtained in moderate to excellent yields and excellent enantioselectivities. As above, more crowded substrates gave better enantioselectivities. For example, the change of iodine to smaller halides, such as Br or Cl, led to lower enantiomeric excesses. The method also allows for the synthesis of compounds with both C–N axial chirality and P-stereogenic chirality.



**Scheme 15.** Pd-Catalyzed asymmetric allylic alkylation of *ortho*-anilides.



Scheme 16. Lewis base organocatalyzed allylic alkylation of anilides

Scheme 17. Atroposelective *N*-allylic alkylation of phosphamides.

### 2.3. Atroposelective construction of the aromatic ring

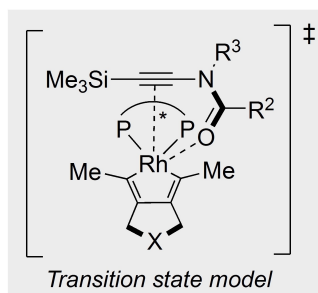
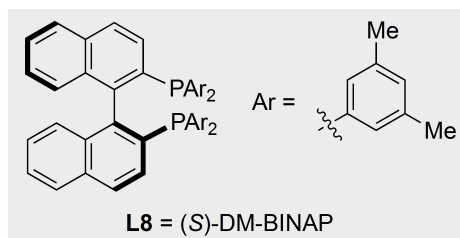
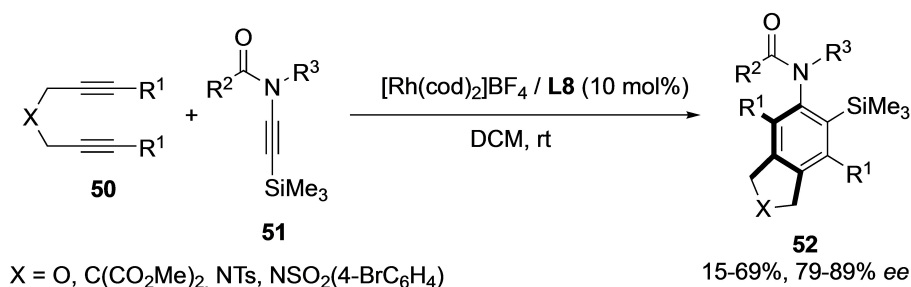
A different strategy for the atroposelective synthesis of axially chiral anilides was developed by Tanaka and co-workers.<sup>[42]</sup> In this case, a rhodium-catalyzed enantioselective intermolecular [2+2+2] cycloaddition of 1,6-diynes **50** with trimethylsilylamides **51** (Scheme 18) was accomplished under mild conditions to afford enantioenriched products **52** in high enantioselectivity although in low-to-moderate yield. The enantioselectivity was determined by the preferential coordination of the carbonyl group of **51** to a rhodacyclopentadiene intermediate and by the steric interactions between substituent  $R^3$  and the  $PAR_2$  group of the (*S*)-DM-BINAP ligand **L8**.

### 2.4. Atroposelective C–H activation/functionalization

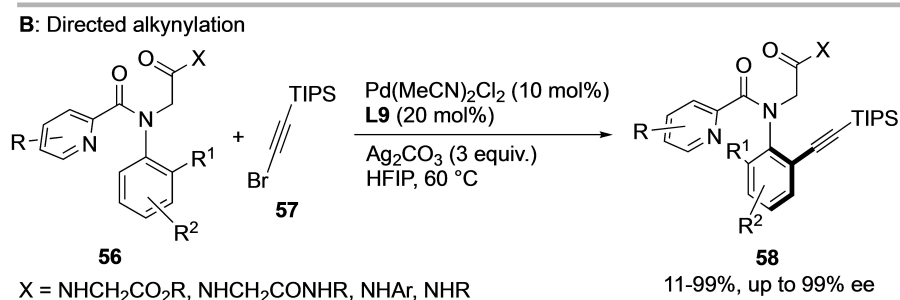
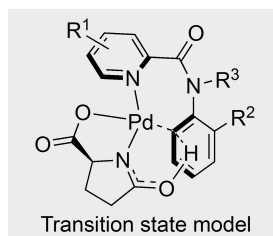
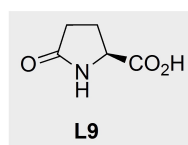
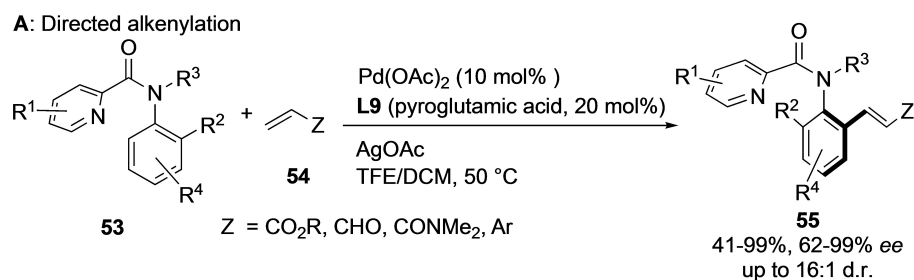
Axially chiral anilides **55** have also been prepared by Shi and co-workers<sup>[43]</sup> using a Pd<sup>II</sup>-catalyzed C–H olefination of racemic *N*-aryl picolinamides **53** (Scheme 19A). Using L-pyroglutamate **L9** as a chiral ligand, the reaction with alkenes **54** proceeds via dynamic kinetic resolution to afford the coupling products in

excellent yields and enantioselectivities. Both electron-donating and electron-withdrawn groups on the pyridine ring ( $R^1$ ) are tolerated, but the size of the *ortho*-substituents on the aryl ring ( $R^2$ ) plays an important role in the enantiocontrol, with the smallest groups such as methoxy leading to racemic products. Additionally, a variety of *Z* substituents were well tolerated. Finally, a broad range of electronically different olefins proved to be suitable reaction partners. As a particular case, simple aliphatic alkenes provide formal C–H allylation products (after double bond migration) in moderate yields and high ee's. Mechanistically, the concerted metalation-deprotonation event was determined to be the enantiodetermining step. Further analysis revealed that a distortion provoked by the amino acid ligand is responsible for the chiral induction during the C–H bond activation event.

Later, the same group developed a related strategy for the Pd-catalyzed alkynylation of peptoid derivatives **56** with bromoalkyne **57** (Scheme 19B). Using the same Pd precatalyst and ligand **L9**, the C–H alkynylation proceeds efficiently in the presence of  $Ag_2CO_3$  to afford a wide variety of axially chiral *N*-aryl peptoids **58** in good yields and with excellent enantioselectivities.<sup>[44]</sup>

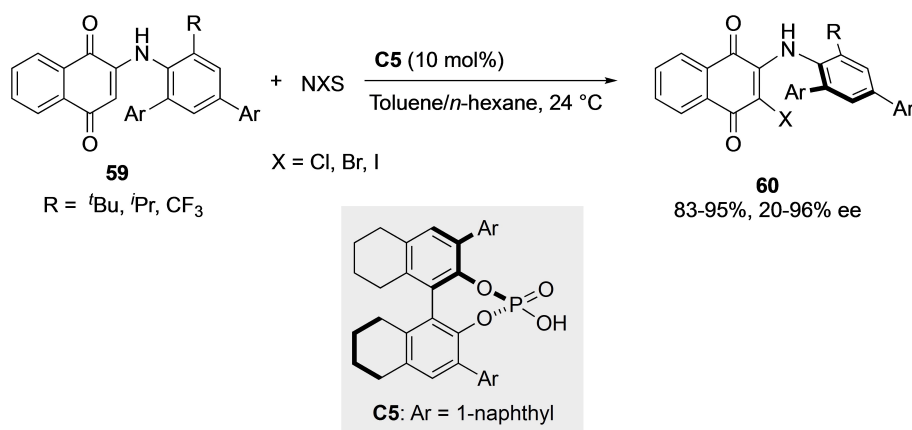


Scheme 18. Rhodium-catalyzed enantioselective intermolecular [2 + 2 + 2] cycloaddition.

Scheme 19. Atroposelective Pd<sup>II</sup>-catalyzed C–H functionalization of *N*-aryl picolinamides via DKR.

Very recently, Gustafson and co-workers<sup>[45]</sup> reported an elegant approach for the synthesis of a family of *N*-aryl quinoids **60**, which exist as configurationally stable atropisomers. The strategy exploits the presence of a strong intramolecular

N–H...O hydrogen bond that locks the 'exo' conformation in the parent quinoids **59** (Scheme 20). Direct C–H halogenation using phosphoric acid catalyst **C5** provides configurational stability to the C(aryl)–N axis of the products, which were



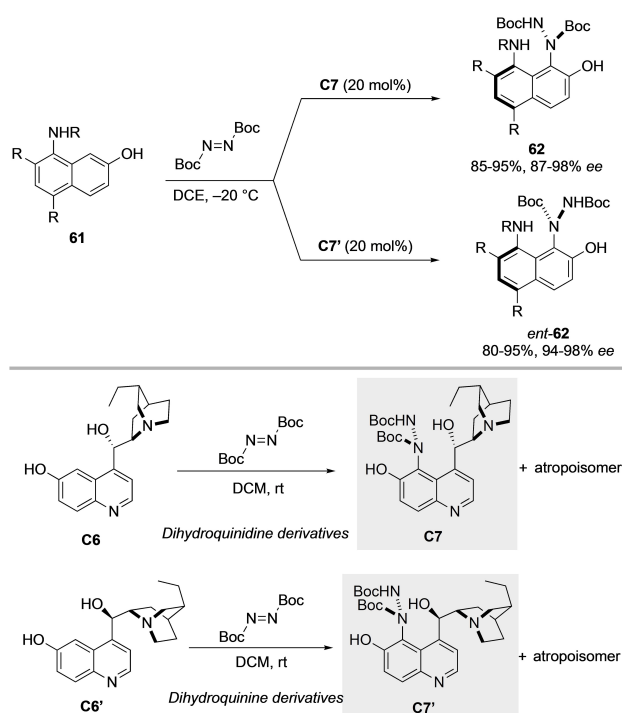
Scheme 20. Synthesis of *N*-aryl quinoids by CPA-catalyzed direct C–H halogenation.

obtained in excellent yields and enantioselectivities when a bulky  $\text{R}^1$  group (such as *tert*-butyl) is installed in the *ortho* position. The reaction worked well for a variety of aryl substitutions, although a poorer enantiocontrol was observed when the aryl groups in the aniline moiety are replaced by methyl groups, suggesting that an interaction between the *ortho*-aryl group and the catalyst is key for the enantioselectivity. Additional studies revealed that the products were configurationally stable under thermal and acidic conditions.

## 2.5 Atroposelective direct formation of the stereogenic C–N bond

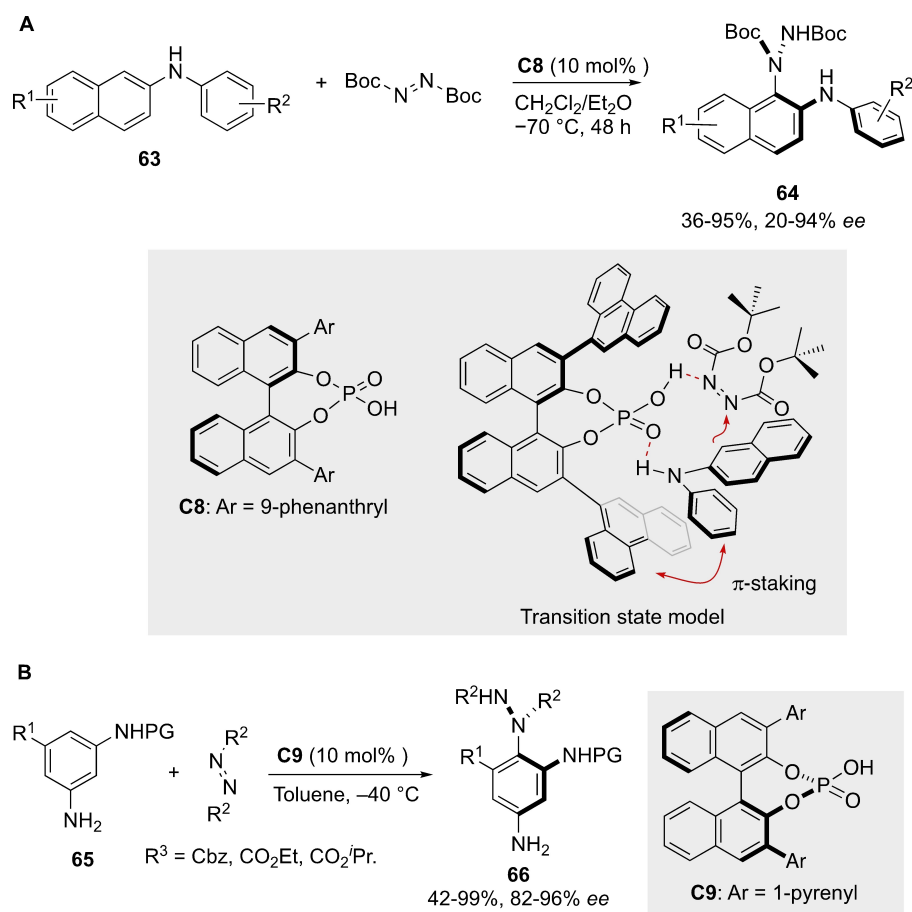
The group of Jørgensen also reported a highly regio- and enantioselective synthesis of unprecedented C–N atropisomers **62** through a cinchona-alkaloid organocatalyzed asymmetric Friedel-Crafts amination of 2-naphtols **61** with azodicarboxylates (Scheme 21).<sup>[46]</sup> After screening a large number of catalysts, the quinidine and quinine derivatives **C6** and **C6'** were initially identified as promising candidates, reaching *ee*'s up to 88%. Remarkably, selective amination took place selectively on substrate **61**, although the cinchona-alkaloid catalyst **C6** is also susceptible to amination under the reaction conditions. In fact, these catalysts also react under forcing conditions to afford derivatives **C7** and **C7'**, thus generating atropisomerism in cinchona alkaloids. Interestingly, these pseudo-enantiomeric derivatives proved to be better catalysts, efficiently affording 1,8-diamino-2-naphthol derivatives in excellent yields and enantioselectivities. The X-ray structure of **C7** showed a hydrogen bond between the quinuclidine nitrogen and the hydrogen atom bound to hydrazine, which blocks the basic site of this alkaloid.

In 2019, Zhang's group reported a related approach for the atroposelective synthesis of axially chiral arylhydrazine derivatives **64** by intermolecular enantioselective C–H amination of *N*-aryl-2-naphthylamides **63** with azodicarboxylates using a chiral phosphoric acid (CPA) catalyst **C8** (Scheme 22A).<sup>[47]</sup> The control of selectivity is provided by a  $\pi$ - $\pi$  stacking interaction between



Scheme 21. Organocatalyzed synthesis of naphthamides by the group of Jørgensen.

the *N*-phenyl substituent of the substrate and the phenanthryl group of the catalyst, in combination with a dual H-bonding interaction. The reaction failed for *N,N*-disubstituted naphthylamines, demonstrating the key role of the N–H bond on reactivity. On the other hand, the introduction of protecting groups such as benzyl or *tert*-butyl on nitrogen led to low enantioselectivities, indicating the importance of the synergistic control by  $\pi$ - $\pi$  and dual H-bonding interactions. The enantioselectivity of the reaction was also sensitive to the size of the azodicarboxylate reagent, with di-*tert*-butyl azodicarboxylate giving the best results. This methodology was later extended by Yang and co-workers<sup>[48]</sup> to the synthesis of related hydrazines **66**. In this case, a very similar chiral phosphoric acid catalyst **C9**



**Scheme 22.** Atroposelective CPA-catalyzed C–H amination of N-aryl-2-naphthylamides and anilides.

was used in the enantioselective amination of 1,3-benzenediamines **65** with azodicarboxylate derivatives (Scheme 22B). A wide variety of substrates with different acyl, aryl, sulfonyl and alkoxycarbonyl protecting groups in the secondary amine were well tolerated. However, the enantioselectivity drops when benzoyl groups are incorporated at this position. Importantly, the use of different azodicarboxylates as the aminating reagents afforded the corresponding product in excellent yields and enantioselectivities. The obtained axially chiral anilides **66** presented the highest configurational stabilities reported to date.

### 3. N-Aryl Five-Membered Heterocycles

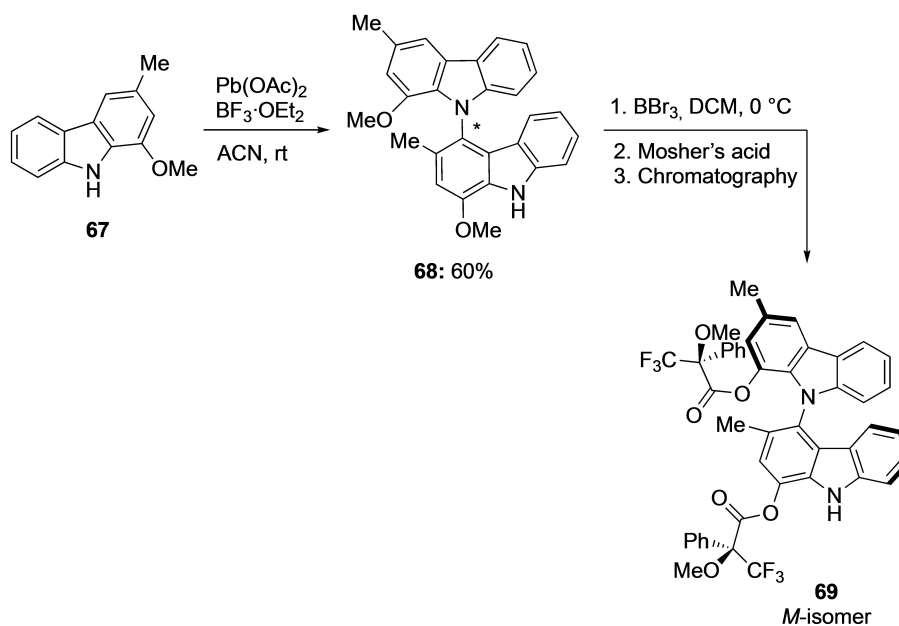
#### 3.1. Pyrrole, indole/indoline, and carbazole derivatives

The enantioselective synthesis of *N*-aryl pyrrole, indole/indoline, and carbazole atropisomers has received increasing attention in recent years, for potential applications as chiral ligands and intermediates in natural product synthesis. In these systems, the rotation about the C–N axis becomes easier than in biaryl compounds because of the relatively larger CNC angles associated with a five-membered heterocyclic ring.

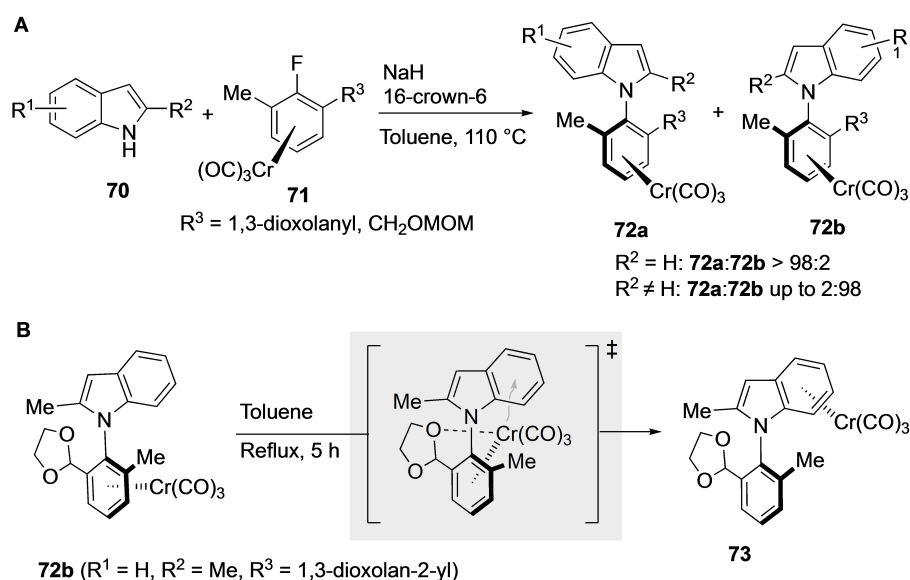
#### 3.1.1. Early examples

In 2001, Bringmann et al.<sup>[49]</sup> reported the first total synthesis of the natural product Murrastifoline-F **68** through an oxidative C–N homocoupling of carbazole precursor **67** with Pb(OAc)<sub>2</sub>. Due to the restricted rotation around the C–N bond, the two enantiomers of the coupling product were observed through liquid chromatography-circular dichroism (LC-CD). After cleavage of the methoxy groups and further derivatization with Mosher's acid, the resulting diastereomers **69** were separated by preparative thin-layer chromatography, allowing the determination of their absolute configurations with the *M*-isomer being the major product (Scheme 23). Comparison with the Murrastifoline-F natural product isolated from the root extract of the curry leaf plant *Murraya koenigii* (Rutaceae), allowed to determine the presence of a 56:44 mixture in favor of the *M*-enantiomer in the natural source mixture.

Few years later, Uemura and co-workers reported the stereoselective synthesis of axially chiral *N*-aryl indoles **72** through a nucleophilic substitution reaction of haloarene chromium complexes **71**, featuring planar chirality, with indoles **70** (Scheme 24, A).<sup>[50]</sup> The stereochemistry of the C–N axis was determined by the position of the substituent R<sup>1</sup>. When the indole ring was unsubstituted or 3-methyl substituted, the



Scheme 23. Total synthesis of Murrastifoline-F.

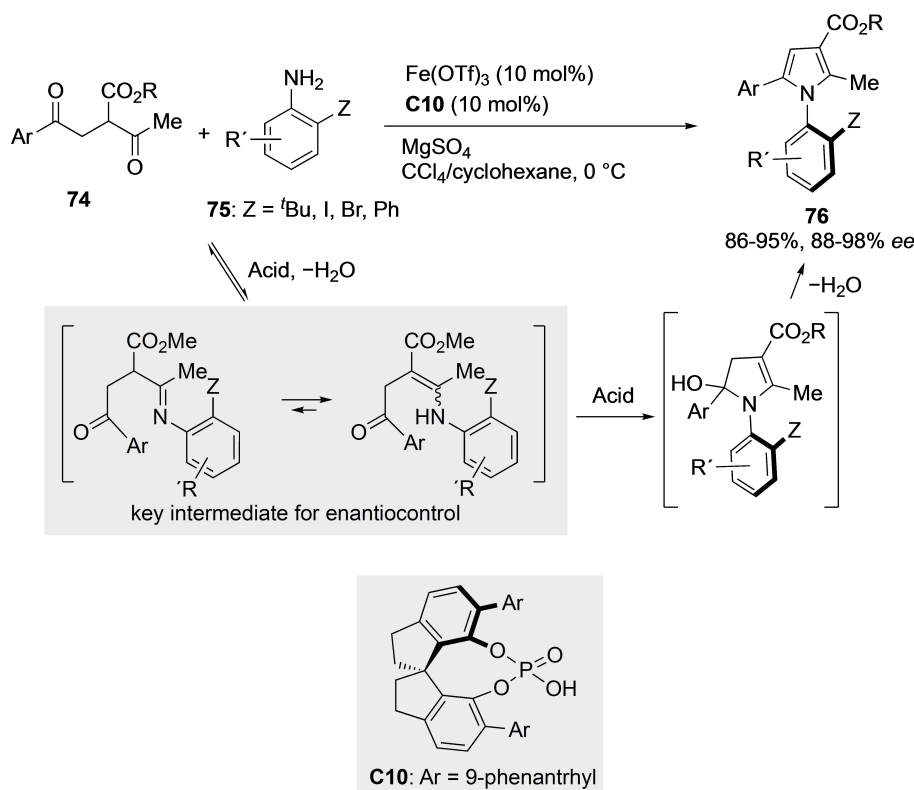
Scheme 24. Stereoselective synthesis of axially chiral *N*-aryl indoles.

resulting chromium moiety was oriented *anti* with respect to the indole aryl ring, whereas when it was 2-methyl substituted, the benzene ring of the indole was oriented *syn* toward the chromium tricarbonyl group, even for sterically hindered indole compounds. It was also found that in product **72b** containing a 1,3-dioxolanyl group, the chromium tricarbonyl group migrated from the *N*-aryl to the indole arene ring to yield complex **73** after heating in toluene (Scheme 24, B). When the 1,3-dioxolane group was changed to a methyl group, migration did not occur. X-Ray analysis revealed that the 1,3-dioxolane was oriented toward the chromium tricarbonyl group in the migrated product, suggesting that the former might play a role in

assisting the transfer of the tricarbonyl chromium group by coordination.

### 3.1.2. Atroposelective cyclization

In 2017, Tan and co-workers described the first catalytic asymmetric Paal-Knorr reaction between functionalized 1,4-diketones **74** and anilines **75** to obtain axially chiral *N*-arylpyrroles **76**. High enantiomeric excesses were observed by using again BINOL-derived phosphoric acid **C10** as the catalyst (Scheme 25).<sup>[51]</sup> Based on previous knowledge on the Paal-Knorr



**Scheme 25.** Catalytic asymmetric Paal-Knorr reaction for the synthesis of axially chiral *N*-arylpyrroles.

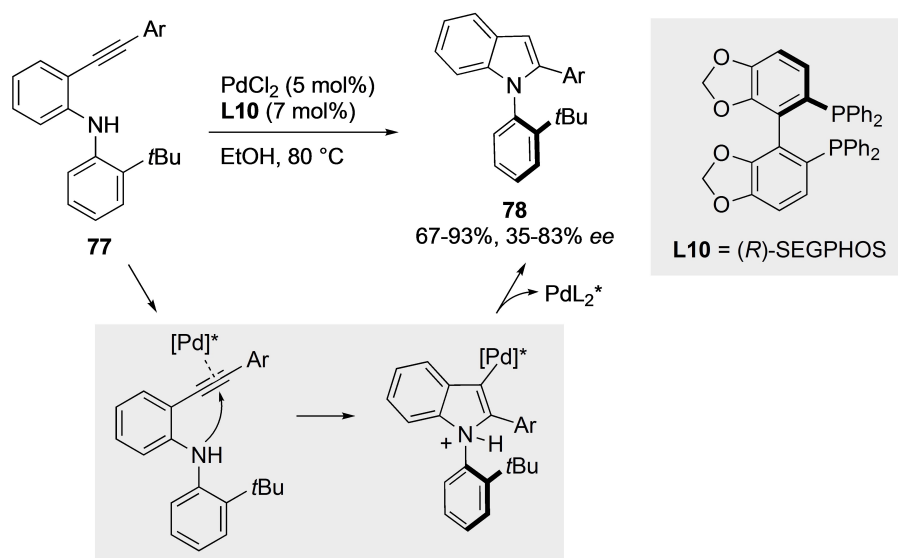
reaction mechanism, the authors envisaged the ability of the chiral phosphoric acid to assist in the intramolecular nucleophilic addition step. It was also found that the reaction could be further speeded up by adding Fe(OTf)<sub>3</sub> as a Lewis acid cocatalyst. Remarkably, the *ortho* Z group in anilines **75** was not restricted to *tert*-butyl: iodine, bromo, and phenyl groups could also be employed, giving the expected products in good to excellent enantiomeric excesses. Mechanistically, the formation of an enamine key intermediate was proposed to control the stereoselection. Finally, the authors also observed an unexpected solvent-dependent inversion of the enantioselectivity.

Kitagawa et al. reported in 2010<sup>[52a]</sup> and further expanded in 2016<sup>[52b]</sup> a Pd-catalyzed 5-*endo*-hydroaminocyclization of *ortho*-alkynylanilines **77** for the synthesis of axially chiral indoles **78**, obtained in moderate to good enantioselectivities by using (*R*)-SEGPHOS **L10** as the chiral ligand (Scheme 26). This transformation represents the first transition metal-catalyzed asymmetric synthesis of such a structural motif. The reaction works well for aromatic alkynes but was sluggish for highly deactivated (R=2-NO<sub>2</sub>C<sub>6</sub>H<sub>4</sub>) and aliphatic derivatives (R=*n*-C<sub>4</sub>H<sub>9</sub>). In these cases, the addition of AgOTf was necessary to increase the reactivity by generating more active cationic palladium species. It was also found that the presence of an *ortho*-substituent in the aromatic alkyne was important to improve the enantioselectivity (60% *ee* for R=Ph, 80–83% *ee* for *ortho*-substituted substrates). The authors attributed this observation to the dynamic axial chirality generated around the C-(alkynyl)–C(phenyl) bond. Because chirality transfer occurs

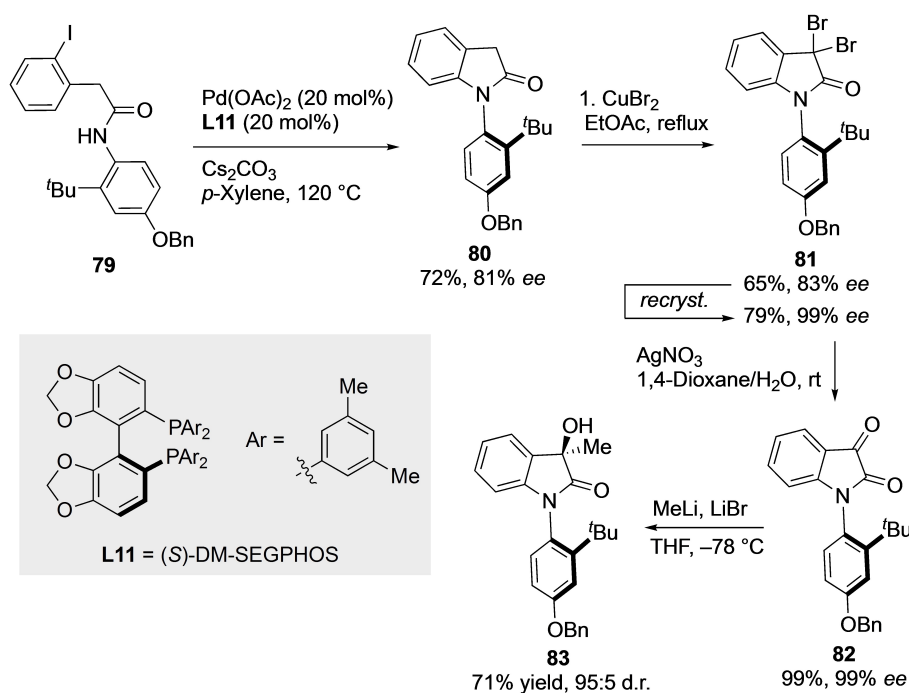
during the N–C bond formation step, substrates with a bulky *ortho*-substituent transferred more effectively the chiral information from the ligand through the C(alkynyl)–C(phenyl) bond.

In 2015, Nakazaki and co-workers developed a methodology to access *N*-arylisatins with C–N axial chirality by means of an enantioselective intramolecular *N*-arylation reaction (Scheme 27).<sup>[53]</sup> Cyclization of amide **79** using Pd(OAc)<sub>2</sub>/*S*-DM-SEGPHOS **L11** as the catalyst afforded *N*-aryloxindole **80** in 81% *ee*. This product was transformed into dibrominated derivative **81**, which was enantioenriched to >99% *ee* by recrystallization and subsequently transformed into *N*-arylisatin **82** under mild conditions without erosion of the enantiomeric purity. Finally, this material was subjected to a diastereoselective 1,2-addition of MeLi, which took place from the less hindered face of the isatin, the one opposite to the *tert*-butyl group, to afford the 3,3-disubstituted oxindole scaffold **83**, in good yield and high diastereoselectivity.

The group of Lin described the first three-component cascade heteroannulation reaction of 2,3-diketoesters **84**, *ortho*-substituted aryl anilines **85** and 1,3-cyclohexanediones **86** using a chiral spirocyclic phosphoric acid organocatalyst **C11** (Scheme 28).<sup>[54]</sup> Under optimal conditions, substituents with different electronic properties in the aromatic ring of the 2,3-diketoester were tolerated, giving axially chiral *N*-arylindoles **87** in excellent yields and enantioselectivities. The reaction also tolerates structural modifications in anilines (R<sup>2</sup>) and 1,3-cyclohexanediones (R<sup>3</sup>), thus expanding the scope of the method.



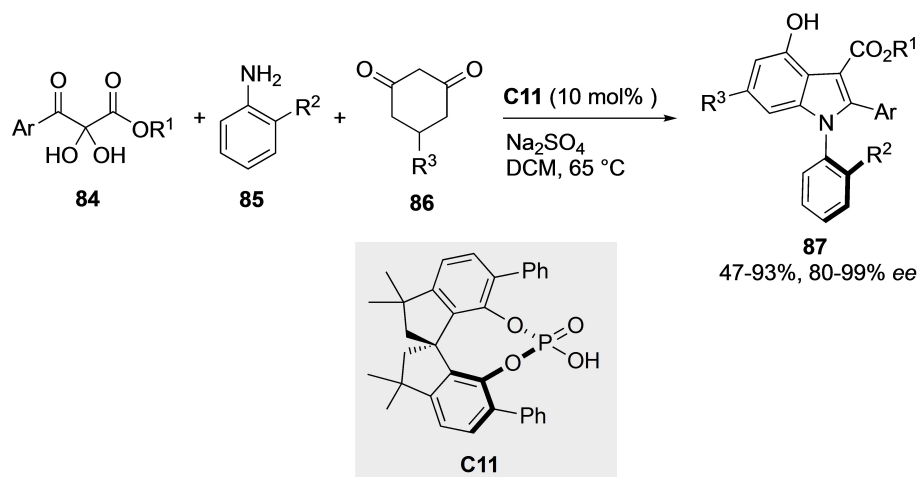
Scheme 26. Pd-Catalyzed enantioselective synthesis of axially chiral indoles.

Scheme 27. Palladium-catalyzed intramolecular *N*-arylation for the synthesis of enantioenriched *N*-aryloxindoles.

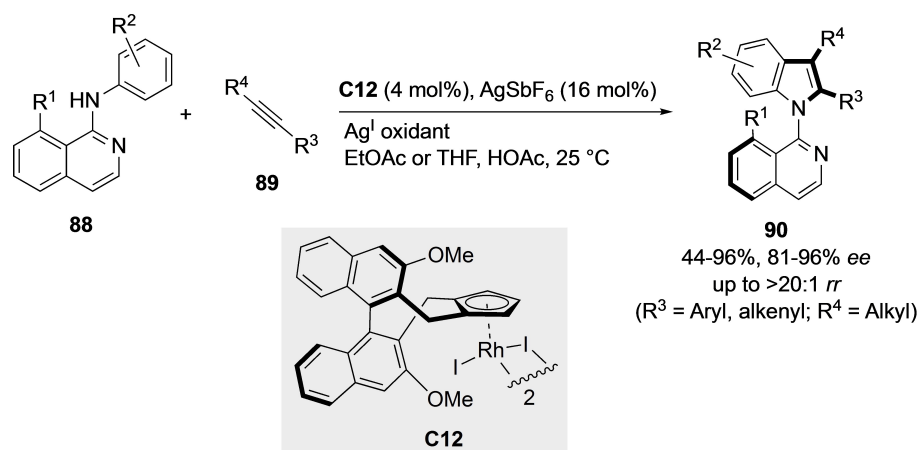
Very recently, Wang, Lan, Li and coworkers also reported an interesting approach to axially chiral *N*-isoquinolyl indole derivatives **90**.<sup>[55]</sup> Using the isoquinoline N atom as a directing group, a Rh<sup>III</sup>-catalyzed C–H activation of anilines **88** was used for an oxidative [3 + 2] annulation with alkynes **89** (Scheme 29). Using Cramer's Cp<sup>OMe</sup>Rh<sup>III</sup>/AgSbF<sub>6</sub> catalyst **C12** and Ag(I) salts as the oxidant, the reaction proceeds under mild conditions with high enantioselectivity and high functional group tolerance. Interestingly, good to excellent regioselectivities were observed

for alkyl-aryl alkynes and substituted 1,3-enynes when AgOPiv or MeSO<sub>3</sub>Ag were used as the oxidants, respectively.

Finally, Yan and co-workers have recently reported on the synthesis of complex azepine derivatives featuring a C–N stereogenic axis incorporated into a bridged heterobiaryl skeleton.<sup>[56]</sup> Starting from alkynyl naphthol substrates **91** bearing a carbazole moiety, reaction with *N*-bromosuccinimide (NBS) in the presence of squaramide organocatalyst **C13** afforded the products **92** in good yields and with excellent enantio- and diastereoselectivities (Scheme 30). The bifunc-



**Scheme 28.** Organocatalyzed heteroannulation reaction for the synthesis of N-arylindole esters.



**Scheme 29.** Rhodium(III)-catalyzed C–H activation of anilines for the synthesis of axially chiral N-isoquinolyl indole derivatives.

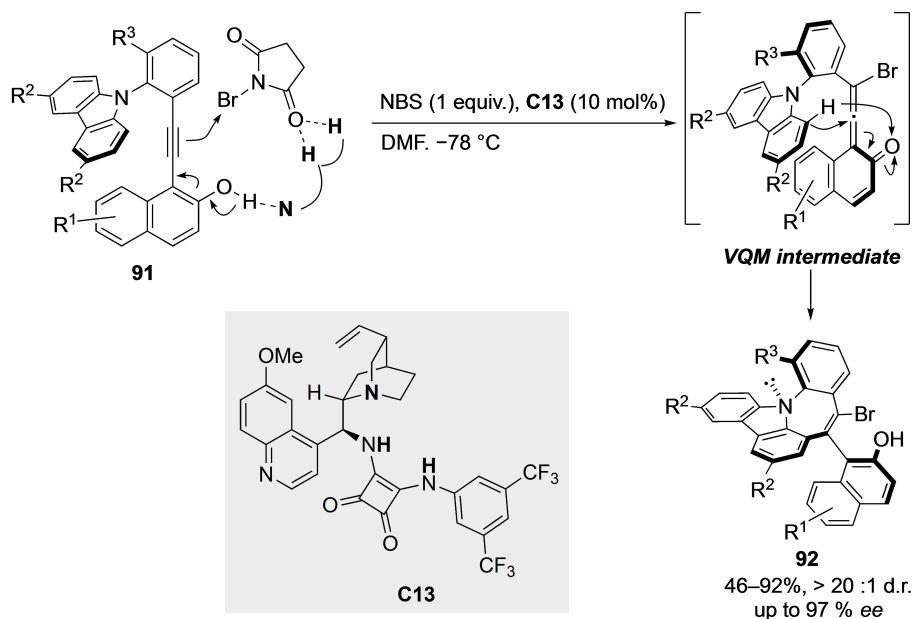
tional activation by the catalyst facilitates a highly stereocontrolled electrophilic bromination to generate reactive bromo-functionalized tetrasubstituted chiral vinylidene *ortho*-quinone methide (VQM) intermediates. Subsequently, intramolecular electrophilic aromatic substitution at the C1 position of the carbazole moiety affords the final products, which exhibited interesting optical properties and  $\text{Ru}^{3+}$ -induced fluorescence responses that suggest potential applications in optoelectronic materials and heavy metal ion detection.

### 3.1.3. Atroposelective C–H activation/functionalization

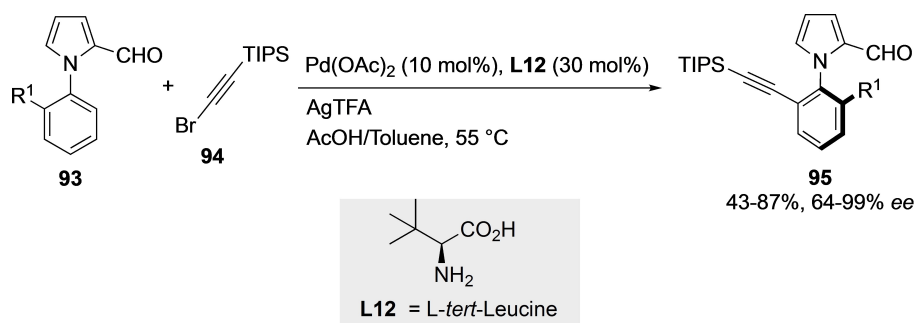
In 2019, Shi and co-workers described a palladium-catalyzed C–H alkylation of aryl pyrroles **93** with bromoalkynes **94** for the synthesis of pyrrole derivatives **95** displaying axial chirality (Scheme 31).<sup>[57]</sup> This elegant approach, inspired by the seminal work by the group of Yu<sup>[58]</sup> and applied previously to the resolution of biaryls,<sup>[59]</sup> is based on the transient directing group formed by condensation of the formyl group of **93** with L-*tert*-

leucine **L12**, thus enabling a regio- and atroposelective C–H activation to afford the alkynylated products in excellent yields and enantioselectivities up to >99% ee. These products exhibit high configurational stability, as no erosion of ee values was observed, even after heating at 120 °C. Nevertheless, sterically bulky substituents in the *ortho* position to the axis are needed to maintain the configurational stability and to ensure good enantioselectivities.

Xie, Zhang and co-workers developed later a similar Pd<sup>II</sup>-catalyzed atroposelective C–H olefination of N-aryl indoles **96** with electron-poor alkenes **97** (Scheme 32A).<sup>[60]</sup> The authors reported on three different situations depending on the substitution pattern of the starting material: For atroposelective C–H olefination/desymmetrization reactions [Z = H, R<sup>2</sup>(*meta*) = R<sup>2</sup>(*meta*)], a wide variety of alkenylated products **98a** could be prepared in good yields and high enantioselectivities using Pd(OAc)<sub>2</sub> as the precatalyst, L-valine **L13** as the ligand and benzoquinone (BQ) as an external oxidant. Similar results were also obtained in the catalytic C–H olefination/dynamic kinetic resolution of configurationally labile N-aryl indoles. Finally, for



Scheme 30. Organocatalytic construction of complex azepines featuring C–N axial chirality.



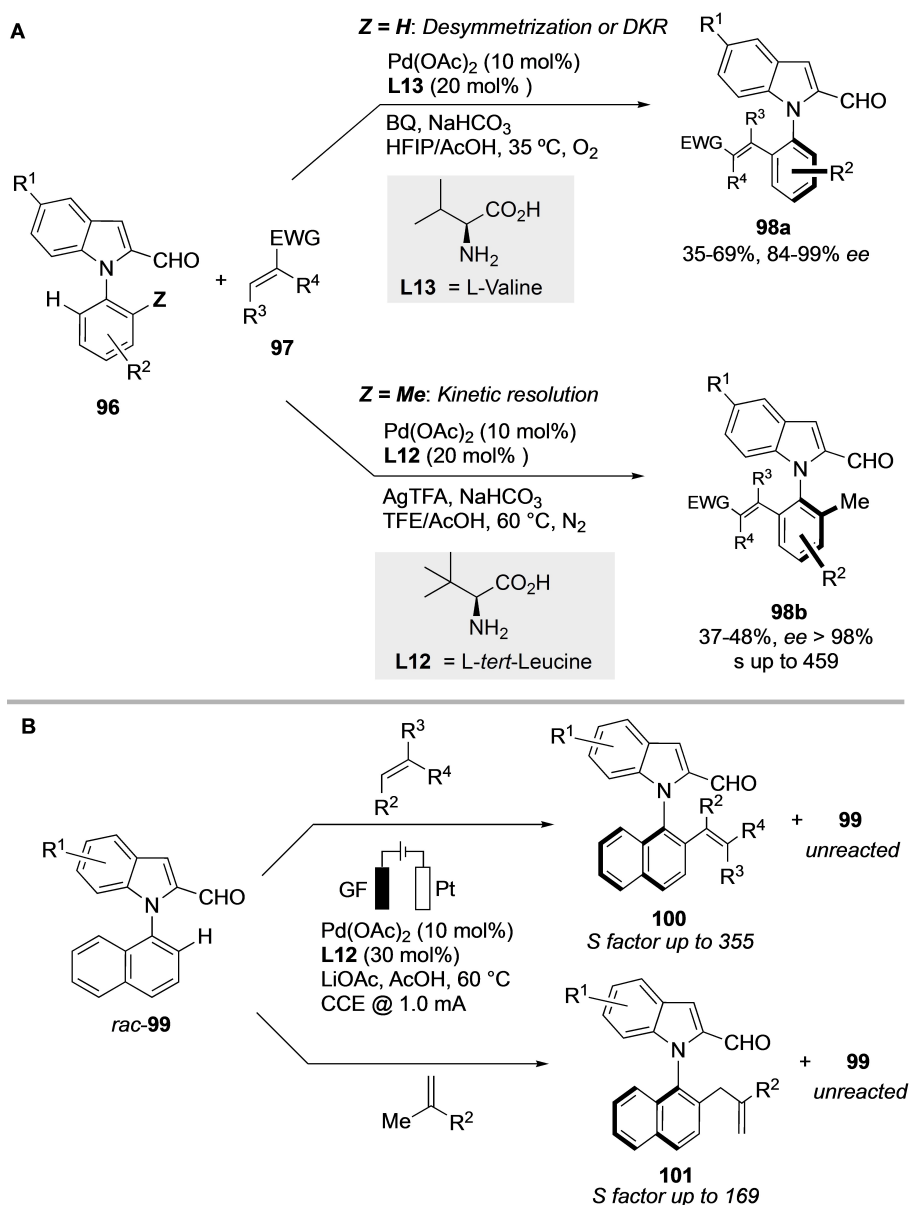
Scheme 31. Palladium-catalyzed atroposelective C–H alkylation.

racemic, configurationally stable substrates with more sterically demanding substituents, a catalytic C–H alkenylation via kinetic resolution was developed. In this last case, the alkenylated *N*-aryl indoles **98b** were obtained with excellent selectivity factors of up to 459 by using *tert*-leucine **L12** as the ligand and AgTFA as the oxidant. All synthesized products present high configurational stability at rt. Very recently, Ackermann and co-workers recently reported developed a similar kinetic resolution of *N*-naphthyl indole carbaldehydes **99** into alkenylated products **100**, but an electrocatalytic approach was used to avoid the need of an external oxidant (Scheme 32B).<sup>[61]</sup> Excellent selectivity factors of up to  $S=355$  were achieved in the reaction with a variety of electron-poor olefins, including, acrylates, vinyl phosphonates, vinyl sulfones, maleimides and fluorinated alkenes. Interestingly, an unprecedented allylic selectivity was observed with 1,1-disubstituted alkenes, and the atroposelective allylation could also be performed to obtain products **101** with excellent selectivity factors of up to  $S=169$ .

Subsequently, Wang et al. presented an alternative method to construct C–N axial chirality through a Rh<sup>III</sup>-catalyzed Satoh-

Miura-type reaction of *N*-aryloxindoles **102** and alkynes **103**. Using catalyst **C14** with a spirocyclic cyclopentadienyl ligand, chiral *N*-aryloxindoles **104** were obtained with high yields and enantioselectivities (Scheme 33).<sup>[62]</sup> This dual C–H activation reaction tolerates both electron withdrawing and electron donating groups in the *N*-phenyl ring and in the diaryl alkynes. Mechanistic studies revealed that the C–H activation step proceeds by a carboxylate-assisted concerted metalation-deprotonation mechanism affording a six-membered rhodacyclic intermediate in which the bulky isobutyrate additive helps to better differentiate the two enantiotopic C–H bonds.

Very recently, Kwon and co-workers<sup>[63]</sup> reported a Pictet-Spengler reaction of *N*-aryl indoles **105** with paraformaldehyde for the atroposelective synthesis of *N*-aryl-tetrahydro- $\beta$ -carboline **107** ( $R_4=H$ , Scheme 34). Previous studies on acid-catalyzed atroposelective C-2 functionalization of unprotected indoles indicated the need for a bifunctional activation that includes acidic activation of the electrophile and interaction between the phosphate counterion and the indole N–H. The absence of a N–H group in these substrates, however, was addressed by

Scheme 32. Atroposelective C–H olefination of *N*-aryl indoles.

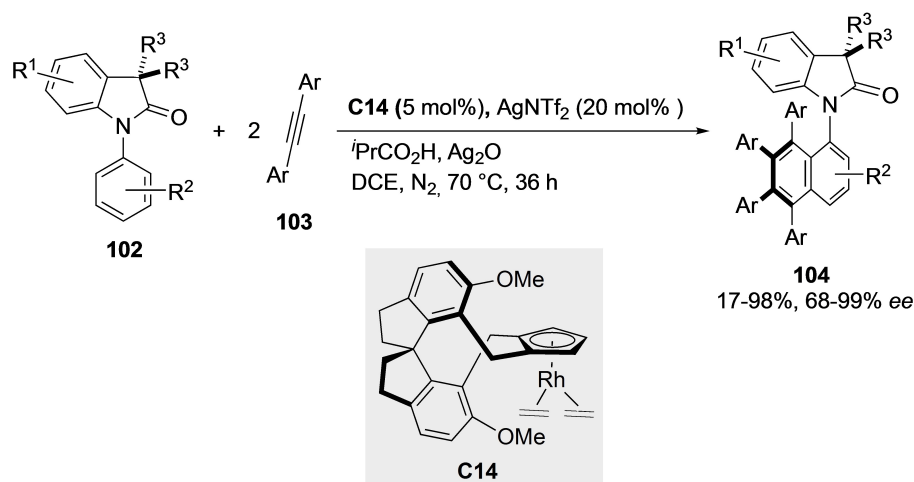
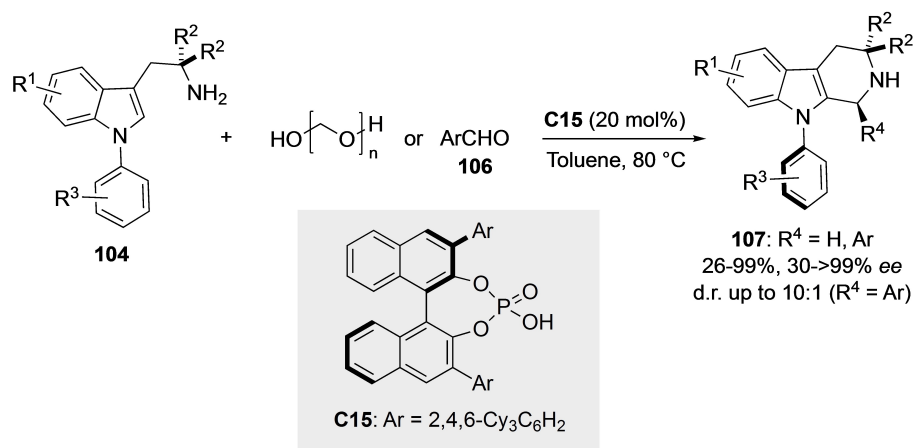
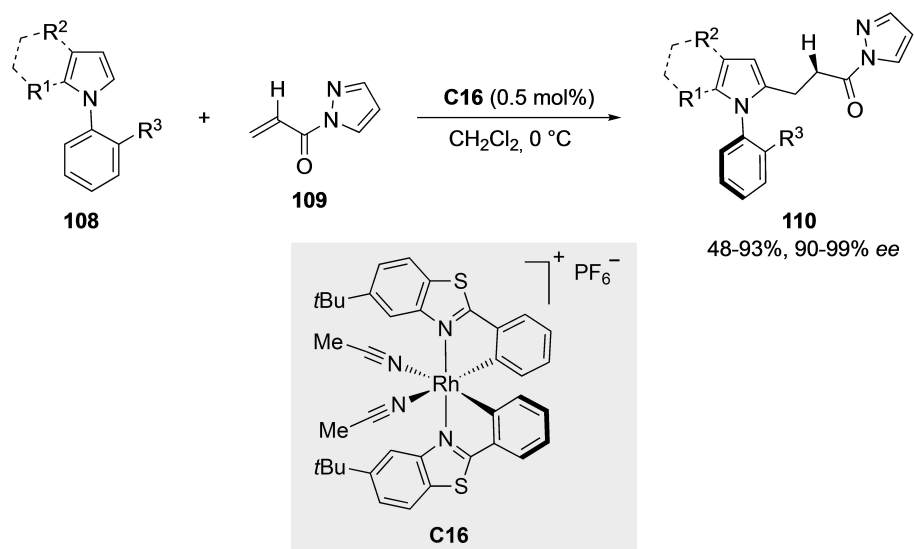
introducing an *ortho*-amino hydrogen bond donor ( $\text{R}^3$ ) into the bottom aromatic ring. Thus, the use of chiral phosphoric acid **C15** afforded excellent yields and enantioselectivities with a variety of substrates that contain electron-donating or electron-withdrawing groups. In addition to paraformaldehyde, the reaction also works with different activated benzaldehydes **106**, which additionally allows to control both central and axial chirality elements (4:1 to 10:1 d.r., > 99% ee).

Very recently, Meggers and co-workers described an atroposelective alkylation of *N*-arylpyrroles **108** achieved by nucleophilic addition to *N*-acryloyl-1H-pyrazoles **109** using a chiral-at-rhodium Lewis acid catalyst **C16** possessing a unique helical (chiral-at-rhodium) chirality (Scheme 35).<sup>[64]</sup> Different substitution patterns were tolerated in the coupling partners affording structurally diverse axially chiral *N*-arylpyrroles **110** in

high yields and excellent atroposelectivities (up to > 99% ee). *N*-arylpyrroles with different  $\text{R}^3$  groups on the phenyl ring could be used with excellent results. Thus, halogen-containing substrates and those with free hydroxy, amino, or strong deactivating nitro groups were tolerated. The thermal configurational stability was analyzed in products with the smaller  $\text{R}^3$  substituents. Even in these cases, no erosion of the enantiomeric excess was observed after heating at 80 °C for 18 h.

### 3.1.4. Atroposelective construction of the C–N stereogenic axis

Direct N–C coupling in hindered systems usually requires harsh reaction conditions that compromise the configurational stability of the C–N axis. Looking for a synthetic solution to this

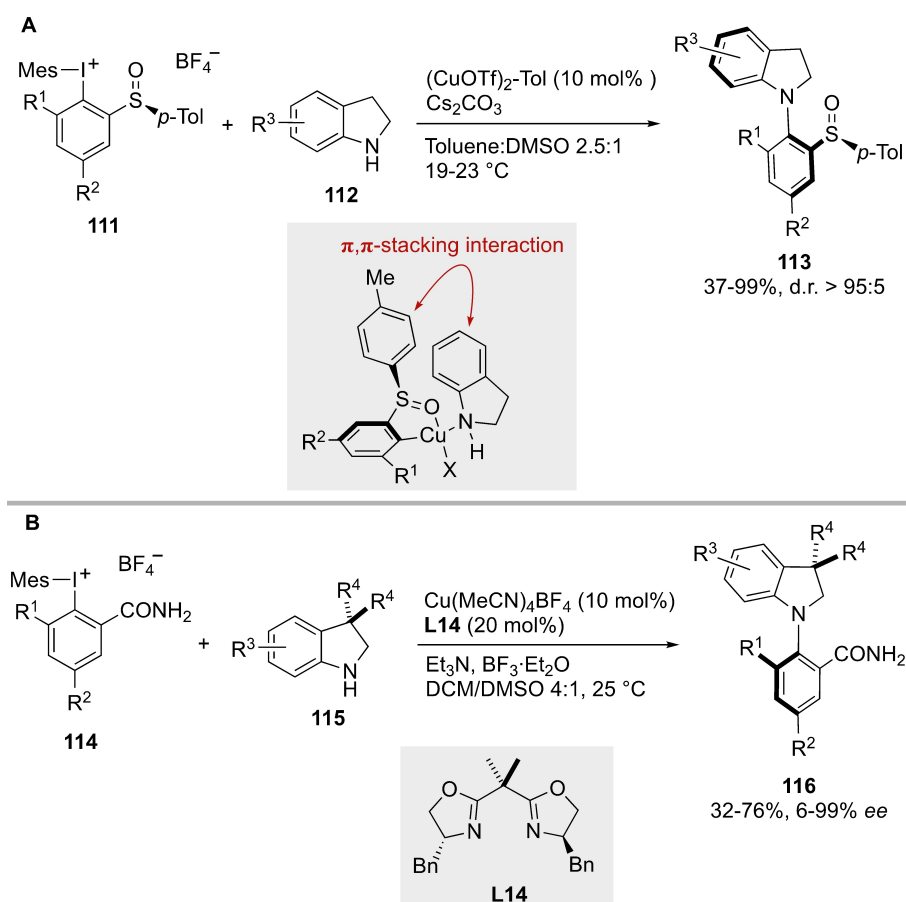
Scheme 33. Satoh-Miura-type reaction of *N*-aryloxindoles and alkynes.Scheme 34. Atroposelective synthesis of *N*-aryl-tetrahydro-β-carbolines.

Scheme 35. Atroposelective alkylation using a chiral at-rhodium catalyst.

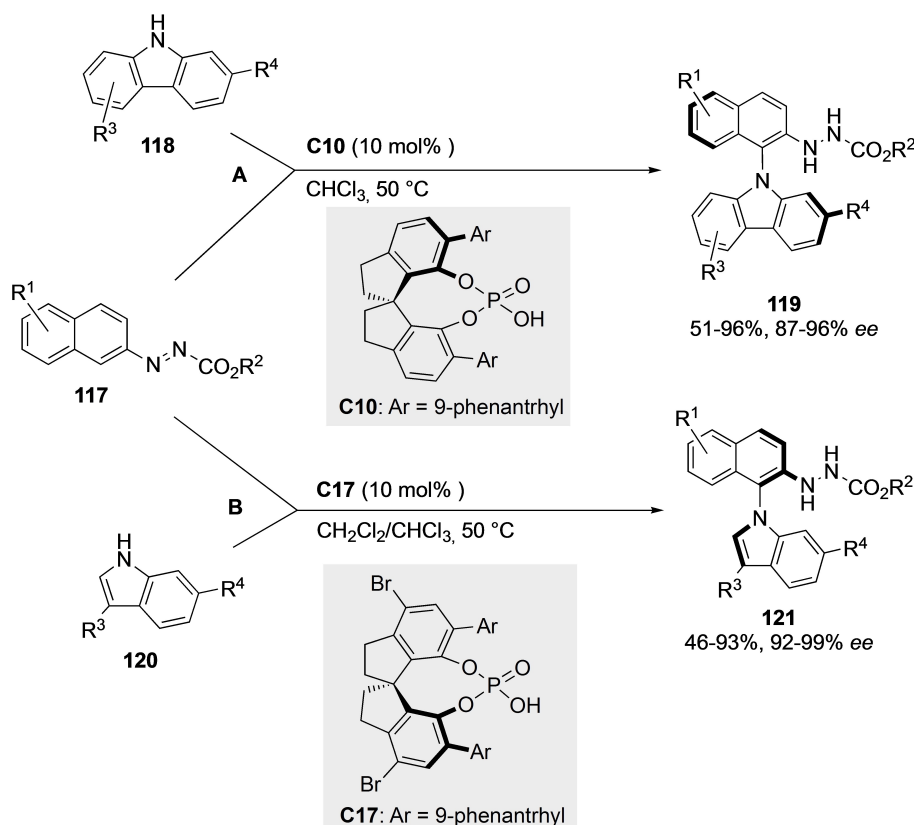
problem, the group of Colobert, Wencel-Delord and co-workers introduced in 2018 the use of hypervalent iodine reagents as highly electrophilic coupling partners for the distereoselective synthesis of axially chiral *N*-arylated indolines **113** via Cu-catalyzed Ullmann coupling (Scheme 36A).<sup>[65]</sup> Taking advantage of the high reactivity of sterically encumbered chiral iodanes **111**, the reaction with indolines **112** could be performed at low temperature furnishing these axially chiral C–N motifs in a highly atroposelective manner. A traceless sulfoxide auxiliary placed in the *ortho*-position of the iodine substituent was chosen to control the stereochemical course of the reaction. It was found that Cu<sup>I</sup> salts performed better than Cu<sup>II</sup> salts, and that the nature of the iodane counteranion had a minor impact on selectivity. Structurally diverse iodane and indolines worked well under the optimized conditions, leading to higher selectivities for the more sterically hindered substrates. A proposed mechanism suggested that the chemoselectivity was controlled by a  $\pi,\pi$ -stabilizing interaction between the *p*-tolyl group of the chiral auxiliary and the aromatic part of the indoline. More recently, the same group reported on the development of a catalytic asymmetric version of the same reaction (Scheme 36B).<sup>[66]</sup> Thus, the reaction between indolines **115** and dissymmetric mesityl-aryl iodanes **114** bearing an unsubstituted primary amide was efficiently catalyzed by a Cu(I)/bisoxazoline **L14** chiral complex, leading to *N*-aryl indo-

lines **116**. The reaction tolerates both Br and F substituents at different positions of the indoline ring, which is important for further functionalization and biological applications. The nature of the R<sup>1</sup> group in the hypervalent iodine reagent is of critical importance: substrates with reduced steric hindrance deliver nearly racemic products. On the other hand, halogen-substituted iodanes are suitable reaction partners, affording the corresponding indolines in good yields and enantioselectivities. The crystal structure of one of the products (R<sup>1</sup> = R<sup>2</sup> = OMe, R<sup>3</sup> = 7–Br, R<sup>4</sup> = H) showed an intermolecular hydrogen bond between the N atom of the indoline and the amide motif, which highlights the importance of the latter in the efficiency of the reaction. Moreover, preliminary mechanistic studies revealed the occurrence of a nonlinear amplification involving multi-metallic copper species, together with a very fast initial rate of the reaction.

Conversely, Tan et al. reported an acid-catalyzed atroposelective C–H amination of azonaphthalenes **117** with carbazoles **118** for the synthesis of axially chiral *N*-arylcarbazoles **119**, reaching good to excellent enantioselectivities by using spinol-derived chiral phosphoric acid **C10** as the catalyst (Scheme 37A).<sup>[67]</sup> This was the first organocatalytic method for the synthesis of such chiral motifs and represents an alternative to metal-catalyzed cross-coupling reactions for C–N bond formation. Since this reaction is redox neutral, no external



**Scheme 36.** Axially chiral *N*-arylated indolines by Cu-catalyzed Ullmann coupling.



**Scheme 37.** Atroposelective C–H amination of arenes for the synthesis of chiral *N*-aryl carbazoles and indoles.

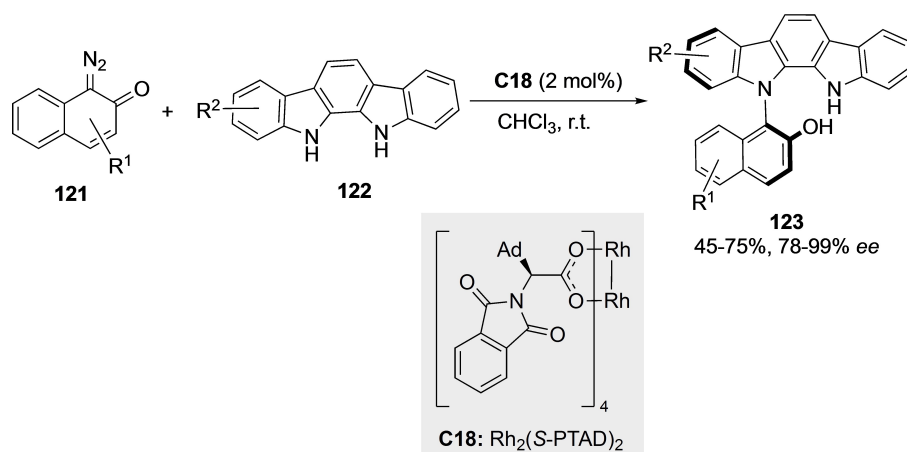
oxidant was needed. A sterically hindered group at the C2 position of the carbazole substrate ensures configurational stability on the resulting products. Replacement of the  $R^2$  group in the ester functionality consistently gave the desired products in excellent yields and with a similar high enantiocontrol. The electronic nature and position of the  $R^1$  groups also had a limited effect on enantioselectivity. The authors propose a CPA-assisted central to axial chirality transfer process through H-bond activation and rearomatization. Indoles **120** were also effective in this transformation, although a bulky  $R^3$  substituent at C3 was required to generate the desired products **121** and a different catalyst **C17** was required to obtain optimal results (Scheme 37, B). Furthermore, it was found that the introduction of a methyl group at C3 of the azonaphthalene **117** significantly increased the yield and also had a positive impact on the enantioselectivity.

More recently, Wang and co-workers reported on a highly atroposelective synthesis of axially chiral *N*-arylindolocarbazoles **123**.<sup>[68]</sup> To this end, the authors developed a Rh(II)-catalyzed intermolecular N–H insertion of diazonaphthoquinone **121**-derived carbenes into indolocarbazole precursors **122**. The reaction proceeds under mild conditions to afford moderate to good yields and excellent enantioselectivities by using phthalimido-derived dirhodium catalyst  $\text{Rh}_2(\text{S-PTAD})_2$  **C18** (Scheme 38). The reaction exhibits a wide substrate scope, providing satisfactory results for a variety of diazonaphthoquinones and indolocarbazoles, regardless of the electronic and steric nature

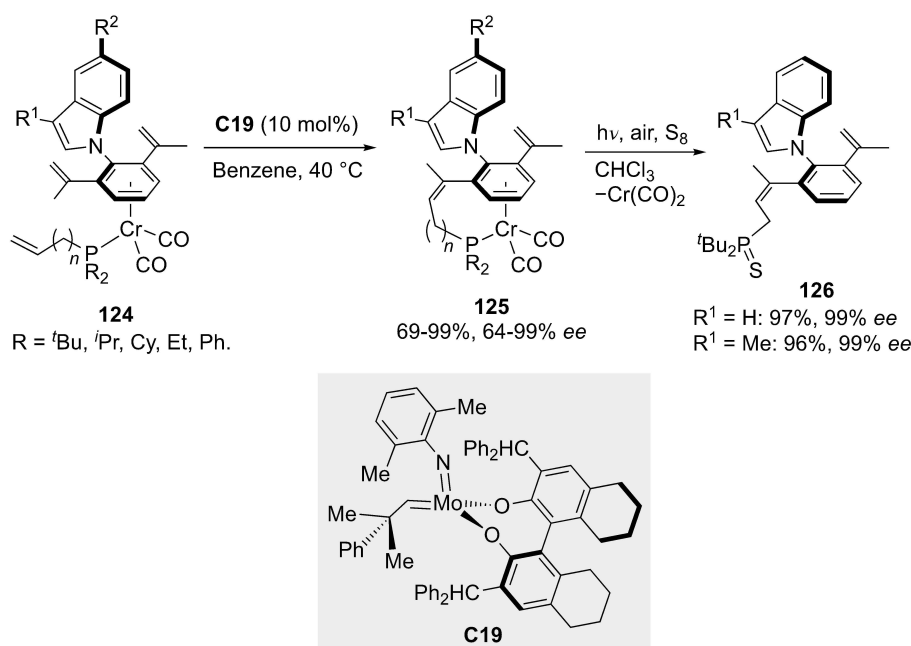
of the substituents. Moreover, the methodology can be used for late-stage functionalization of natural products and bioactive molecules and for the synthesis of novel chiral phosphoric acids (CPAs).

### 3.1.5. Atroposelective desymmetrization of achiral heterobiaryls

Kamikawa and co-workers reported the desymmetrization of planar-prochiral ( $\pi$ -arene)chromium complexes **124** via an enantioselective ring-closing metathesis catalyzed by (*R*)-Mo-alkylidene catalyst **C10**, generating *N*-arylindoles **125** with both planar and axial chirality (Scheme 39).<sup>[69]</sup> These substrates contain  $\eta^6$ -diisopropenyl-2-*N*-indolyl ligands, in which the orientation of the aryl ring of the indole is *anti* with respect to the  $\text{Cr}(\text{CO})_2$  group. The presence of electron-donating groups on the phosphine moiety was crucial to obtain good reactivity and high enantioselectivity. For substrates with poorer electron-donating groups on the allylphosphine, the reaction did not occur. The proximal isopropenyl groups slow down the rotation around the ( $\pi$ -arene)-indolyl single bond, and their orientation is therefore fixed in the *anti*-configuration. Mechanistically, the first metathesis takes place between the catalyst and the P-allyl group, which is the less sterically hindered olefin. The ring-closing metathesis is then favored because the more electron-donating  $\text{PR}_2$  group increases the electron density at the two isopropenyl groups through the chromium atom. As ligation of



**Scheme 38.** Asymmetric Rh-catalyzed carbene insertion reaction for the synthesis of axially chiral *N*-arylindolocarbazoles.



**Scheme 39.** Enantioselective ring-closing metathesis for the synthesis of *N*-arylindoles.

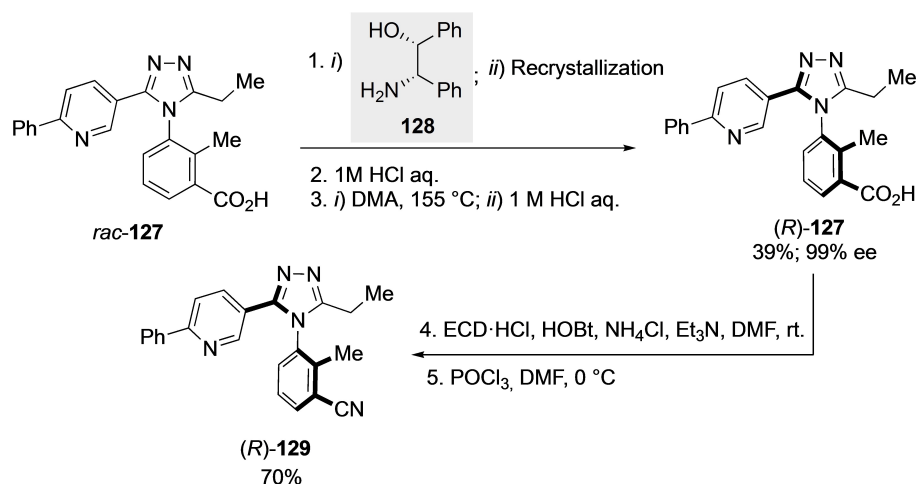
a  $\pi$ -arene moiety in (arene)chromium complexes is electronically neutral, the  $\pi$ -arene can be detached under mild conditions (exposure of the chloroform solution to sunlight under air) giving axially chiral *N*-arylindoles **126** with complete retention of the enantiomeric purity. Elemental sulfur was used to trap the released phosphine. It was also determined that the geometry of the internal olefin formed was exclusively *cis*.

### 3.2. Axially chiral triazole derivatives

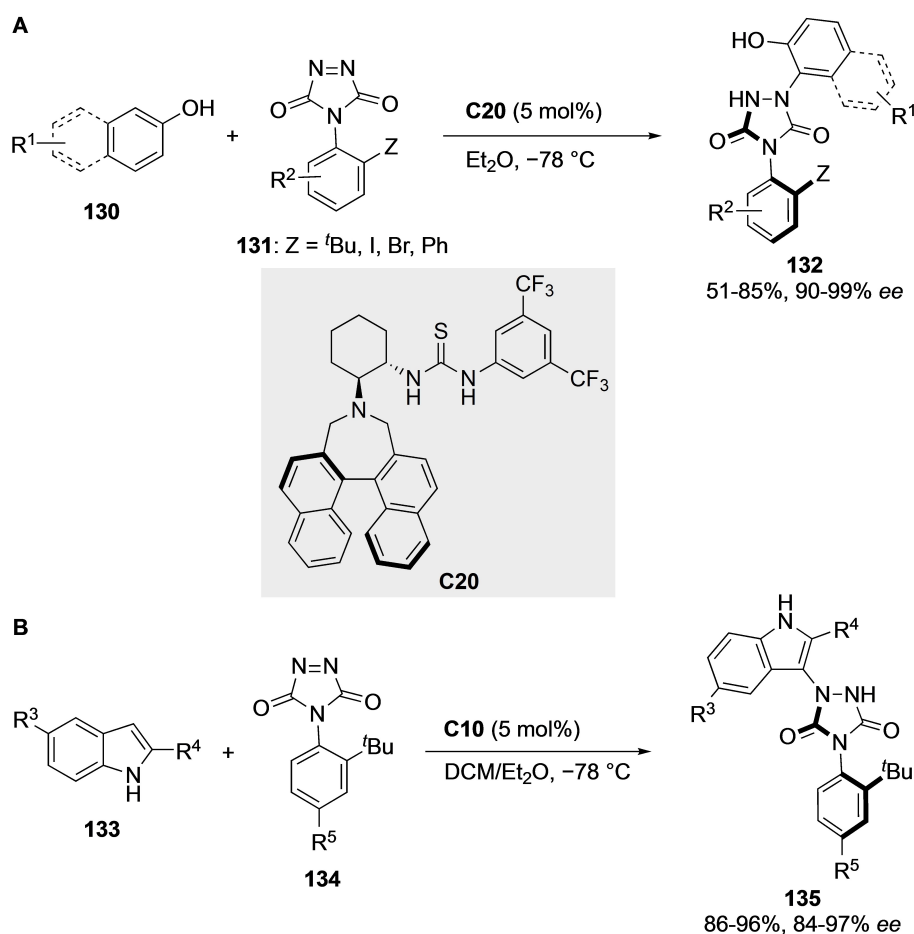
Triazoles, prominent representatives of heterocyclic compounds, are key structural motifs in a plethora of biologically active compounds and useful building blocks in the synthesis of natural products. As is the case with axially chiral pyrroles and

indoles, the wider angles next to the axis in these five-membered ring compounds are responsible for their limited configurational stability with respect to biaryl derivatives.

Sugane and co-workers were the first to report a method to resolve phenyl triazole derivatives **127** via diastereomeric salt formation, identifying (*1R,2S*)-2-amino-1,2-diphenylethanol [(*1R,2S*)-ADPE] **128** as the most suitable and effective resolving agent (Scheme 40).<sup>[70]</sup> Salt formation was afforded after stirring for 4 h, and the resulting precipitate was recrystallized to afford the desired product (*R*)-**127** in excellent yield and enantioselectivity. The resolving agent was further removed in acidic media and the undesired (*S*)-**127** was almost quantitatively recycled to racemate by heating in DMA and then reused to prepare additional (*R*)-**127**. Finally, the carboxyl group was transformed into a cyano group to obtain an important GlyT1



Scheme 40. Resolution of phenyl triazole derivatives.

Scheme 41. Synthesis of axially chiral *N*-aryltriazole derivatives.

inhibitor (*R*)-**129** in good yield and in enantiomerically pure form.

In 2016, Tan and co-workers described an organocatalytic asymmetric approach to an interesting class of axially chiral *N*-aryltriazole derivatives **132** (Scheme 41A).<sup>[71]</sup> The authors used a

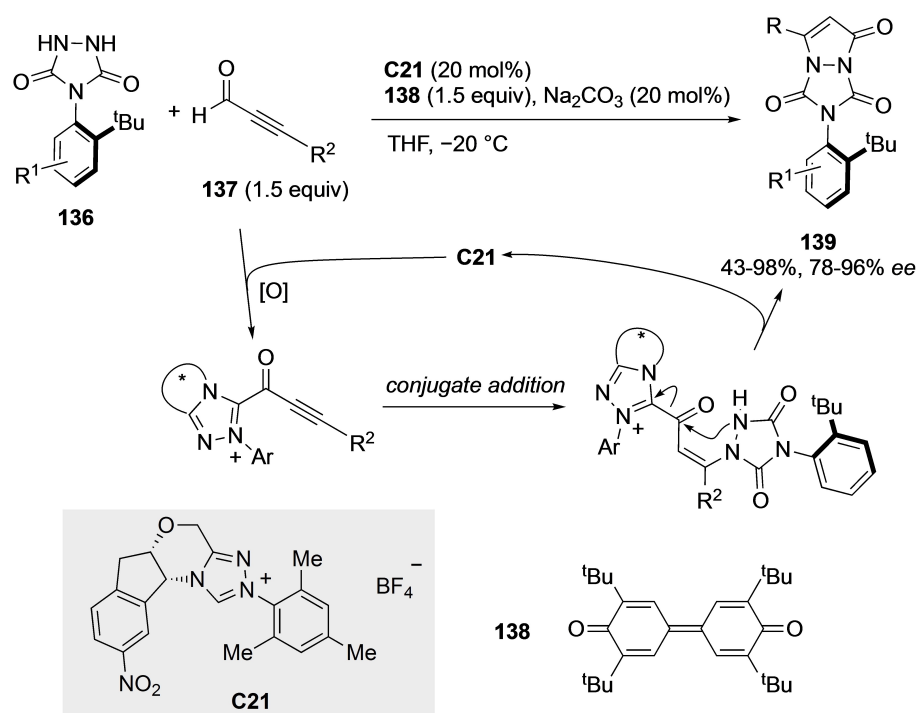
bifunctional thiourea-based organocatalyst **C20** for the desymmetrization of the triazolidiones **131** in Friedel-Crafts type amination of phenols/naphthols **130**, transferring central and axial chirality from the catalyst into a stereogenic axis located far from the reaction site. A variety of phenols and 2-naphthols

were tolerated, with limited influence of the electronic properties of the aromatic ring substituents on stereoselectivity. Similar conclusions were also drawn from the effect of substitution on the aromatic ring of triazolidiones **131**. Additionally, the *ortho*-substituent on arylurazole was not only restricted to *tert*-butyl group. Thus, iodo, bromo, or phenyl groups at the *ortho* position also afford excellent enantioselectivities. The use of indoles **133** as nucleophiles needed further optimization, resulting in the identification of spirocyclic phosphoric acid **C10** as the optimal catalyst to obtain *N*-aryltriazole derivatives **135** from triazolidiones **134** (Scheme 41B). The electronic nature, size, or substitution pattern of the triazolidione and substituted indoles have only minimal effects on yields and enantioselectivities. All products **132** and **135** presented high thermal stability and both reactivity and stereoselectivity were retained in large-scale production.

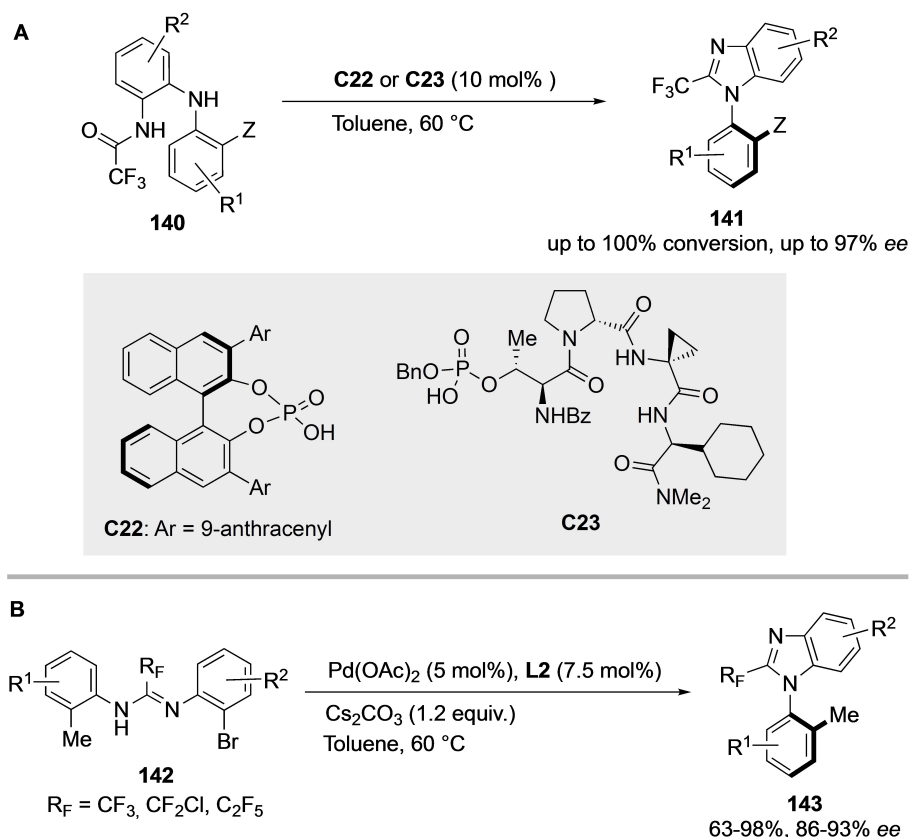
Very recently, Chi and co-workers reported on the synthesis of related axially chiral pyrazolo[1,2-*a*]triazole derivatives **139**.<sup>[72]</sup> In this case, the products are formed via an atroposelective [3 + 2] annulation/desymmetrization of urazoles **136** in their reaction with ynals **137**. Optimal enantioselectivities were achieved using the triazolium NHC catalyst **C21** in the presence of quinone **138** as an external oxidant (Scheme 42). The C–N stereogenic axis is generated by atroposelective addition of a nitrogen atom of the urazole to the acylazolium intermediate formed upon activation of ynal **137** with the catalyst and subsequent oxidation.

### 3.3. Axially chiral benzimidazole derivatives

Recently, Toste, Miller and co-workers presented a comparative study of two distinct catalyst **C22** and **C23** that are effective for the atroposelective cyclodehydration of *ortho*-substituted aniline derivatives **140** to afford *N*-aryl benzimidazoles **141** (Scheme 43A).<sup>[73]</sup> Catalyst **C22** is a C<sub>2</sub>-symmetric chiral phosphoric acid, while catalyst **C23** is a peptide-based phosphoric acid in which standard variations of the peptide sequence led to significant improvements in selectivity. Both catalysts gave similar results with several substrates bearing electron-donating and electron-withdrawing groups. However, for compounds that presented substitution at C7 (R<sup>2</sup>=7-Me, 7-Et, 7-*i*Pr, 7-Ph, 7-OMe), phosphoric acid **C22** was a less selective catalyst (44–83% ee). On the other hand, both catalysts showed low enantioselectivities with *ortho*, *ortho'*-disubstituted substrates. Mechanistic DFT studies and experimental results suggested that the cyclization was the rate- and stereo-determining step. Steric effects on both the catalyst and the substrate dictate the enantioselectivity for catalyst **C22**. For catalyst **C23**, conformational adjustments minimize repulsive interactions. Similar benzimidazoles **143** have also been synthesized in a simple manner using an intramolecular Buchwald-Hartwig amination of amidines **142** (Scheme 43B).<sup>[74]</sup> Excellent yields and enantioselectivities were achieved using the common combination of Pd(OAc)<sub>2</sub> as the precatalyst and (*S*)-BINAP **L2** as the ligand. It is noteworthy that the stereochemical result strongly depends on the nature of the amidine substituent in C1. Excellent enantioselectivities were achieved for trifluoromethylated substrates (R<sub>F</sub>=CF<sub>3</sub>) and slightly lower ee's were observed for other fluorinated derivatives (R<sub>F</sub>=CF<sub>2</sub>Cl or



**Scheme 42.** NHC-catalyzed atroposelective desymmetrization of urazoles.



**Scheme 43.** Cyclization approaches for the synthesis of axially chiral *N*-aryl benzimidazoles.

$\text{C}_2\text{F}_5$ ). However, the enantioselectivity drops substantially when simple alkyl- or aryl-substituted amidine substrates are used instead.

An alternative methodology for the atroposelective synthesis of axially chiral *N*-aryl benzimidazoles has recently been reported by Fu and co-workers.<sup>[75]</sup> In this approach, the reaction of *N*-(aryl)benzene-1,2-diamines **144** with dicarbonyl compounds **145** or **146** proceeds with C–C bond cleavage of the latter, yielding products **147** and **148**, respectively. In both cases, hindered phosphoric acid **C24** was identified as the best catalyst, affording both types of products with moderate to good yields and excellent enantioselectivities (Scheme 44).

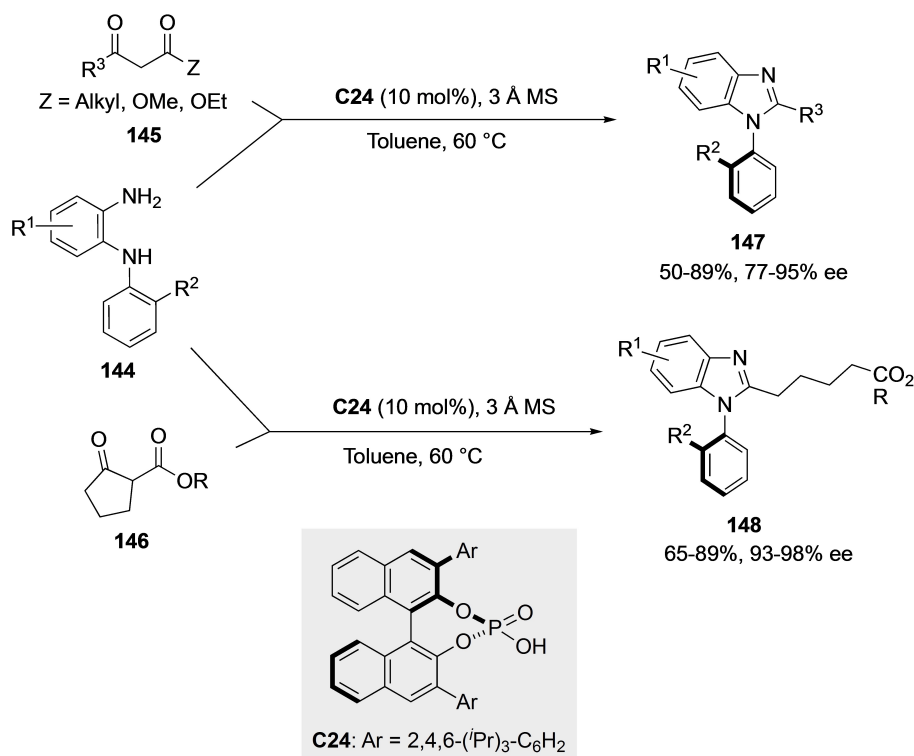
Furthermore, an atroposelective synthesis of axially chiral *N*-arylbenzimidazoles **151** have also been very recently reported by Tan and co-workers.<sup>[76]</sup> The strategy relies on the use of chiral phosphoric acid (CPA) catalysis for the C–N bond formation between 2-naphthylamine derivatives **149** and nitrosoarenes **150** as the electrophilic amination reagent (Scheme 45). Best results were collected with the previously developed spirocyclic catalysts **C17**. The reaction proceeds by dehydration of the initially formed addition intermediate, followed by isomerization of the resulting diimine (either by two consecutive reduction and oxidation steps or by a direct [1,5]-H migration), a second C–N bond formation in the stereodetermining step (SDS), and a final oxidative aromatization. Remarkably, the

nitroso group acts as both an electrophilic and nucleophilic site in the two C–N bond-forming events.

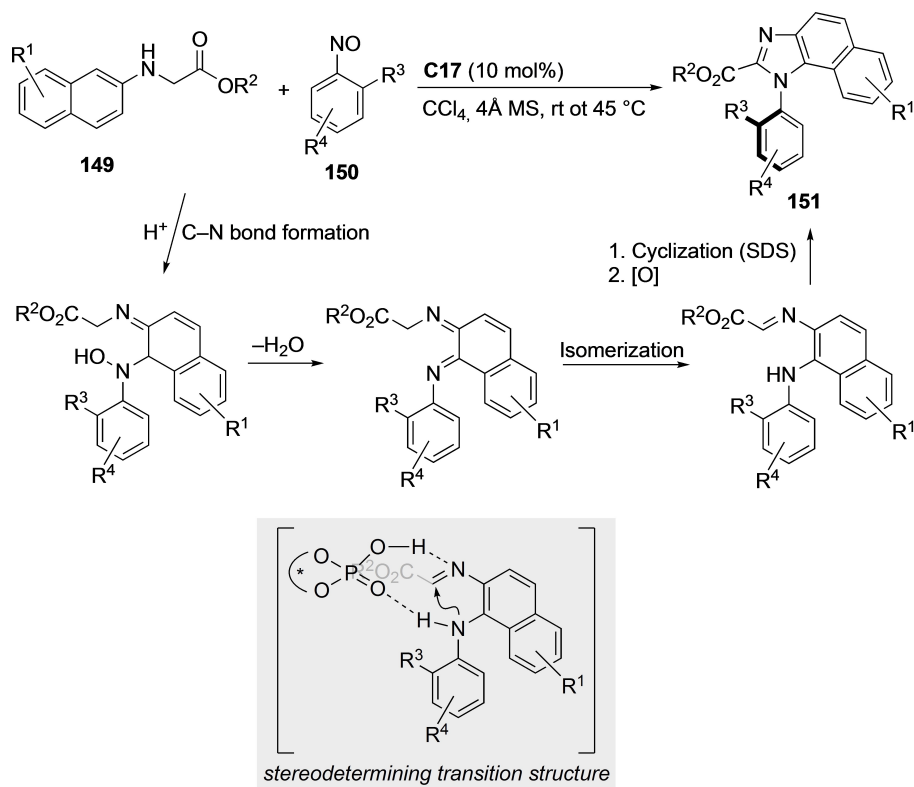
### 3.4. Axially chiral cyclic imides

Simpkins and co-workers reported the asymmetric synthesis of axially chiral imides **153** by enantioselective deprotonation of succinimide **152** with a chiral lithium amide base (Scheme 46).<sup>[77]</sup> In this way, the *anti*-isomer of the desired monoalkylated product was obtained with moderate yields but excellent enantioselectivities. A kinetic resolution via double alkylation of the minor enantiomer is responsible for the high enantiomeric excesses observed. The reaction provides straightforward access to a range of target molecules and could be applied to the total synthesis of (+)-hinokinin, whose enantiomer is present in a lignin natural product.

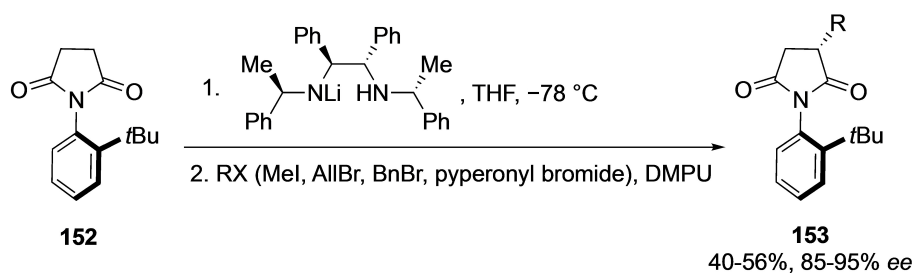
In 2007, Hayashi and co-workers developed a highly enantio- and diastereoselective construction of axially chiral *N*-arylsuccinimides **156** by a rhodium-catalyzed asymmetric 1,4-addition reaction of aryl boronic acids **155** to *N*-aryl succinimides **154** (Scheme 47).<sup>[78]</sup> Optimal results were obtained by using chiral diene ligand **L15**, thus reaching high yields, good diastereoselectivity and excellent enantioselectivities for a wide range of boronic acids. Different  $R^1$  and  $R^2$  substituents were tolerated, with the best results obtained for the more hindered



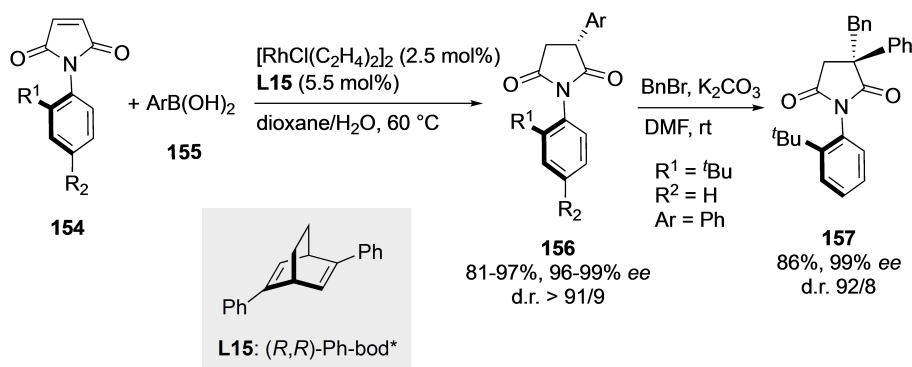
**Scheme 44.** Atroposelective construction of axially chiral *N*-aryl benzimidazoles involving carbon – carbon bond cleavage.



**Scheme 45.** Atroposelective construction of axially chiral *N*-aryl benzimidazoles involving carbon – carbon bond cleavage.



Scheme 46. Enantioselective deprotonation for the synthesis of axially chiral imides.

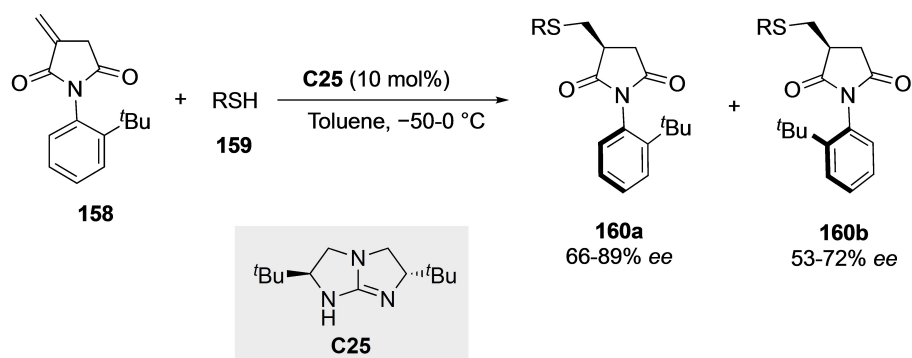
Scheme 47. Rhodium-catalyzed asymmetric 1,4-addition for the synthesis of axially chiral *N*-arylsuccinimides.

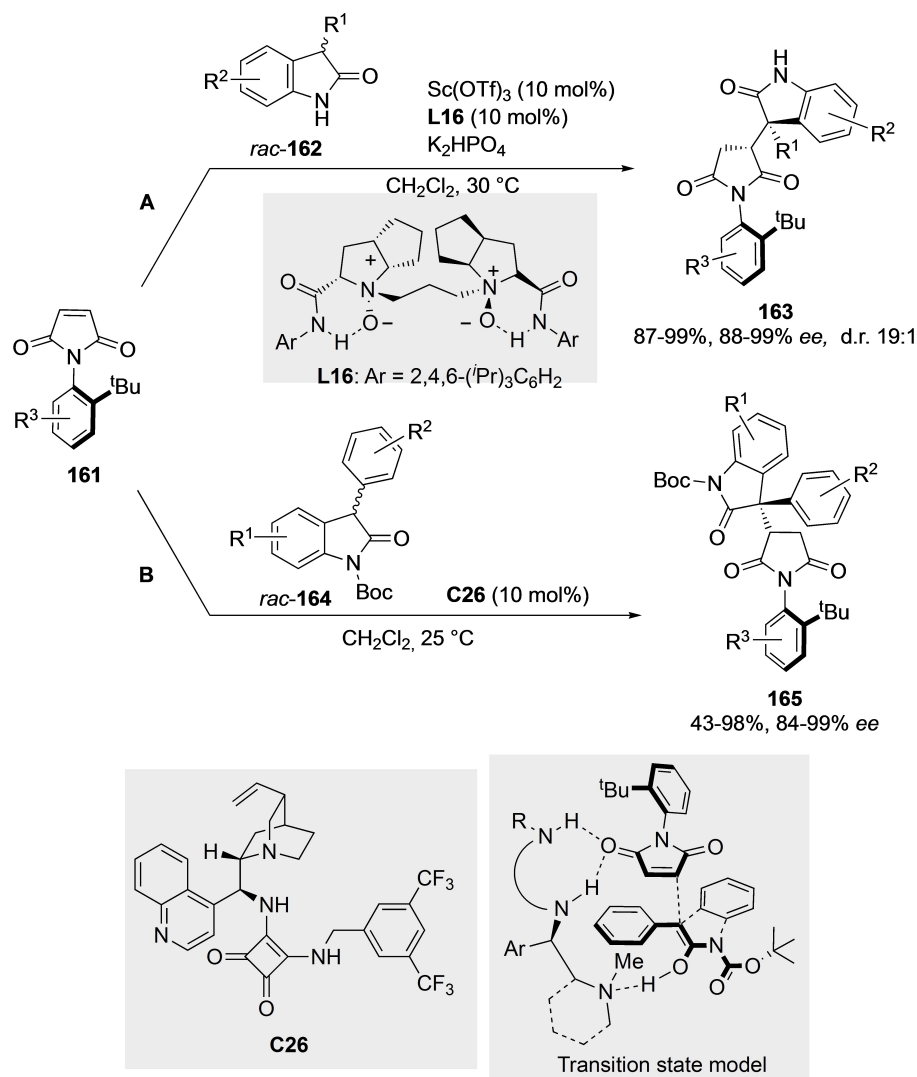
derivatives. It was also found that the stereochemical information of the C–N axis could be efficiently transferred in subsequent transformations. This was exemplified by a diastereoselective alkylation of **156** that led to derivative **157** featuring an all-carbon quaternary stereogenic center.

Later, Tan et al. described a thia-Michael addition/enantioselective protonation sequence of *N*-substituted itaconimides **158** with thiols **159** to obtain a 1:1 atropisomeric mixture of *anti*- and *syn*-*N*-arylsuccinimides **160a** and **160b** (Scheme 48).<sup>[79]</sup> Using using *tert*-butylthiol and chiral guanidine **C25** as the catalyst, a higher ee value was observed for the *anti*-diastereomer (89%) relative to the *syn*-diastereomer (72%). The atropisomerization rate was experimentally measured to be

$32.4\text{ kcal mol}^{-1}$  ( $\text{R} = \text{tBu}$ ), in good agreement with the value of  $30.9\text{ kcal mol}^{-1}$  at 298 K obtained from DFT calculations.

A Michael addition of unprotected 3-substituted-2-oxindoles **162** to *N*-arylmaleimide derivatives **161** was reported by Feng et al. in 2015 (Scheme 49A).<sup>[80]</sup> Using a  $\text{Sc}(\text{OTf})_3/\text{N,N}'$ -dioxide catalytic system based on ligand **L16**, adducts **163** were obtained in excellent yields and enantioselectivities. The addition of  $\text{K}_2\text{HPO}_4$  as the base accelerates the reaction and allows to obtain only one of the possible isomers. A broad scope was demonstrated, with oxindole and maleimide derivatives with different substituents, including halogens, being suitable reaction partners. Later, Bencivenni et al.<sup>[81]</sup> also demonstrated the ability of a squaramide-functionalized cinchonidine derivative **C26** to promote the reaction of the same

Scheme 48. Synthesis of *N*-arylsuccinimides by a guanidine-catalyzed thia-Michael addition/ protonation sequence:



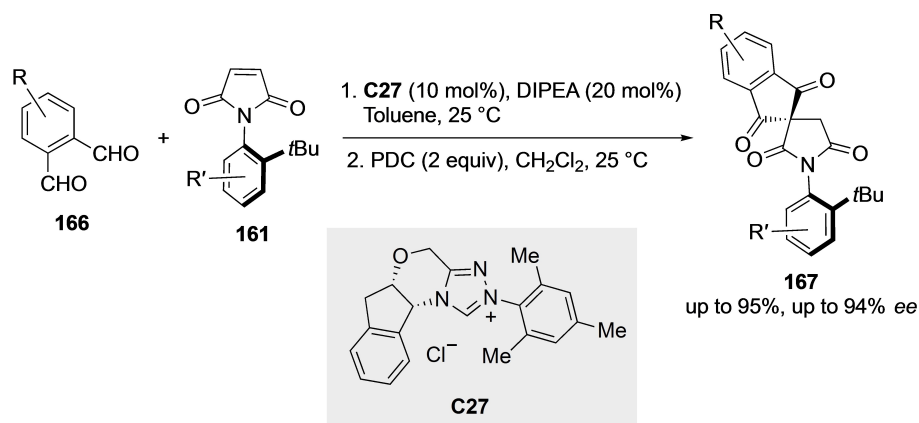
**Scheme 49.** A: Scandium-catalyzed Michael addition of 3-substituted-2-oxindoles to arylmaleimide derivatives. B: Organocatalytic atroposelective desymmetrization of maleimides.

maleimides **161** with *N*-Boc protected oxindoles **164** for the synthesis of adducts **165** (Scheme 49B). The bifunctional character of the catalyst containing a tertiary amine was essential to interact with the acidic proton at C3 of the oxindole and simultaneously as H-bond donor to coordinate the imide carbonyl, ensuring in this way a well-defined geometry in the transition state. Under optimal conditions, it was shown that the presence of diverse electron-withdrawing and electron-donating groups at the oxindole core did not affect the reactivity of the system. Furthermore, no loss of reactivity or stereoselectivity was observed with *para* or *meta* substituents in the maleimide. On the other hand, excellent results were obtained with halogenated maleimides, although a lower reactivity was observed for the larger ones.

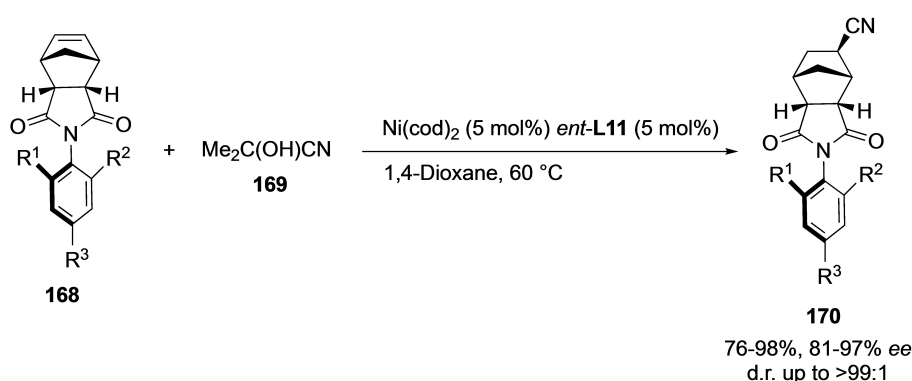
A related strategy for the atroposelective synthesis of spirocyclic *N*-aryl succinimides **167** has also been recently reported.<sup>[82]</sup> The method is also based on a desymmetrization of maleimides **161**, making use in this case of a NHC-catalyzed

Stetter-aldol/oxidation sequence from dialdehydes **166** (Scheme 50). Using triazolium salt **C27** as the carbene precursor in the presence of DIPEA as the base and thiourea as an additive, a variety of products were obtained in good yields and enantioselectivities.

Lastly, axially chiral *N*-aryl succinimides **170** have been prepared from *N*-aryl 5-norbornene-2,3-dicarboximides **168** using a nickel-catalyzed enantioselective hydrocyanation with cyanohydrin **169** as a hydrogen cyanide surrogate (Scheme 51).<sup>[83]</sup> The desymmetrization process proceeds with generation of central and remote N–C axial chirality, reaching high levels of enantioselectivity by using (*R*)-DM-SEGPHOS ligand *ent*-**L11**. The absence of a nonlinear effect (NLE) suggests that a monomeric [Ni**L11**] complex is the catalytically active species, and control experiments confirmed the key role of the carbonyl groups of the substrate. Finally, computational DFT studies revealed that reductive elimination is the enantiodetermining step.



**Scheme 50.** NHC-catalyzed synthesis of axially chiral *N*-Aryl succinimides.



**Scheme 51.** Synthesis of axially chiral *N*-Aryl succinimides: Ni-catalyzed desymmetrization of norbornene derivatives by hydrocyanation.

## 4. N-Aryl/Vinyl Six-Membered Heterocycles

### 4.1. Axially chiral lactams

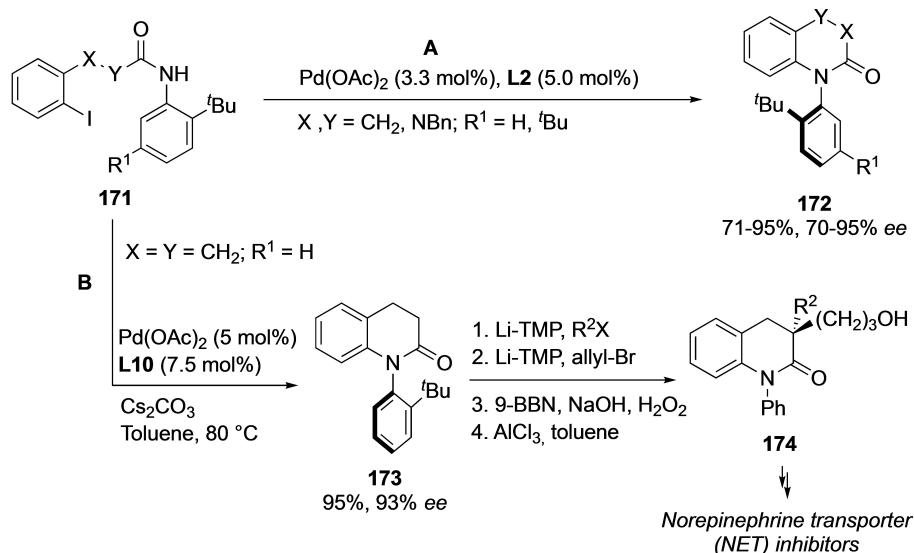
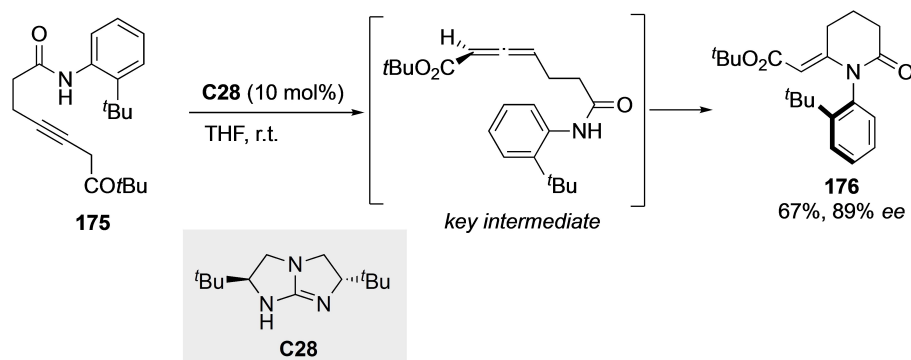
The above-mentioned intermolecular anilide *N*-arylation by Taguchi and co-workers (Scheme 10) could also be applied in an intermolecular fashion to anilide derivatives **171** for the atroposelective synthesis of cyclic products **172**.<sup>[34]</sup> Good *ee*'s and excellent yields were observed by using a modified catalyst system comprising Pd(OAc)<sub>2</sub>/*S*-BINAP **L2** (Scheme 52A). This methodology was later applied by the authors to the synthesis of dihydroquinolinone derivatives **173** using a Pd(OAc)<sub>2</sub>/*R*-SEGPHOS **L10** catalyst (Scheme 52B).<sup>[84]</sup> The synthesis of **174** precursor of a norepinephrine transporter (NET) inhibitor, was then carried out by diastereoselective  $\alpha$ -alkylation of the corresponding lactam enolate, where the attack of the electrophile occurs preferentially from the opposite side or the *ortho-tert*-butyl group, generating finally a quaternary carbon. *anti*-Markovnikov hydration of the allyl group followed by *trans-tert*-butylation was then performed under mild conditions to afford the target product.

In 2010, Tan and co-workers described an intramolecular hetero-Michael reaction of alkynylamide **175** for the synthesis of axially chiral lactam **176**. Using Brønsted base-catalyst **C28**,

this transformation proceeds via isomerization into chiral allene intermediates followed by cyclization (Scheme 53).<sup>[85]</sup> Limitations in the preparation of related atropisomeric six-membered lactams were encountered due to difficulties in the synthesis of suitable alkyne substrates.

Tanaka and co-workers have also described an atroposelective Rh(I)-catalyzed [2+2+2] cycloaddition reaction of diynes **177** with *ortho*-substituted phenyl isocyanates **178** for the synthesis of axially chiral *N*-aryl-2-pyridones **179** (Scheme 54A).<sup>[86]</sup> The optimal cationic catalyst was generated in situ from [Rh(cod)<sub>2</sub>]BF<sub>4</sub> and (*R*)-BINAP *ent*-**L2**. Under the optimized conditions, it was observed that an increase of the steric hindrance of the alkyl substituent at the 2-position of substrates **178** led to higher *ee* values but at expenses of yield. Conversely, substituents such as 2-OMe and 2-Cl afforded good yields but moderate *ee*'s. On the other hand, malonate-derived-diynes, 1,3-diol-derived diynes, 1,6-diynes and ethylene-linked 1,7-diynes could all participate in the reaction although moderate enantioselectivities were reached.

Using the same approach, Takeuchi et al. later described that the alternative catalyst formed in situ from [Ir(cod)Cl]<sub>2</sub> and chiral diphosphines can also be used in the same transformation, reaching optimal enantioselectivities by using **L17** as the ligand (Scheme 54B).<sup>[87]</sup> The use of iridium instead of

Scheme 52. Asymmetric intramolecular *N*-arylation for the synthesis of atropisomeric lactams.

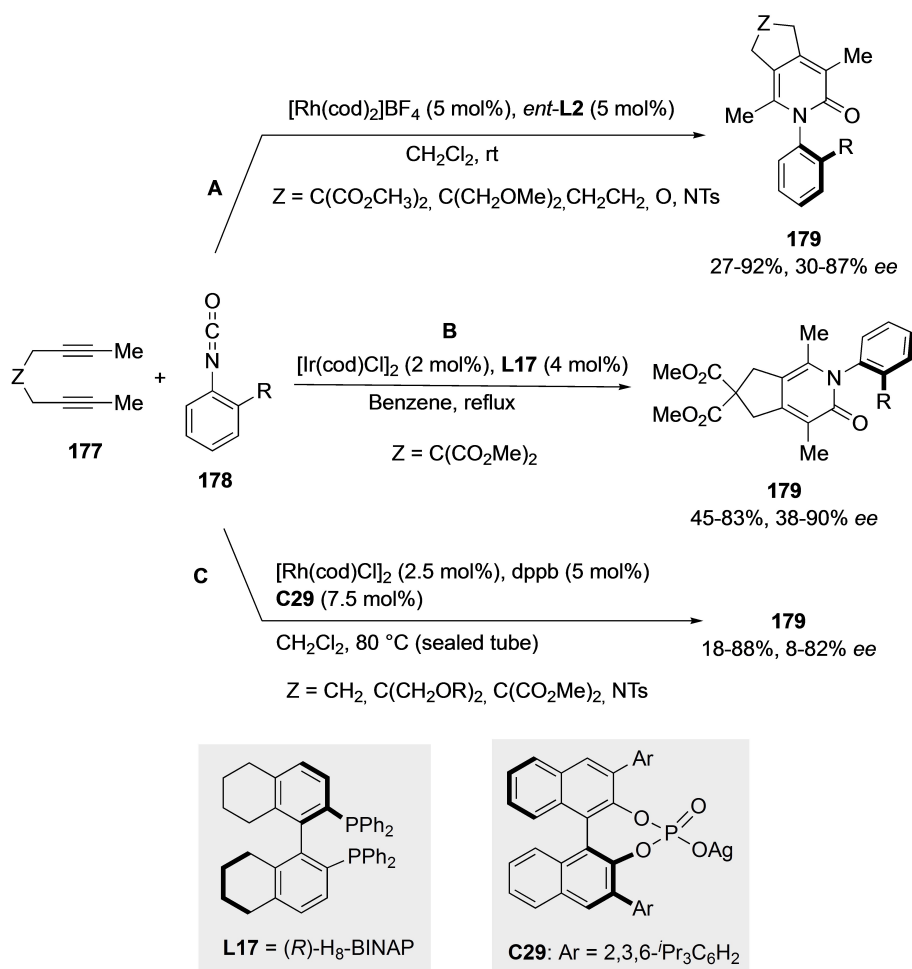
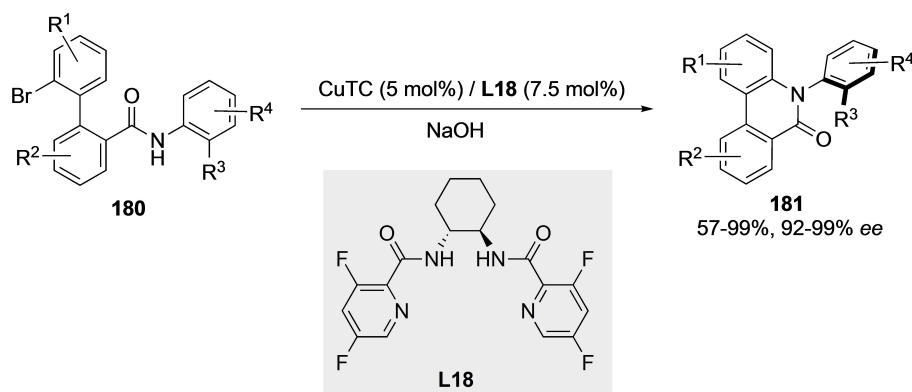
Scheme 53. Base-catalyzed isomerization–Michael addition for the synthesis of axially chiral lactams

rhodium or nickel has advantages, as the catalyst does not require preactivation. Under optimized conditions, the reaction worked well for a wide range of isocyanates **178**. As in the precedent case, the higher the steric hindrance of *R*, the lower the observed yield. The reaction tolerates *ortho*-halophenyl isocyanates, with the bromo derivative giving a yield lower than that of the chlorine, although good enantioselectivities were observed in both cases. Alternatively, Ollivier and co-workers used in the same reaction an anion metathesis between the rhodium catalyst [Rh(cod)Cl]<sub>2</sub> and a chiral silver phosphate **C29** in order to generate in situ a catalytically active [Rh(I)][phosphate] chiral complex (Scheme 54C).<sup>[88]</sup> An H<sub>2</sub> atmosphere was initially used to accelerate decoordination of the cyclooctadiene ligand, but similar results were also obtained without H<sub>2</sub> premix, although a higher temperature was required to generate the catalytically active species. The presence of bulky *R* substituents in **178** provided better *ee*'s under optimized conditions, but the use of halogenated derivatives (*R* = Cl, Br) was detrimental to both yield and enantioselectivity. Regarding the scope of the diynes **177**, good results were

obtained when *Z* was a diester, cyclic acetal, and *N*-tosyl group, but lower yields and selectivities were observed for an unsubstituted tether, indicating the underlying positive gem-dialkyl effect on the reaction.

Gu and co-workers developed a copper-catalyzed enantioselective Ullmann-type amination reaction for the construction of C–N atropisomers (Scheme 55).<sup>[89]</sup> Using diamide **L18** as the optimal ligand, a series of biaryl bromo anilides **180** afforded the corresponding lactams **181** in excellent selectivities. Different substitution patterns in the biaryl skeleton and in the aniline fragment were well tolerated. *Ortho*-substituted alkyl substrates (*R*<sup>3</sup>) in the latter, however, afforded lower yields due to steric hindrance, but the enantioselectivities remained excellent. Racemization studies indicated the need to work under mild conditions (below 60 °C), to avoid racemization.

In 2016, Kitagawa et al.<sup>[90]</sup> reported on the atroposelective synthesis of C–N axially chiral *N*-aryl phenanthridin-6-ones **183** via Pd-catalyzed intramolecular Buchwald-Hartwig amination from bromo amides **182** (Scheme 56). Using (*R*)-DTBM-SEGPHOS **L4** as ligand, *ortho*-ethyl and *ortho*-methyl substituted products

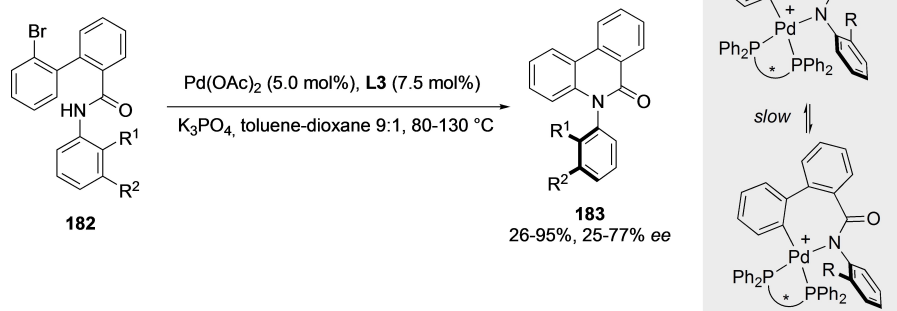
Scheme 54. Atroposelective cycloaddition of diynes with isocyanates for the synthesis of axially chiral *N*-aryl-2-pyridones.

Scheme 55. Ullmann-type amination to obtain axially chiral lactams.

were obtained with moderate yield and enantioselectivity (25 and 68% *ee* respectively) although racemization of the products was also observed. Surprisingly, the use of bulky *ortho-tert*-butyl substituents led to poor yield and enantioselectivity, although these results could be improved by heating the reaction at 130 °C. This behavior was attributed to a high rotational barrier

around the C–N chiral axis in the Pd-amine diastereomeric intermediates.

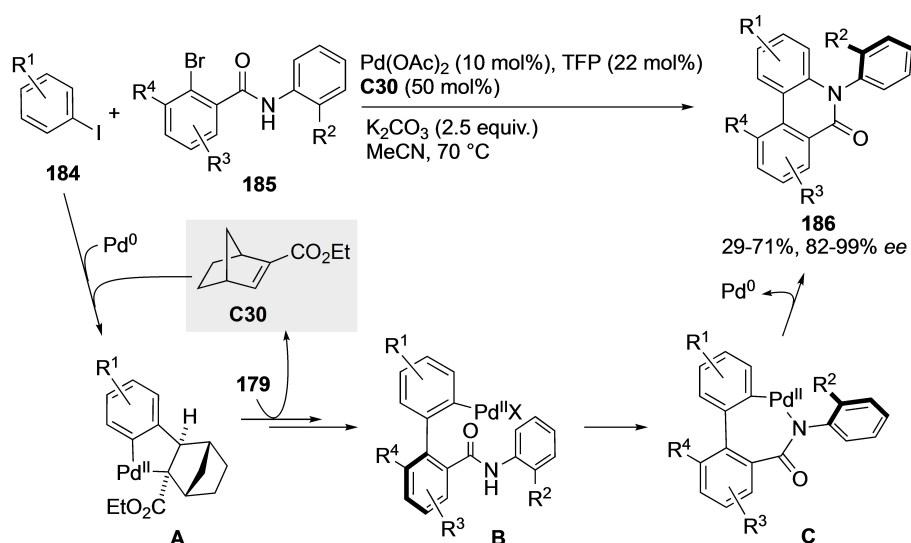
Very recently, Hong, Zhou and co-workers have developed an elegant approach for the synthesis of axially chiral *N*-arylphenanthridinones.<sup>[91]</sup> The strategy relies on cooperative palladium/chiral norbornene (Pd/NBE\*) catalysis, in what can be

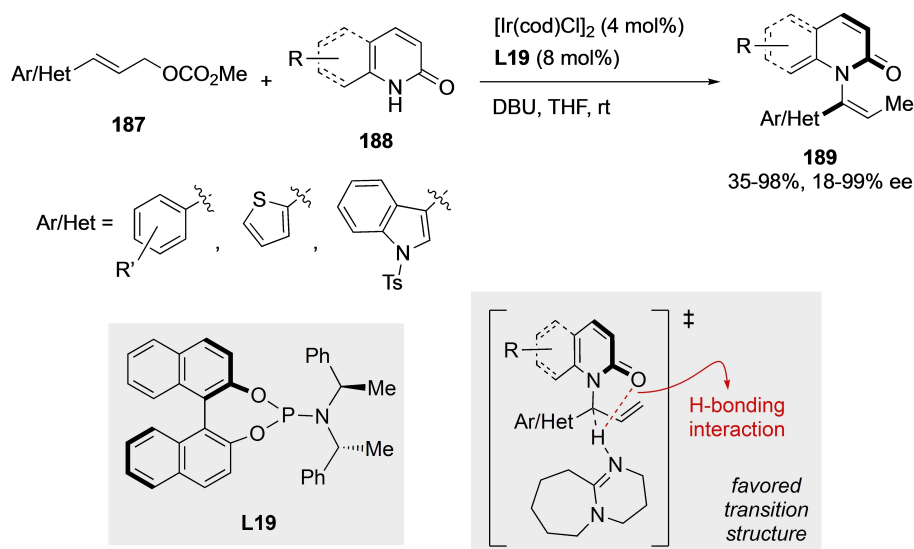


Scheme 56. Atroposelective synthesis of phenanthridin-6-ones.

considered as a variant of the Catellani reaction with an intramolecular amidation as the termination event. Thus, starting from *ortho*-substituted iodoarenes **184** and *ortho*-bromoanilides **185**, an optimized catalyst formed by Pd(OAc)<sub>2</sub>, tri(2-furyl)phosphine (TFP) and 2-ethyl ester-substituted norbornene **C30** provided the desired products **186** in good yields and excellent enantioselectivities (Scheme 57). The process, supported by DFT calculations, starts with the oxidative addition of the Pd<sup>0</sup> catalyst to iodoarene **184**, NBE\* **C30** insertion, and C–H activation leading to palladacycle intermediate **A**. Oxidative addition to **185** followed by reductive elimination and extrusion of the NBE transient mediator **C30** affords the key Pd<sup>II</sup> intermediate **B**, featuring a transient C–C stereogenic axis from which the final C–N stereogenic axis originates with high levels of stereoselectivity during the final intramolecular amidation step via intermediate **C** and the final axial-to-axial chirality transfer to the N–C axis.

Very recently, He and co-workers<sup>[92]</sup> described the synthesis of axially chiral pyridones **189** through an iridium-catalyzed enantioselective allylic amination of cinnamyl carbonates **187** followed by a stereospecific central-to-axial chirality transfer process (Scheme 58). As a remarkable singularity, the C–N bond is built on an *N*-styryl moiety instead of the common *N*-aryl unit. The reaction proceeds smoothly using an iridacycle catalyst generated in situ with a chiral phosphoramidite ligand **L19**. The C–H amination procedure tolerates different *para*- and *meta*-substituted carbonates bearing electron-neutral, electron-donating, and electron-withdrawing groups, as well as difunctionalized derivatives, affording the corresponding products in excellent yields and enantioselectivities. Bulky substituents and heterocyclic rings were also tolerated, but a lower *ee* was obtained with *ortho*-substituted derivatives. Remarkably, the electronic properties of substituents on 2-quinolinol substrates have an important impact on enantioselectivity with electron-withdrawing groups

Scheme 57. Axial-to-axial chirality transfer approach for the synthesis of axially chiral *N*-arylphenanthridinones.



**Scheme 58.** Atroposelective synthesis of *N*-styryl pyridones.

at C4, resulting in a decrease in enantiocontrol. Density functional theory (DFT) studies revealed that the stereospecificity during the central-to-axial chirality transfer ([1,3]-H transfer) can be explained by the stabilizing H-bonding interaction between the base and the amide carbonyl group in the favored transition structure.

#### 4.2. Quinazolinone derivatives

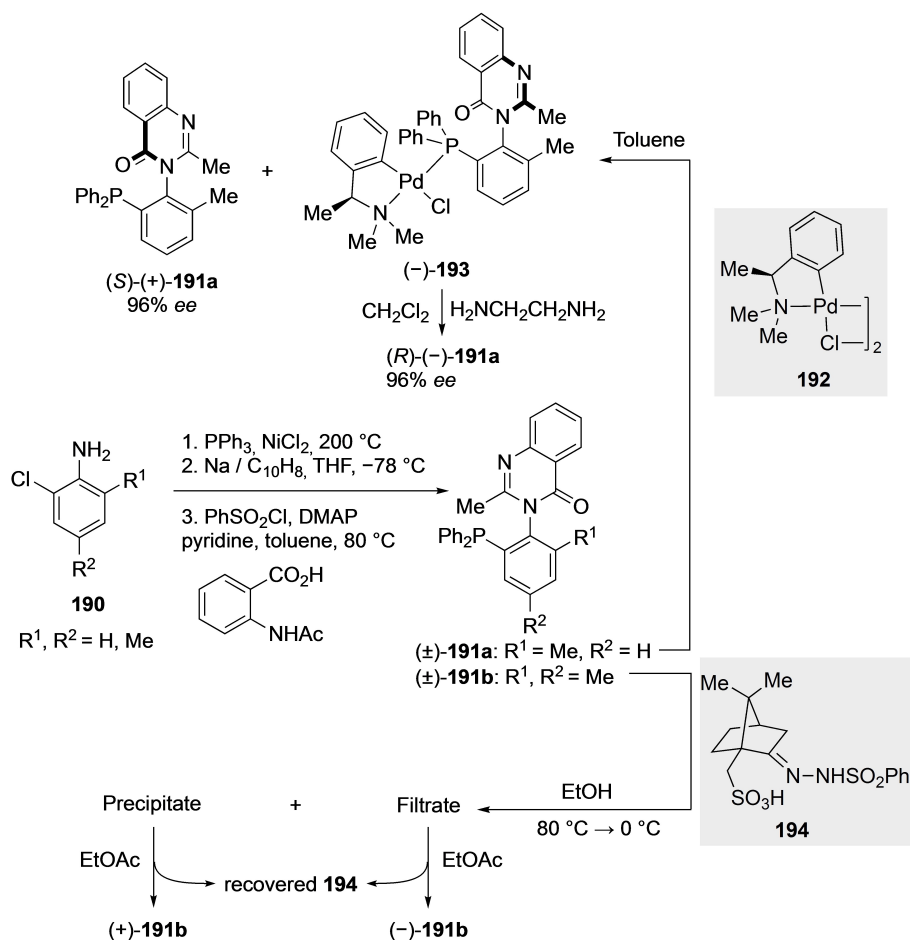
*N*-Aryl quinazolinone derivatives are privileged heterocyclic structures in medicinal chemistry as they possess a wide spectrum of biological activities.<sup>[93]</sup> Their high rotational barrier compared to other axially chiral C–N compounds also makes them good chiral ligands candidates for asymmetric catalysis. Until 2006, quinazolinone derivatives could only be obtained in enantiomerically pure form after chromatographic separation in chiral stationary phases<sup>[94]</sup> or classical resolution with chiral resolving agents. For example, Virgil and co-workers<sup>[95]</sup> described in 1998 the synthesis of different racemic quinazolinone ligands **191 a,b** from 2-chloroanilines **190** (Scheme 59) and the resolution of the former, which was accomplished by means of chiral palladium dimer **192**, a conventional resolving agent for monophosphines. Enantiomerically pure quinazolinone complex **193** and unreacted (*S*)-(+)-**191 a** were obtained with high enantioselectivities. A more convenient strategy for larger-scale synthesis was applied to the resolution of analogue **191 b** with (*S*)-camphorsulfonic acid (benzenesulfonyl)hydrazone **194** as the resolving agent.

In 2006, Natsugari and co-workers reported a method for the atroposelective synthesis of quinazolinone derivatives **197**, obtained by condensation of precursors **195** with chiral amino acids and subsequent dehydrative cyclization of the resulting compounds **196** (Scheme 60).<sup>[96]</sup> The diastereoselectivity was found to depend on the type of substrate and reaction

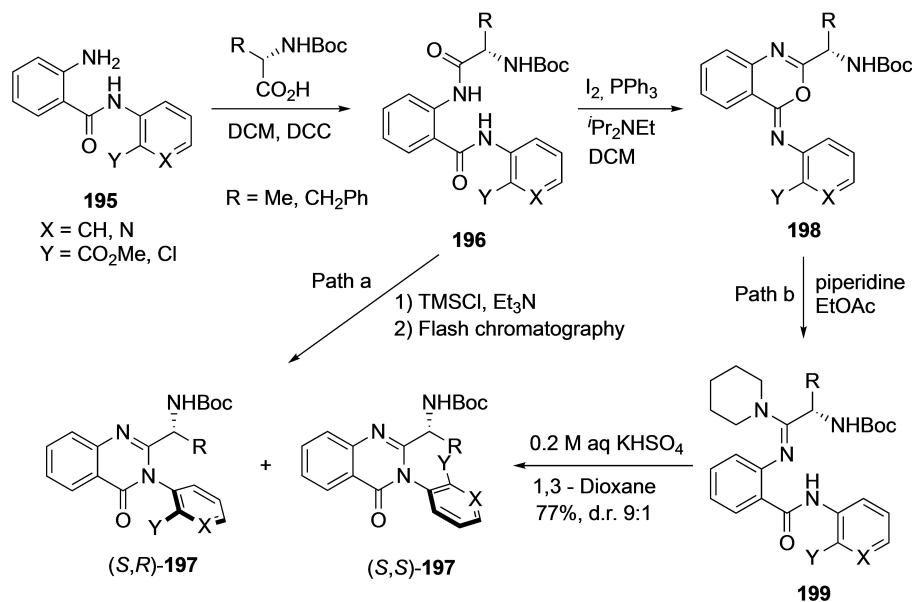
conditions employed. Using TMSCl/Et<sub>3</sub>N (path a) the reaction gave almost equal amounts of diastereomers (*S,R*)-**197** and (*S,S*)-**197**, which could be easily separated by flash chromatography. The second method (path b) consists of the alternative cyclization of amidine **199** under milder conditions. This in turn was prepared from **196** by treatment with I<sub>2</sub>, PPh<sub>3</sub>, and DIPEA, followed by reaction of the resulting product **198** with piperidine. In this case, the reaction occurred to yield (*S,R*)-**197** in good yield and much better diastereoselectivity (d.r. up to 9:1).

Miller described an efficient method to access a wide range of substituted tribrominated 3-arylquinazolin-4(3H)-ones **201** through an atroposelective tribromination reaction of precursors **200** (Scheme 61).<sup>[97]</sup> High enantioselectivities were achieved by using a tertiary amine-embedded  $\beta$ -turn peptide catalyst **C31**. Even in the absence of *ortho*-substituents in the phenol ring, quinazolinones **200** present a modest rotational barrier around the C–N axis (18.8 kcal/mol for R<sup>1</sup>=Me, R<sup>3</sup>=H) Therefore, the slow addition of NBS over 2.5 h was necessary for an efficient DKR to occur. A screening of truncated peptide catalysts provided evidenced that the  $\beta$ -turn secondary structure is important to achieve high levels of enantioinduction in this reaction. Under optimized conditions, it was possible to achieve good yields and high enantioselectivities for substrates possessing alkyl substituents at the 2-position (R<sup>1</sup>) or electron-donating and withdrawing groups at the phenol ring (R<sup>3</sup>), suggesting a weak effect of distal substitution on enantioselectivity. However, electron-withdrawing groups or lack of substitution at the 2-position (R<sup>1</sup>) led to products with a lower rotational barrier around the chiral axis, resulting in lower levels of enantioselectivity. Mechanistically, the chiral axis is set after the first bromination reaction at *ortho*-position.

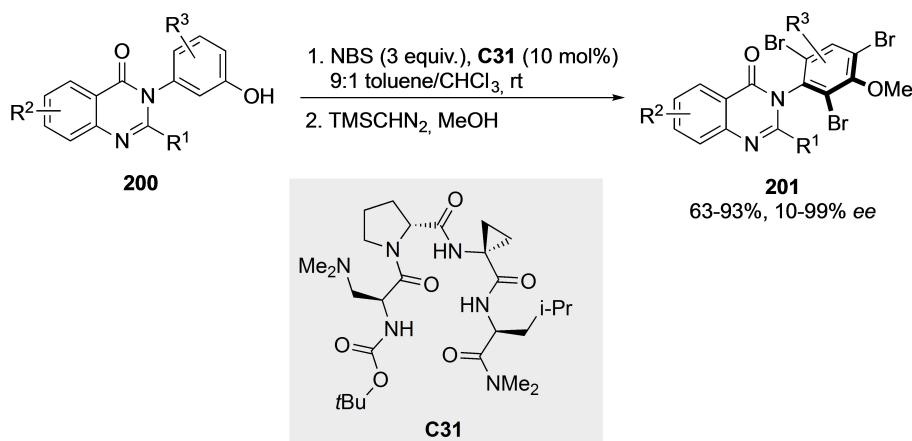
Based on the results previously described by Miller, Kitagawa et al. reported in the following year a reductive desymmetrization of chiral quinazolinone derivatives **202** into



Scheme 59. Classical resolution of racemic quinazolones.



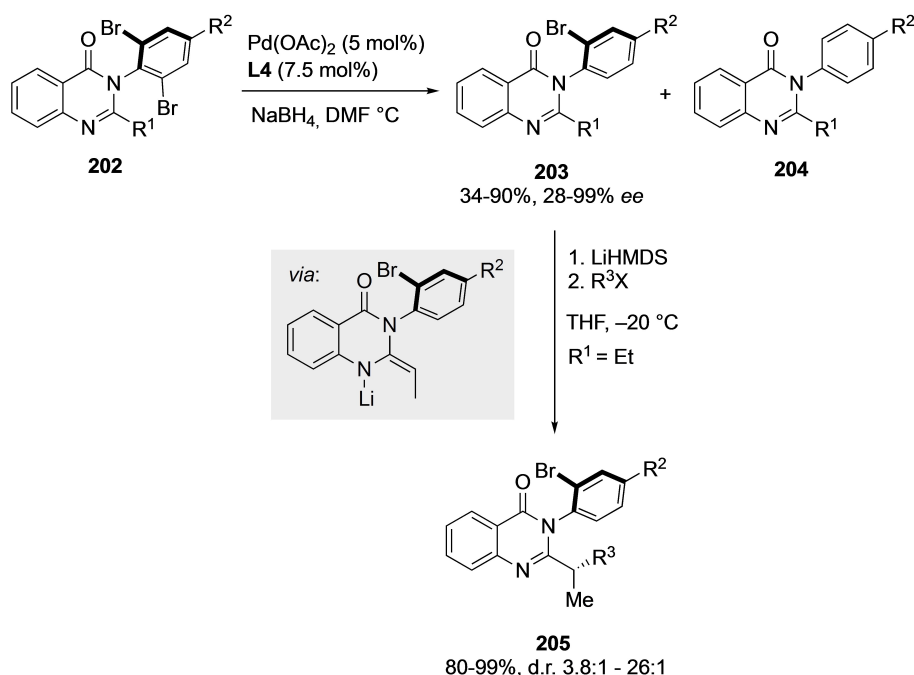
Scheme 60. Diastereoselective dehydrative cyclization for the synthesis of quinazolone derivatives.



**Scheme 61.** Atroposelective tribromination of *N*-arylquinazolinones.

debrominated derivatives **203** using palladium catalysts based on (*R*)-DTBM-SEGPHOS **L4** as the ligand (Scheme 62).<sup>[98]</sup> As an important strategic advance, the presence of an hydroxyl group at the C3 position of the phenyl ring, which hampered the synthesis of bioactive quinazolinone products in the previous method, is not required. During the optimization of the reaction, it was found that the enantioselectivity could be improved by decreasing the reaction temperature to 0 °C. Furthermore, reducing the amount of  $\text{NaBH}_4$  resulted in a considerable increase in the chemical yield of **203** at the expense of that of the fully dibrominated byproduct **204**, although lower enantioselectivities were achieved. This result suggests that the enantioselectivity is determined not only by the desymmetrization process (the first dehydrodebromination),

but also by a kinetic resolution of **203** (the second dehydrobromination). The outcome of the reaction was significantly influenced by the  $\text{R}^2$  substituent, with alkyl groups affording a remarkable increase in enantioselectivity. However, the presence of methoxy or chlorine groups in  $\text{R}^2$  was found to decrease enantioselectivity due to the influence of inductive effects. Later, the same research group developed a diastereoselective  $\alpha$ -alkylation reaction of lithium enamines, prepared from mebroqualone derivatives **203** ( $\text{R}^1 = \text{Et}$ ).<sup>[99]</sup> Under optimized conditions, the resulting  $\alpha$ -alkylation products **205** were obtained in good yields and diastereomeric ratios (up to 99% yield and up to d.r. = 26:1). The diastereoselectivity was found to be strongly dependent on the bulkiness of the  $\text{R}^2$  group. Thus, bulky alkyl halides, in particular isopropyl iodide, afforded



**Scheme 62.** Reductive desymmetrization of chiral quinazolinones.

the best results. The relative (*P,S*)-configuration of the major diastereomer could be explained by the steric repulsion between the R<sup>3</sup> and the *ortho*-bromo groups.

#### 4.3. Other six-membered heterocycles

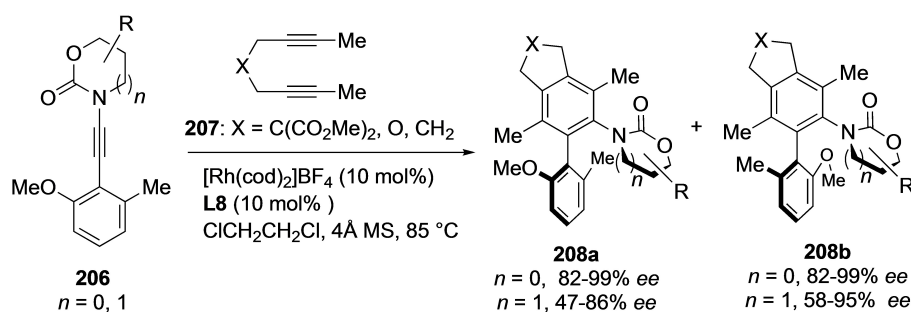
The synthesis of biaryls compounds **208** featuring both C–C and C–N axial chirality were reported by Hsung et al. in 2007. These products were obtained by a Rh(I)-catalyzed asymmetric [2+2+2] cycloaddition of ynamines **206** with 1,6-diyne **207** (Scheme 63).<sup>[100]</sup> Using (*S*)-DM-BINAP **L8** as the ligand, cycloadditions of achiral 6-membered 2-oxazinone rings (*n*=1) afforded products with good yields and enantioselectivities, with the diastereomer **208b** being formed preferentially (d.r. up to 8:1). In the case of ynamides containing 5-membered 2-oxazolidinones (*n*=0), the resulting chiral biaryls were also obtained in good yields and good to excellent enantioselectivities (82 to 99% *ee*), but with moderate diastereoselectivity (d.r. 1:1 to 1:6). The key step of the reaction is the chelation of the Rh metal by both the methoxy and carbonyl groups and the following cycloaddition yielding the major stereoisomer.

Kitagawa and co-workers described the enantioselective synthesis of C–N axially chiral quinolinone derivatives **211** by a palladium-catalyzed amination/cyclization of ynones **209** with *ortho-tert*-butyl aniline **210** (Scheme 64).<sup>[101]</sup> Low enantioselectivities and yields were observed when bidentate phosphines

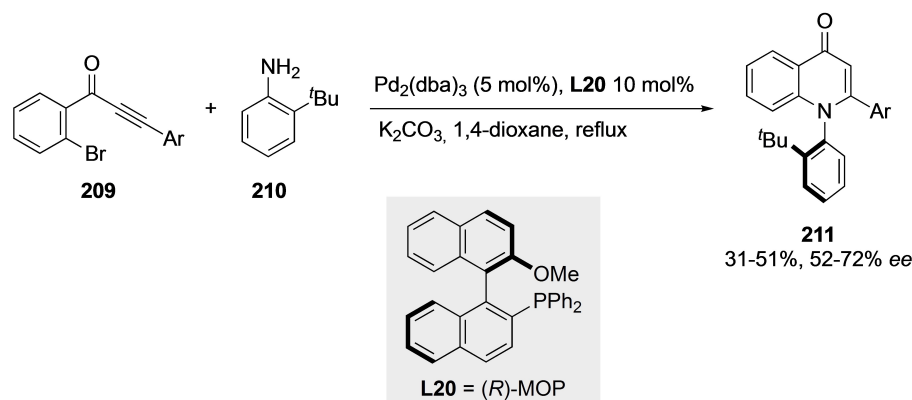
were used as ligands, while monodentate derivatives such as (*R*)-MOP **L20** provided better results. As a limitation, ethynyl ketones with nonaromatic substituents were unproductive in the reaction.

Murata and co-workers developed a cyclization reaction of ureas **212** for the synthesis of axially chiral uracil derivatives **213** through the combined use of (*R*)-ALBO as a chiral auxiliary and quinidine **C32** as a chiral organic base catalyst (Scheme 65).<sup>[102]</sup> The chiral auxiliary was placed in the *ortho*-position of the substituted *N*-phenyl group to effectively control the enantioselective cyclization. It was also found that the absolute configuration of the stereocenter at C9 of the catalyst **C32** is crucial to achieve high diastereoselectivity due to the formation of an intermolecular hydrogen bond between the hydroxyl group and the urea carbonyl group. Finally, removal of the (*R*)-ALBO auxiliary was successfully achieved to obtain the corresponding phenol derivative **214** under mild acidic conditions without significant racemization.

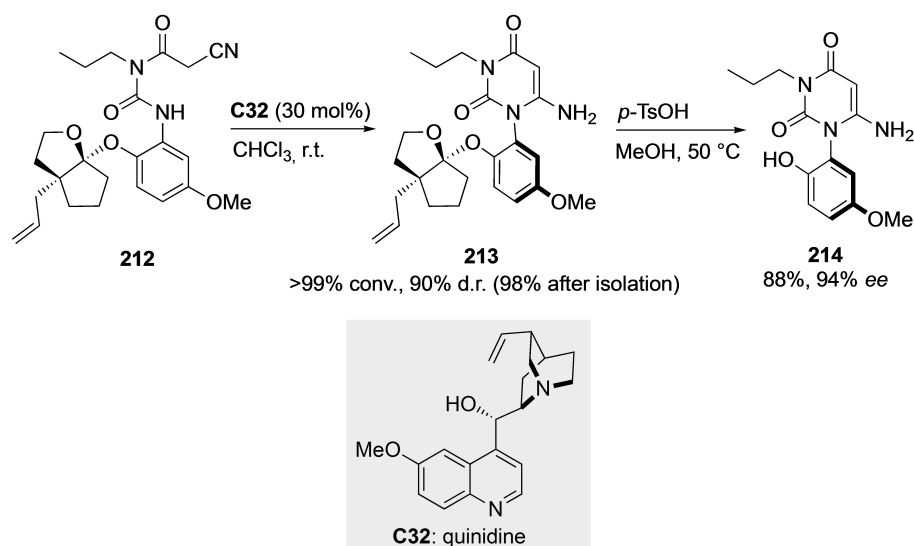
Finally, NHC catalysis has been exploited by Jin and co-workers<sup>[103]</sup> for the atroposelective cycloaddition of thioureas **215** with ynals **216** for the synthesis of axially chiral *N*-aryl thiazines **217** (Scheme 66). Moderate yields, but excellent enantioselectivities were achieved using triazolium salt **C33** as the NHC precatalyst, DMAP as the base and furan as the solvent in the presence of Sc(OTf)<sub>3</sub> and 5 Å MS as beneficial additives to improve the yield of the thiazine product. The reaction involves NHC-catalyzed addition of **215** to acylazolium intermediate **I**,



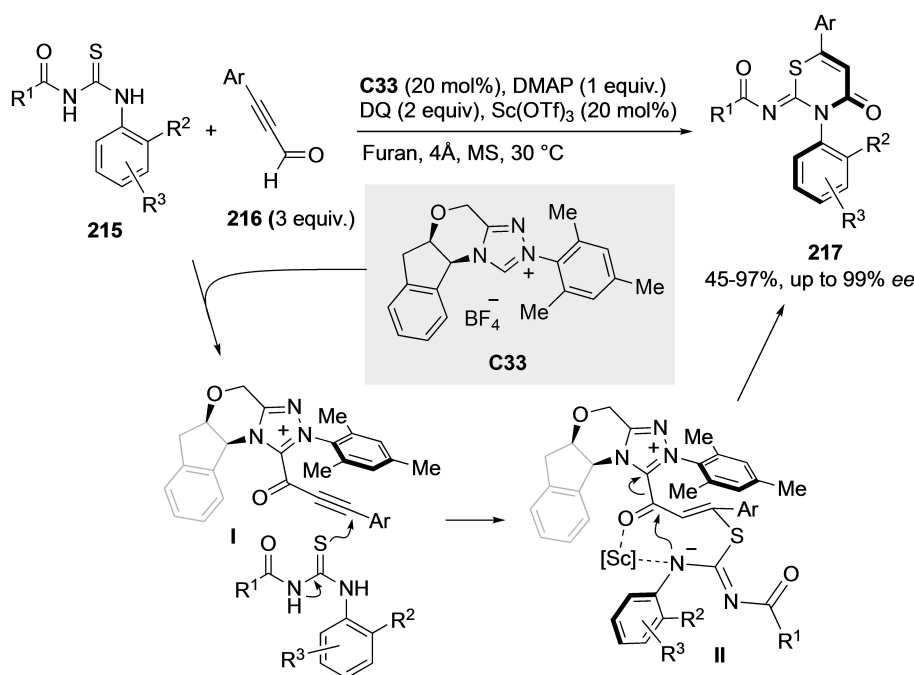
**Scheme 63.** Asymmetric synthesis of heterobiaryl cyclic carbamates.



**Scheme 64.** Hydroamination/cyclization sequence for the synthesis of axially chiral quinazolinones.



Scheme 65. Atroposelective synthesis of axially chiral uracil derivatives.



Scheme 66. Atroposelective synthesis of axially chiral thiazine derivatives.

leading to key intermediate **II**, which undergoes a face-selective intramolecular lactam formation. The reaction tolerates various functionalities, and it was found that the size of substituent  $R^2$  on the *N*-phenyl moieties of the thiazine products plays a significant role in both chirality induction and stereochemical stability. As a limitation, aliphatic ynals are not suitable substrates in this reaction, leading to complex reaction mixtures.

In conclusion, the development of new synthetic methods for accessing axially chiral C–N atropisomers has emerged as a relevant goal in asymmetric catalysis. A minor number of these

strategies have nonetheless been reported when compared with those for the synthesis of axially chiral biaryl scaffolds. Reasons for this difference include the lower configurational stability of the formers due to the high degree of freedom of their conformers and the reduced steric congestion around the C–N axis, in particular for the more challenging 5-membered ring atropisomers. This review has covered enantioselective strategies for the synthesis of atropisomers that display a stereogenic C–N bond, starting from the seminal work of Curran and Simpkins, and putting emphasis on catalytic asymmetric methods. The preparation of new families of atropisomers,

including anilides and axially chiral C–N heterocycles, has also been discussed. Creative strategies based on transition metal-catalyzed and organocatalyzed reactions that allow an efficient transfer of chiral information from the catalyst to a C–N stereogenic axis have been revised. Interestingly, many of these methods have found applications in the synthesis of natural products and biologically active molecules, and as chiral ligands for enantioselective catalysis. Nevertheless, the design of novel methods for the syntheses of these motifs remains challenging, and new innovative strategies need clearly to be developed. We expect that this review will help researchers to have an updated perspective of the state-of-the-art in this fast-growing field and will stimulate the development of new approaches for the synthesis of this important family of compounds.

## Acknowledgements

We thank the Spanish Ministerio de Ciencia e Innovación (Grants PID2019-106358GB-C21, PID2019-106358GB-C22, contracts RYC-2017-22294 for V.H. and BES-2017-081561 P.R.-S.), European funding (ERDF), and Junta de Andalucía (Grants P18-FR-3531, P18-FR-644, US-1262867, US-1260906).

## Conflict of Interest

The authors declare no conflict of interest.

- [1] M. Oki, *Top. Stereochem.* **1983**, *14*, 1–81.
- [2] G. H. Christie, J. Kenner, *J. Chem. Soc. Trans.* **1922**, *120*, 614–620.
- [3] R. Noyori, *Angew. Chem. Int. Ed.* **2002**, *41*, 2008–2022; *Angew. Chem.* **2002**, *114*, 2108–2123.
- [4] a) D. Zhang, Q. Wang, *Coord. Chem. Rev.* **2015**, *286*, 1–16; b) J. Wencel-Delord, A. Panossian, F. R. Leroux, F. Colobert, *Chem. Soc. Rev.* **2015**, *44*, 3418–3430; c) P. Loxq, E. Manoury, R. Poli, E. Deydier, A. Labande, *Coord. Chem. Rev.* **2016**, *308*, 131–190; d) J. M. Lassaletta, *Atropisomerism and Axial Chirality*, 1st ed.; World Scientific: New Jersey, **2019**; e) M. Mancinelli, G. Bencivenni, D. Pecorari, A. Mazzanti, *Eur. J. Org. Chem.* **2020**, 4070–4086; f) V. Corti, G. Bertuzzi, *Synthesis* **2020**, *52*, 2450–2468; g) D.-J. Cheng, Y.-D. Shao, *Adv. Synth. Catal.* **2020**, *362*, 3081–3099; h) J. A. Carmona, C. Rodríguez-Franco, R. Fernández, V. Hornillos, J. M. Lassaletta, *Chem. Soc. Rev.* **2021**, *50*, 2968–2983; i) J. K. Cheng, S. H. Xiang, S. Li, L. Ye, B. Tan, *Chem. Rev.* **2021**, *121*, 4805–4902; j) Q. Zhao, C. Peng, Y.-T. Wang, G. Zhan, B. Han, *Org. Chem. Front.* **2021**, *8*, 2772–2785; k) C.-X. Liu, W.-W. Zhang, S.-Y. Yin, Q. Gu, S.-L. You, *J. Am. Chem. Soc.* **2021**, *143*, 14025–14040.
- [5] a) G. Bringmann, T. Gulder, T. A. M. Gulder, M. Breuning, *Chem. Rev.* **2011**, *111*, 563–639; b) M. C. Kozlowski, B. J. Morgan, E. C. Linton, *Chem. Soc. Rev.* **2009**, *38*, 3193–3207; c) J. E. Smyth, N. M. Butler, P. A. Keller, *Nat. Prod. Rep.* **2015**, *32*, 1562–1583; d) A. Zask, J. Murphy, G. A. Ellestad, *Chirality* **2013**, *25*, 265–274.
- [6] a) I. Takahashi, Y. Suzuki, O. Kitagawa, *Org. Prep. Proced. Int.* **2014**, *46*, 1–23; b) E. Kumarasamy, R. Raghunathan, M. P. Sibi, J. Sivaguru, *Chem. Rev.* **2015**, *115*, 11239–11300; c) D. Bonne, J. Rodriguez, *Chem. Commun.* **2017**, *53*, 12385–12393; d) O. Kitagawa, *Acc. Chem. Res.* **2021**, *54*, 719–730.
- [7] a) L. H. Bock, R. Adams, *J. Am. Chem. Soc.* **1931**, *53*, 374–376; b) L. H. Bock, R. Adams, *J. Am. Chem. Soc.* **1931**, *53*, 3519–3522.
- [8] a) D. P. Curran, N. C. DeMello, *J. Chem. Soc. Chem. Commun.* **1993**, 1314–1317. b) D. P. Curran, H. Qi, S. J. Geib, N. C. DeMello, *J. Am. Chem. Soc.* **1994**, *116*, 3131–3132; c) S. Thayumanavan, P. Beak, D. P. Curran, *Tetrahedron Lett.* **1996**, *37*, 2899–2902; d) D. P. Curran, G. R. Hale, S. J. Geib, A. Balog, Q. B. Cass, A. L. G. Degani, M. Z. Hernandez, L. C. G. Freitas, *Tetrahedron: Asymmetry* **1997**, *8*, 3955–3975; e) J. Clayden, *Angew. Chem. Int. Ed. Engl.* **1997**, *36*, 949–951; *Angew. Chem.* **1997**, *109*, 986–988. f) J. Clayden, *Synlett* **1998**, 810–816; g) J. Clayden, in *Organic Synthesis Highlights IV* (Ed.: H.-G. Schmalz), Wiley-VCH, Weinheim, **2000**, pp. 48–52.
- [9] a) P. W. Glunz, *Bioorg. Med. Chem. Lett.* **2018**, *28*, 53–60; b) S. T. Toenjes, J. L. Gustafson, *Future Med. Chem.* **2018**, *10*, 409–422.
- [10] H. Hammer, B. M. Bader, C. Ehnert, C. Bundgaard, L. Bunch, K. Hoestgaard-Jensen, O. H. Schroeder, J. F. Bastlund, A. Gramowski-Voß, A. A. Jensen, *Mol. Pharmacol.* **2015**, *88*, 401–420.
- [11] A. Mannschreck, E. von Angerer, *J. Chem. Educ.* **2009**, *86*, 1054–1059.
- [12] a) L.-K. Yang, R. P. Glover, K. Yonganathan, J. P. Sarnaik, A. J. Godbole, D. D. Soejarto, A. D. Buss, M. S. Butler, *Tetrahedron Lett.* **2003**, *44*, 5827–5829; b) G. Bringmann, T. Gulder, M. Reichert, F. Meyer, *Org. Lett.* **2006**, *8*, 1037–1040.
- [13] C. Ito, Y. Thoyama, M. Omura, I. Kjiura, H. Furukawa, *Chem. Pharm. Bull.* **1993**, *41*, 2096–2100.
- [14] G. Bringmann, S. Tasler, H. Endress, J. Kraus, K. Messer, M. Wohlfarth, W. Lobin, *J. Am. Chem. Soc.* **2001**, *123*, 2703–2711.
- [15] P. Schneider, G. Schneider, *Chem. Commun.* **2017**, *53*, 2272–2274 and references cited therein.
- [16] B. A. Lanman, J. R. Allen, J. G. Allen, A. K. Amegadzie, K. S. Ashton, S. K. Booker, J. J. Chen, N. Chen, M. J. Frohn, G. Goodman, D. J. Kopecky, L. Liu, P. Lopez, J. D. Low, V. Ma, A. E. Minatti, T. T. Nguyen, N. Nishimura, A. J. Pickrell, A. B. Reed, Y. Shin, A. C. Siegmund, N. A. Tamayo, C. M. Tegley, M. C. Walton, H. L. Wang, R. P. Wurz, M. Xue, K. C. Yang, P. Achanta, M. D. Bartberger, J. Canon, L. S. Hollis, J. D. McCarter, C. Mohr, K. Rex, A. Y. Saiki, T. San Miguel, L. P. Volak, K. H. Wang, D. A. Whittington, S. G. Zech, J. R. Lipford, V. J. Cee, *J. Med. Chem.* **2020**, *63*, 52–65.
- [17] S. H. Watterson, G. V. De Lucca, Q. Shi, C. M. Langevine, Q. Liu, D. G. Batt, M. Beaudoin Bertrand, H. Gong, J. Dai, S. Yip, et al., *J. Med. Chem.* **2016**, *59*, 9173–9200.
- [18] J. Chandrasekhar, R. Dick, J. Van Veldhuizen, D. Koditek, E.-I. Lepist, M. E. McGrath, L. Patel, G. Phillips, K. Sedillo, J. R. Somoza, et al., *J. Med. Chem.* **2018**, *61*, 6858–6868.
- [19] S. R. Selness, R. V. Devraj, B. Devadas, J. K. Walker, T. L. Boehm, R. C. Durley, H. Shieh, L. Xing, P. V. Rucker, K. D. Jerome, et al., *Bioorg. Med. Chem. Lett.* **2011**, *21*, 4066–4071.
- [20] J. Wang, W. Zeng, S. Li, L. Shen, Z. Gu, Y. Zhang, J. Li, S. Chen, X. Jia, *ACS Med. Chem. Lett.* **2017**, *8*, 299–303.
- [21] T. Sugane, T. Tobe, W. Hamaguchi, I. Shimada, K. Maeno, J. Miyata, T. Suzuki, T. Kimizuka, S. Sakamoto, S. Tsukamoto, *J. Med. Chem.* **2013**, *56*, 5744–5756.
- [22] a) T. Mino, Y. Tanaka, Y. Hattori, T. Yabusaki, H. Saotome, M. Sakamoto, T. Fujita, *J. Org. Chem.* **2006**, *71*, 7346–7353; b) N. Debono, Y. Canac, C. Duhayon, R. Chauvin, *Eur. J. Inorg. Chem.* **2008**, 2991–2999; c) I. Abdellah, N. Debono, Y. Canac, L. Vendier, R. Chauvin, *Chem. Asian J.* **2010**, *5*, 1225–1231; d) I. Abdellah, M. Boggio-Pasqua, Y. Canac, C. Lepetit, C. Duhayon, R. Chauvin, *Chem. Eur. J.* **2011**, *17*, 5110–5115; e) T. Mino, K. Nishikawa, M. Asano, Y. Shima, T. Ebisawa, Y. Yoshida, M. Sakamoto, *Org. Biomol. Chem.* **2016**, *14*, 7509–7519; f) L. Kong, J. Morvan, D. Pichon, M. Jean, M. Albalat, T. Vives, S. Colombel-Rouen, M. Giorgi, V. Dorcet, T. Roisnel, C. Crevisy, D. Nuel, P. Nava, S. Humbel, N. Vanthuyne, M. Mauduit, H. Clavier, *J. Am. Chem. Soc.* **2020**, *142*, 93–98.
- [23] For a recent review on methods based on stereoselective C–N bond formation see: J. Frey, S. Choppin, F. Colobert, J. Wencel-Delord, *Chimia* **2020**, *74*, 883–889.
- [24] D. P. Curran, H. Qi, S. J. Geib, N. C. DeMello, *J. Am. Chem. Soc.* **1994**, *116*, 3131–3132.
- [25] A. D. Hughes, D. A. Price, O. Simpkins, N. S. Simpkins, *Tetrahedron Lett.* **1996**, *37*, 7607–7610.
- [26] a) O. Kitagawa, H. Izawa, T. Taguchi, *Tetrahedron Lett.* **1997**, *38*, 4447–4450. b) O. Kitagawa, H. Izawa, K. Sato, A. Dobashi, T. Taguchi, *J. Org. Chem.* **1998**, *63*, 2634–2640.
- [27] A. D. Hughes, N. S. Simpkins, *Synlett* **1998**, 967–968.
- [28] O. Kitagawa, S.-I. Momose, Y. Fushimi, T. Taguchi, *Tetrahedron Lett.* **1999**, *40*, 8827–8831.
- [29] a) T. Hata, H. Koide, N. Taniguchi, M. Uemura, *Org. Lett.* **2000**, *2*, 1907–1910. b) H. Koide, T. Hata, M. Uemura, *J. Org. Chem.* **2002**, *67*, 1929–1935.
- [30] A. Ates, D. P. Curran, *J. Am. Chem. Soc.* **2001**, *123*, 5130–5131.
- [31] J. Clayden, H. Turner, *Tetrahedron Lett.* **2009**, *50*, 3216–3219.
- [32] O. Kitagawa, M. Kohriyama, T. Taguchi, *J. Org. Chem.* **2002**, *67*, 8682–8684.
- [33] J. Terauchi, D. P. Curran, *Tetrahedron: Asymmetry* **2003**, *14*, 587–592.

- [34] a) O. Kitagawa, M. Takahashi, M. Yoshikawa, T. Taguchi, *J. Am. Chem. Soc.* **2005**, *127*, 3676–3677. b) O. Kitagawa, M. Yoshikawa, H. Tanabe, T. Morita, M. Takahashi, Y. Dobashi, T. Taguchi, *J. Am. Chem. Soc.* **2006**, *128*, 12923–12931.
- [35] Y. Kikuchi, C. Nakamura, M. Matsuoka, R. Asami, O. Kitagawa, *J. Org. Chem.* **2019**, *84*, 8112–8120.
- [36] D. Li, S. Wang, S. Ge, S. Dong and X. Feng, *Org. Lett.* **2020**, *22*, 5331–5336.
- [37] Z. Gao, C.-X. Yan, J. Qian, H. Yang, P. Zhou, J. Zhang, G. Jiang, *ACS Catal.* **2021**, *11*, 6931–6938.
- [38] a) S. Shirakawa, K. Liu, K. Maruoka, *J. Am. Chem. Soc.* **2012**, *134*, 916–919. b) K. Liu, X. Wu, S. B. J. Kan, S. Shirakawa, K. Maruoka, *Chem. Asian J.* **2013**, *8*, 3214–3221.
- [39] Y. Liu, X. Feng, H. Du, *Org. Biomol. Chem.* **2015**, *13*, 125–132.
- [40] S.-L. Li, C. Yang, Q. Wu, H.-L. Zheng, X. Li, J.-P. Cheng, *J. Am. Chem. Soc.* **2018**, *140*, 12836–12843.
- [41] G.-H. Yang, H. Zheng, X. Li, J.-P. Cheng, *ACS Catal.* **2020**, *10*, 2324–2333.
- [42] K. Takana, K. Takeishi, K. Noguchi, *J. Am. Chem. Soc.* **2006**, *128*, 4586–4587.
- [43] Q.-J. Yao, P.-P. Xie, Y.-J. Wu, Y.-L. Feng, M.-Y. Teng, X. Hong, B.-F. Shi, *J. Am. Chem. Soc.* **2020**, *142*, 18266–18276.
- [44] Y.-J. Wu, P.-P. Xie, G. Zhou, Q.-J. Yao, X. Hong, B.-F. Shi, *Chem. Sci.* **2021**, *12*, 9391–9397.
- [45] S. D. Vaidya, S. T. Toenjes, N. Yamamoto, S. M. Maddox, J. L. Gustafson, *J. Am. Chem. Soc.* **2020**, *142*, 2198–2203.
- [46] a) S. Brandes, M. Bella, A. Kjærsgaard, K. A. Jørgensen, *Angew. Chem. Int. Ed.* **2006**, *45*, 1147–1151; *Angew. Chem.* **2006**, *118*, 1165–1169. b) S. Brandes, B. Niess, M. Bella, A. Prieto, J. Overgaard, K. A. Jørgensen, *Chem. Eur. J.* **2006**, *12*, 6039–6052.
- [47] H.-Y. Bai, F.-X. Tan, T.-Q. Liu, G.-D. Zhu, J.-M. Tian, T.-M. Ding, Z.-M. Cheng, S.-Y. Zhang, *Nat. Commun.* **2019**, *10*, 3063.
- [48] D. Wang, Q. Jiang, X. Yang, *Chem. Commun.* **2020**, *56*, 6201–6204.
- [49] G. Bringmann, S. Tasler, H. Endress, J. Kraus, K. Messer, M. Wohlfarth, W. Lobin, *J. Am. Chem. Soc.* **2001**, *123*, 2703–2711.
- [50] a) K. Kamikawa, S. Kinoshita, H. Matsuoka, M. Uemura, *Org. Lett.* **2006**, *8*, 1097–1100. b) K. Kamikawa, S. Kinoshita, M. Furuoy, S. Takemoto, H. Matsuoka, M. Uemura, *J. Org. Chem.* **2007**, *72*, 3394–3402.
- [51] L. Zhang, J. Zhang, J. Ma, D.-J. Cheng, B. Tan, *J. Am. Chem. Soc.* **2017**, *139*, 1714–1717.
- [52] a) N. Ototake, Y. Morimoto, A. Mokuya, H. Fukaya, Y. Shida, O. Kitagawa, *Chem. Eur. J.* **2010**, *16*, 6752–6755. b) Y. Morimoto, S. Shimizu, A. Mokuya, N. Ototake, A. Saito, O. Kitagawa, *Tetrahedron* **2016**, *72*, 5221–5229.
- [53] A. Nakazaki, K. Miyagawa, N. Miyata, T. Nishikawa, *Eur. J. Org. Chem.* **2015**, *21*, 4603–4606.
- [54] L. Wang, J. Zhong, X. Lin, *Angew. Chem. Int. Ed.* **2019**, *58*, 15824–15828; *Angew. Chem.* **2019**, *131*, 15971–15975.
- [55] L. Sun, H. Chen, B. Liu, J. Chang, L. Kong, F. Wang, Y. Lan, X. Li, *Angew. Chem. Int. Ed.* **2021**, *60*, 8391–8395; *Angew. Chem.* **2021**, *133*, 8472–8476.
- [56] S. Huang, H. Wen, Y. Tian, P. Wang, W. Qin, H. Yan, *Angew. Chem. Int. Ed.* **2021**, *60*, 21486–21493; *Angew. Chem.* **2021**, *133*, 21656–21663.
- [57] S. Zhang, Q.-J. Yao, G. Liao, X. Li, H. Li, H.-M. Cheng, X. Hong, B.-F. Shi, *ACS Catal.* **2019**, *9*, 1956–1961.
- [58] F.-L. Zhang, K. Hong, T.-J. Li, H. Park, J.-Q. Yu, *Science* **2016**, *351*, 252–256.
- [59] Q.-J. Yao, S. Zhang, B.-B. Zhan, B.-F. Shi, *Angew. Chem. Int. Ed.* **2017**, *56*, 6617–6621; *Angew. Chem.* **2017**, *129*, 6717–6721.
- [60] J. Zhang, Q. Xu, J. Wu, J. Fan, M. Xie, *Org. Lett.* **2019**, *21*, 6361–6365.
- [61] U. Dhawa, T. Wdowik, X. Hou, B. Yuan, J. C. A. Oliveira, L. Ackermann, *Chem. Sci.* **2021**, *12*, 14182–14188.
- [62] H. Li, X. Yan, J. Zhang, W. Guo, J. Jiang, J. Wang, *Angew. Chem. Int. Ed.* **2019**, *58*, 6732–6736. *Angew. Chem.* **2019**, *131*, 6804–6808.
- [63] A. Kim, A. Kim, S. Park, S. Kim, H. Jo, K. M. Ok, S. K. Lee, J. Song, Y. Kwon, *Angew. Chem. Int. Ed.* **2021**, *60*, 12279–12283; *Angew. Chem.* **2021**, *133*, 12387–12391.
- [64] C.-X. Ye, S. Chen, F. Han, X. Xie, S. Ivlev, K. N. Houk, E. Meggers, *Angew. Chem. Int. Ed.* **2020**, *59*, 13552–13556; *Angew. Chem.* **2020**, *132*, 13654–13658.
- [65] J. Rae, J. Frey, S. Jerhaoui, S. Choppin, J. Wencel-Delord, F. Colobert, *ACS Catal.* **2018**, *8*, 2805–2809.
- [66] J. Frey, A. Malekafzali, I. Delso, S. Choppin, F. Colobert, J. Wencel-Delord, *Angew. Chem. Int. Ed.* **2020**, *59*, 8844–8848; *Angew. Chem.* **2020**, *132*, 8929–8933.
- [67] W. Xia, Q.-J. An, S.-H. Xiang, Y.-B. Wang, B. Tan, *Angew. Chem. Int. Ed.* **2020**, *59*, 6775–6779; *Angew. Chem.* **2020**, *132*, 6841–6845.
- [68] Q. Ren, T. Cao, C. He, M. Yang, H. Liu, L. Wang, *ACS Catal.* **2021**, *11*, 6135–6140.
- [69] a) S. Kinoshita, K. Kamikawa, *Tetrahedron* **2016**, *72*, 5202–5207. b) K. Kamikawa, S. Arae, W.-Y. Wu, C. Nakamura, T. Takahashi, M. Ogasawara, *Chem. Eur. J.* **2015**, *21*, 4954–4957.
- [70] T. Sugane, N. Hamada, T. Tobe, W. Hamaguchi, I. Shimada, K. Maeno, J. Miyata, T. Suzuki, T. Kimizuka, S. Sakamoto, S. Tsukamoto, *Tetrahedron: Asymmetry* **2012**, *23*, 1528–1533.
- [71] J.-W. Zhang, J.-H. Xu, D.-J. Cheng, C. Shi, X.-Y. Liu, B. Tan, *Nat. Commun.* **2016**, *7*, 10677.
- [72] J. Jin, X. Huang, J. Xu, T. Li, X. Peng, X. Zhu, J. Zhang, Z. Jin, Y. R. Chi, *Org. Lett.* **2021**, *23*, 3991–3996.
- [73] Y. Kwon, J. Li, J. P. Reid, J. M. Crawford, R. Jacob, M. S. Sigman, F. D. Toste, S. J. Miller, *J. Am. Chem. Soc.* **2019**, *141*, 6698–6705.
- [74] P. Zhang, X.-M. Wang, Q. Xu, C.-Q. Guo, P. Wang, C.-J. Lu, R.-R. Liu, *Angew. Chem. Int. Ed.* **2021**, *60*, 21718–21722; *Angew. Chem.* **2021**, *133*, 21886–21890.
- [75] Ni. Man, Z. Lou, Y. Li, H. Yang, Y. Zhao, H. Fu, *Org. Lett.* **2020**, *22*, 6382–6387.
- [76] Q.-J. An, W. Xia, W.-Y. Ding, H.-H. Liu, S.-H. Xiang, Y.-B. Wang, G. Zhong, B. Tan, *Angew. Chem. Int. Ed.* **2021**, *60*, 24888–24893; *Angew. Chem.* **2021**, *133*, 25092–25097.
- [77] J. Bennett, P. L. Pickering, N. S. Simpkins, *Chem. Commun.* **2004**, 1392–1393.
- [78] W.-L. Duan, Y. Imazaki, R. Shintani, T. Hayashi, *Tetrahedron* **2007**, *63*, 8529–8536.
- [79] S. Lin, D. Leow, K.-W. Huang, C.-H. Tan, *Chem. Asian J.* **2009**, *4*, 1741–1744.
- [80] J. Zhang, Y. Zhang, L. Lin, Q. Yao, X. Liu, X. Feng, *Chem. Commun.* **2015**, *51*, 10554–10557.
- [81] N. Di Iorio, L. Soprani, S. Crotti, E. Marotta, A. Mazzanti, P. Righi, G. Bencivenni, *Synthesis* **2017**, *49*, 1519–1530.
- [82] S. Bariik, S. Shee, S. Das, R. G. Gonnade, G. Jindal, S. Mukherjee, A. T. Biju, *Angew. Chem. Int. Ed.* **2021**, *60*, 12264–12268; *Angew. Chem.* **2021**, *133*, 12372–12376.
- [83] F. Sun, T. Wang, G.-J. Cheng, X. Fang, *ACS Catal.* **2021**, *11*, 7578–7583.
- [84] O. Kitagawa, D. Kurihara, H. Tanabe, T. Shibuya, T. Taguchi, *Tetrahedron Lett.* **2008**, *49*, 471–474.
- [85] H. Liu, W. Feng, C. W. Kee, D. Leow, W.-T. Loh, C.-H. Tan, *Adv. Synth. Catal.* **2010**, *352*, 3373–3379.
- [86] K. Tanaka, H. Takahashi, T. Suda, M. Hirano, *Synlett* **2008**, *11*, 1724–1728.
- [87] G. Onodera, M. Suto, R. Takeuchi, *J. Org. Chem.* **2012**, *77*, 908–920.
- [88] M. Augé, M. Barbazanges, A. T. Tran, A. Simonneau, P. Elley, H. Amouri, C. Aubert, L. Fensterbank, V. Gandon, M. Malacria, J. Moussa, C. Ollivier, *Chem. Commun.* **2013**, *49*, 7833–7835.
- [89] X. Fan, X. Zhang, C. Li, Z. Gu, *ACS Catal.* **2019**, *9*, 2286–2291.
- [90] T. Hirata, I. Takahashi, Y. Suzuki, H. Yoshida, H. Hasegawa, O. Kitagawa, *J. Org. Chem.* **2016**, *81*, 318–323.
- [91] Z.-S. Liu, P.-P. Xie, Y. Hua, C. Wu, Y. Ma, J. Chen, H.-G. Cheng, X. Hong, Q. Zhou, *Chem.* **2021**, *7*, 1917–1932.
- [92] C. Sun, X. Qi, X. Min, X. Bai, P. Liu, Y. He, *Chem. Sci.* **2020**, *11*, 10119–10126.
- [93] a) J. Junghele, V. Buss, T. Beyrich, T. Jira, *Chirality* **1998**, *10*, 253–261. b) W. M. Welch, F. E. Ewing, J. Huang, F. S. Menniti, M. J. Pagnozzi, K. Kelly, P. A. Seymour, V. Guanowsky, S. Guhan, M. R. Guinn, D. Critchett, J. Lazzaro, A. H. Ganong, K. M. DeVries, T. L. Staigers, B. L. Chenard *Bioorg. Med. Chem. Lett.* **2001**, *11*, 177–181. c) H. H. Sun, C. J. Barrow, R. Cooper, *J. Nat. Prod.* **1995**, *58*, 1575–1580.
- [94] a) C. Roussel, M. Adjimi, A. Chemlal, A. Djafri, *J. Org. Chem.* **1988**, *53*, 5076–5080. b) T. Kawamoto, M. Tomishima, F. Yoneda, *Tetrahedron Lett.* **1992**, *33*, 3169–3172. c) R. S. Atkinson, E. Barker, C. J. Price, D. R. Russel, *J. Chem. Soc. Chem. Commun.* **1994**, 1159–1160.
- [95] X. Dai, A. Wong, S. C. Virgil, *J. Org. Chem.* **1998**, *63*, 2597–2600.
- [96] T. Tokitoh, T. Kobayashi, E. Nakada, T. Inoue, S. Yokoshima, H. Takahashi, H. Natsugari, *Heterocycles* **2006**, *70*, 93–99.
- [97] M. E. Diener, A. J. Metrano, S. Kusano, S. J. Miller, *J. Am. Chem. Soc.* **2015**, *137*, 12369–12377.
- [98] M. Hirai, S. Terada, H. Yoshida, K. Ebine, T. Hirate, O. Kitagawa, *Org. Lett.* **2016**, *18*, 5700–5703.
- [99] M. Matsuoka, M. Goto, A. Wzorek, V. A. Soloshonok, O. Kitagawa, *Org. Lett.* **2017**, *19*, 2650–2653.

- [100] a) J. Oppenheimer, R. P. Hsung, R. Figueroa, W. L. Johnson, *Org. Lett.* **2007**, *9*, 3969–3972. b) J. Oppenheimer, W. L. Johnson, R. Figueroa, R. Hayashi, R. P. Hsung, *Tetrahedron* **2009**, *65*, 5001–5012.
- [101] I. Takahashi, F. Morita, S. Kusagaya, H. Fukaya, O. Kitagawa, *Tetrahedron: Asymmetry* **2012**, *23*, 1657–1662.
- [102] F. Asegawa, Y. Yasukawa, K. Kawamura, H. Tsuchikawa, M. Murata, *Asian J. Org. Chem.* **2018**, *7*, 1648–1653.
- [103] T. Li, C. Mou, P. Qi, X. Peng, S. Jiang, G. Hao, W. Xue, S. Yang, L. Hao, Y. R. Chi, Z. Jin, *Angew. Chem. Int. Ed.* **2021**, *60*, 9362–9367; *Angew. Chem.* **2021**, *133*, 9448–9453.

---

Manuscript received: December 14, 2021  
Accepted manuscript online: February 22, 2022  
Version of record online: March 25, 2022

---